

NOTCH SERVES AS A MOLECULAR BRAKE ON MYOGENESIS, PROTEIN
SYNTHESIS, AND GROWTH IN SKELETAL MUSCLE

by

Joshua Robert Huot

A dissertation submitted to the faculty of
The University of North Carolina at Charlotte
in partial fulfillment of the requirements
for the degree of Doctor of Philosophy in
Biology

Charlotte

2018

Approved by:

Dr. Susan Tsivitse Arthur

Dr. Scott Gordon

Dr. Didier Dréau

Dr. Ian Marriott

Dr. Jeanette Bennett

©2018
Joshua Robert Huot
ALL RIGHTS RESERVED

ABSTRACT

JOSHUA ROBERT HUOT. Notch Serves as a Molecular Brake on Myogenesis, Protein Synthesis, and Growth in Skeletal Muscle. (Under the direction of Dr. SUSAN TSIVITSE ARTHUR)

Aging can be accompanied by aggressive loss of muscle mass (sarcopenia) and is a primary prognosticator for the reduced capacity of the elderly to accomplish basic activities of daily living. Several mechanisms within skeletal muscle lead to development of sarcopenia, including a faulty myogenic response (i.e. repair) and suppressed muscle protein synthesis (MPS) following a physiological stressor (e.g. bout of exercise). Notch has been identified as a key regulatory signaling pathway over the myogenic response, however exact roles of Notch signaling remain controversial. Moreover, regulation of MPS by Notch signaling is an unexplored area. We conducted a myriad of experiments to further elucidate Notch's regulatory role over the myogenic response as well as to determine if Notch has a regulatory role over MPS and skeletal muscle growth. Notch1 shRNA lentiviral (LV) particles (Notch1 knockdown) and an empty LV vector were injected into the left and right gastrocnemius of C57BL/6 mice, respectively (Chapter 2). Following LV administration mice, were separated in exercising (downhill running (DHR)) and non-exercising groups. Notch1 knockdown elevated myogenic regulatory factors and increased embryonic myosin heavy chain positive fibers following DHR. Moreover, Notch1 knockdown elevated MPS rate, albeit through an unknown mechanism. Follow-up experiments conducted on C2C12 cells confirmed that chemical inhibition of Notch, via γ -secretase inhibitor (GSI) treatment elevated myotube hypertrophy and MPS (Chapter 3). In chapter 3, we also demonstrated

that GSI-mediated increases in MPS may occur via modulation of the Phosphatase and Tensin Homolog/Protein Kinase B/Mechanistic Target of Rapamycin signaling pathway. In chapter 4, we demonstrated that GSI treatment is also sufficient to increase MPS independent of AKT and mTOR, likely via Glycogen Synthase Kinase 3 β . This work collectively demonstrates that Notch serves as a molecular brake on skeletal muscle and targeting of Notch may be a useful tactic in combatting muscle wasting conditions.

DEDICATIONS

*To my parents Bob and Diane,
and my wife, Ligia,
this work is dedicated to you.*

ACKNOWLEDGEMENTS

This work would not have been possible without Dr. Susan Arthur. I have the utmost gratitude for you taking me on as student and allowing me to join the Laboratory of Systems Physiology (LSP) 4 years ago. Thank you for putting me in an environment that has allowed me to grow and develop not only as a researcher, but as a person. I would also like to extend a huge thank you to my committee members, Dr. Scott Gordon, Dr. Ian Marriott, Dr. Didier Dréau, and Dr. Jeanette Bennett. I appreciate all of the guidance, feedback, and support you have provided me throughout this process. Thank you to the past and present members of LSP, Dr. Joe Marino, Dr. Marcus Lawrence, Bailey Peck, Jonathan Petrocelli, Cassandra Beach, Dr. Mike Turner, Dr. Reuben Howden, and Dr. Benjamin Gordon for providing a nourishing research environment. I would also like to thank the University of North Carolina at Charlotte Graduate School for the Graduate Assistant Support award that has funded my graduate education. Additionally, I owe thanks to the Sigma Xi Grants-in-Aid of Research Award (Appendix 3) and the Thomas L. Reynolds Graduate Student Research Award (Appendix 4) for helping to fund a portion of this research. I would also like to thank my parents, Bob and Diane, without the love and support that you have shown me from the day I was born none of this would be possible. Lastly, I owe an immense thank you to my wife, Ligia. The individual support system that you have provided me over the past 4 years is truly astonishing, and I could not have done this without you by my side every step of the way. Thank you.

TABLE OF CONTENTS

| | |
|----------------------------------------------------------------------------------------------------------|-----|
| LIST OF TABLES | x |
| LIST OF FIGURES | xi |
| LIST OF ABBREVIATIONS..... | xiv |
| CHAPTER 1: PROPOSED RESEARCH..... | 1 |
| 1.1 Background and Significance..... | 1 |
| 1.2 Innovation..... | 8 |
| 1.3 Specific Aims | 9 |
| 1.4 Approach | 14 |
| CHAPTER 2: EFFECTS OF NOTCH1 KNOCKDOWN ON SKELETAL MUSCLE REMODELING FOLLOWING DOWNHILL RUNNING | 15 |
| 2.1 Introduction | 15 |
| 2.2 Experimental Design and Methods | 16 |
| 2.2.1 Experimental Animals | 16 |
| 2.2.2 Lentiviral Knockdown..... | 17 |
| 2.2.3 Treadmill Familiarization and Downhill Run Exercise Bout..... | 17 |
| 2.2.4 SUnSET Technique and Muscle Tissue Harvesting..... | 18 |
| 2.2.5 Tissue Homogenization and Protein Concentration Assay | 18 |
| 2.2.6 SDS-Page and Western Blotting..... | 19 |
| 2.2.7 Immunofluorescent Staining..... | 20 |
| 2.2.8 Immunofluorescent Quantification..... | 21 |
| 2.2.9 Hematoxylin and Eosin Staining and Quantification | 21 |
| 2.2.10 Statistical Analysis | 22 |
| 2.3 Results | 22 |
| 2.3.1 Lentiviral incorporation and knockdown of Notch1 receptor and signaling.... | 22 |
| 2.3.2 Skeletal muscle injury | 22 |
| 2.3.3 Pax7 expression | 23 |
| 2.3.4 MyoD expression..... | 23 |
| 2.3.5 Myogenin expression..... | 24 |
| 2.3.6 eHMC fibers | 24 |

| | |
|---------------------------------------------------------------------------------------------------------------------|-----------|
| 2.3.7 Muscle wet weight and cross-sectional area..... | 25 |
| 2.3.8 Phosphorylation and total mTOR expression..... | 25 |
| 2.3.9 Mixed muscle protein synthesis | 26 |
| 2.4 Discussion and Conclusion | 26 |
| 2.5 Figures..... | 38 |
| 2.6 Tables | 54 |
| CHAPTER 3: EFFECTS OF NOTCH INHIBITION ON THE MYOGENIC PROGRAM AND PROTEIN SYNTHESIS IN C2C12 CELLS..... | 58 |
| 3.1 Introduction | 58 |
| 3.2 Experimental Design and Methods | 60 |
| 3.2.1 Cell Culture..... | 60 |
| 3.2.2 MTT Proliferation Assay on Myoblasts | 61 |
| 3.2.3 Myosin Heavy Chain Staining..... | 61 |
| 3.2.4 Myotube Fusion and Myotube Area..... | 62 |
| 3.2.5 Protein Synthesis | 62 |
| 3.2.6 Western Blot..... | 63 |
| 3.2.7 Statistical Analysis | 64 |
| 3.3 Results | 64 |
| 3.3.1 GSI reduces Notch signaling and blunts proliferation in C2C12 myoblasts | 64 |
| 3.3.2 GSI elevates myotube formation in differentiating C2C12 myotubes | 64 |
| 3.3.3 GSI elevates protein synthesis and mTOR in C2C12 myoblasts and myotubes | 65 |
| 3.3.4 GSI modulates signaling upstream of mTOR in C2C12 myoblasts and myotubes..... | 66 |
| 3.3.5 GSI elevates protein synthesis and myotube hypertrophy in day 6 myotubes . | 66 |
| 3.4 Discussion and Conclusion | 67 |
| 3.5 Figures..... | 72 |
| 3.6 Tables | 84 |
| CHAPTER 4: GSI-MEDIATED ELEVATIONS IN PROTEIN SYNTHESIS INDEPENDENT OF AKT AND MTOR | 85 |
| 4.1 Introduction | 85 |
| 4.2 Experimental Design and Methods | 86 |

| | |
|-------------------------------------------------------------------------------------|-----|
| 4.2.1 Cell Culture..... | 86 |
| 4.2.2 Myosin Heavy Chain Staining..... | 87 |
| 4.2.3 Myotube Fusion and Myotube Area..... | 87 |
| 4.2.4 Protein Synthesis | 88 |
| 4.2.5 Western Blot..... | 88 |
| 4.2.6 Co-immunoprecipitation..... | 89 |
| 4.2.7 Statistical Analysis | 91 |
| 4.3 Results | 91 |
| 4.3.1 A lack of protein-protein interactions between Notch and mTOR signaling... 91 | |
| 4.3.2 Rapamycin ablates GSI-mediated elevations in myotube formation | 91 |
| 4.3.3 GSI mediates protein synthesis independent of mTOR..... | 92 |
| 4.3.4 API-1 ablates GSI-mediated elevations in myotube formation..... | 93 |
| 4.3.5 GSI mediated increases in mTOR is halted by API-1 | 94 |
| 4.3.6 GSI elevates protein synthesis independent of AKT and mTOR..... | 95 |
| 4.4 Discussion and Conclusion | 96 |
| 4.5 Figures..... | 104 |
| 4.6 Tables | 116 |
| CHAPTER 5: DISSERTATION DISCUSSION | 118 |
| REFERENCES | 132 |
| APPENDIX 1: INSTITUTIONAL ANIMAL CARE AND USE COMMITTEE APPROVAL LETTER..... | 151 |
| APPENDIX 2: INSTITUTIONAL BIOSAFETY APPROVAL LETTER | 153 |
| APPENDIX 3: SIGMA XI STUDENT RESEARCH GRANT..... | 155 |
| APPENDIX 4: THOMAS L. REYNOLDS GRADUATE RESEARCH FELLOWSHIP | 159 |

LIST OF TABLES

| | |
|---------------------------------------------------------|-----|
| TABLE 2.6.1. Treadmill Familiarization Protocol. | 54 |
| TABLE 2.6.2. Antibodies used for Western Blot Analysis. | 55 |
| TABLE 2.6.3. Antibodies used for Immunohistochemistry. | 56 |
| TABLE 2.6.4. Muscle Wet Weights of Young C57BL/6 Mice. | 57 |
| TABLE 3.6.1. Antibodies used for Western Blot Analysis. | 84 |
| TABLE 4.6.1. Antibodies used for Western Blot Analysis. | 116 |
| TABLE 4.6.2. Antibodies used for Immunoprecipitation. | 117 |

LIST OF FIGURES

| | |
|-------------------------------------------------------------------------------------------|----|
| FIGURE 1.1. Overview of Myogenesis. | 1 |
| FIGURE 1.2. Overview of Potential MPS Regulation by Notch. | 6 |
| FIGURE 1.3. Muscle Injury in Aged Mice Following DHR. | 10 |
| FIGURE 1.4. MyoD Expression in Aged Mice Following DHR. | 10 |
| FIGURE 1.5. Percent Change in Myoblast Proliferation. | 11 |
| FIGURE 1.6. Percent Change in Fusion Indices of Day 4 Myotubes. | 11 |
| FIGURE 1.7. Percent Change of mTOR in C2C12 Myoblasts. | 12 |
| FIGURE 1.8. Percent Change of Protein Synthesis in C2C12 Myoblasts. | 12 |
| FIGURE 1.9. Percent Change of mTOR in C2C12 Myotubes. | 13 |
| FIGURE 1.10. Knockdown of Notch1 Receptor. | 14 |
| FIGURE 2.5.1. Experimental Design of Young Mice (n = 30). | 38 |
| FIGURE 2.5.2. Lentiviral Incorporation. | 39 |
| FIGURE 2.5.3. Notch1 Expression in Gastrocnemius Muscle. | 40 |
| FIGURE 2.5.4. Hes1 Expression in Gastrocnemius Muscle. | 41 |
| FIGURE 2.5.5. Muscle Injury in Gastrocnemius. | 42 |
| FIGURE 2.5.6. Pax7 Expression in Gastrocnemius Muscle. | 43 |
| FIGURE 2.5.7. Pax7/fiber in Gastrocnemius Muscle. | 44 |
| FIGURE 2.5.8. MyoD Expression in Gastrocnemius Muscle. | 45 |
| FIGURE 2.5.9. MyoD+/DAPI+ Colocalization in Gastrocnemius Muscle. | 46 |
| FIGURE 2.5.10. Myogenin Expression in Gastrocnemius Muscle. | 47 |
| FIGURE 2.5.11. Myogenin+/DAPI+ Colocalization in Gastrocnemius Muscle. | 48 |
| FIGURE 2.5.12. Percentage of Embryonic Myosin Heavy Chain Fibers in Gastrocnemius Muscle. | 49 |

| | |
|----------------------------------------------------------------------------------------------------|-----|
| FIGURE 2.5.13. CSA Frequency Distribution in Gastrocnemius Muscle. | 50 |
| FIGURE 2.5.14. Average CSA in Gastrocnemius Muscle. | 51 |
| FIGURE 2.5.15. Phosphorylated and Total mTOR in Gastrocnemius Muscle. | 52 |
| FIGURE 2.5.16. Muscle Protein Synthesis Rate in Gastrocnemius Muscle. | 53 |
| FIGURE 3.5.1. GSI Reduces Notch Signaling and Blunts Proliferation in C2C12 Myoblasts. | 72 |
| FIGURE 3.5.2. GSI Reduces Notch Signaling C2C12 Myotubes. | 73 |
| FIGURE 3.5.3. GSI Treatment Increases Indices of Myotube Fusion in C2C12 Myotubes. | 74 |
| FIGURE 3.5.4. GSI Treatment Increases Indices of Myotube Hypertrophy in C2C12 Myotubes. | 75 |
| FIGURE 3.5.5. GSI Treatment Increases Markers of Differentiation in C2C12 Myotubes. | 76 |
| FIGURE 3.5.6. GSI Treatment Elevates Protein Synthesis in C2C12 Myoblasts. | 77 |
| FIGURE 3.5.7. GSI Treatment Elevates Protein Synthesis in C2C12 Myotubes. | 78 |
| FIGURE 3.5.8. GSI Treatment Elevates Upstream mTOR Signaling in C2C12 Myoblasts. | 79 |
| FIGURE 3.5.9. GSI Treatment Elevates Upstream mTOR Signaling in C2C12 Myotubes. | 80 |
| FIGURE 3.5.10. GSI Treatment Elevates Protein Synthesis in Formed C2C12 Myotubes. | 81 |
| FIGURE 3.5.11. Effect of GSI Treatment on Indices of Myotube Fusion in Formed C2C12 Myotubes. | 82 |
| FIGURE 3.5.12. Effect of GSI Treatment on Indices of Myotube Hypertrophy in Formed C2C12 Myotubes. | 83 |
| FIGURE 4.5.1. Immunoprecipitation in C2C12 Myoblasts and Myotubes. | 104 |
| FIGURE 4.5.2. Indices of Fusion in C2C12 Myotubes with GSI and RAP. | 105 |
| FIGURE 4.5.3. Indices of Hypertrophy in C2C12 Myotubes with GSI and RAP. | 106 |

| | |
|---------------------------------------------------------------------------------------------------|-----|
| FIGURE 4.5.4. mTOR Signaling in Cultured C2C12 Myotubes with GSI and RAP. | 107 |
| FIGURE 4.5.5. Muscle Protein Synthesis Rate in Cultured C2C12 Myotubes with GSI and RAP. | 108 |
| FIGURE 4.5.6. Indices of Fusion in Cultured C2C12 Myotubes with GSI and API-1. | 109 |
| FIGURE 4.5.7. Indices of Hypertrophy in C2C12 Myotubes with GSI and API-1. | 110 |
| FIGURE 4.5.8. AKT in Cultured C2C12 Myotubes with GSI and API-1. | 111 |
| FIGURE 4.5.9. mTOR Signaling in Cultured C2C12 Myotubes with GSI and API-1. | 112 |
| FIGURE 4.5.10. Muscle Protein Synthesis Rate in Cultured C2C12 Myotubes with GSI and API-1. | 113 |
| FIGURE 4.5.11. GSK3 β and ABC in Cultured C2C12 Myotubes with GSI and API-1. | 114 |
| FIGURE 4.5.12. Muscle Protein Synthesis Rate in Cultured C2C12 Myotubes with GSI, RAP, and API-1. | 115 |
| FIGURE 5.1. Influence of Notch Over Myogenesis. | 130 |
| FIGURE 5.2. Regulation of Muscle Protein Synthesis. | 131 |

LIST OF ABBREVIATIONS

| | |
|-------|-----------------------------------------------|
| ABC | Activated β -Catenin |
| Akt | Protein Kinase B |
| CSA | Cross-Sectional Area |
| eMHC | Embryonic Myosin Heavy Chain |
| DHR | Downhill Running |
| eEF2 | Eukaryotic Elongation Factor 2 |
| GFP | Green Fluorescent Protein |
| GSI | γ -secretase Inhibitor |
| GSK3 | Glycogen Synthase Kinase 3 |
| Hes1 | Hairy/Enhancer of Split-1 |
| IRS-1 | Insulin Receptor Substrate-1 |
| MPS | Muscle Protein Synthesis |
| MRF | Myogenic Regulatory Factor |
| mTOR | Mechanistic Target of Rapamycin |
| Myc | Avian Myelocytomatosis Viral Oncogene Homolog |
| NICD | Notch Intracellular Domain |
| Pax7 | Paired Box 7 |
| PDK-1 | Phosphoinositide-Dependent Kinase-1 |
| PIP2 | Phosphatidylinositol 4,5-Bisphosphate |
| PIP3 | Phosphatidylinositol (3,4,5)-Trisphosphate |

| | |
|---------|------------------------------------|
| PTEN | Phosphatase and Tensin Homolog |
| P70S6K | 70 kDA Ribosomal Protein S6 Kinase |
| RAP | Rapamycin |
| Ser | Serine |
| Thr | Threonine |
| TSC 1/2 | Tuberous Sclerosis Complex |

CHAPTER 1: PROPOSED RESEARCH

1.1 Background and Significance

Aging can be accompanied by aggressive loss of skeletal muscle mass (sarcopenia), and is a primary factor to a reduced ability of the elderly to accomplish basic activities of daily living [1; 2]. From age 20 to 80 years old, there is approximately a 40% reduction in muscle mass and a 20% decline in muscle cross-sectional area [2]. Moreover, these losses preferentially affect fast-twitch fibers leading to lower muscular

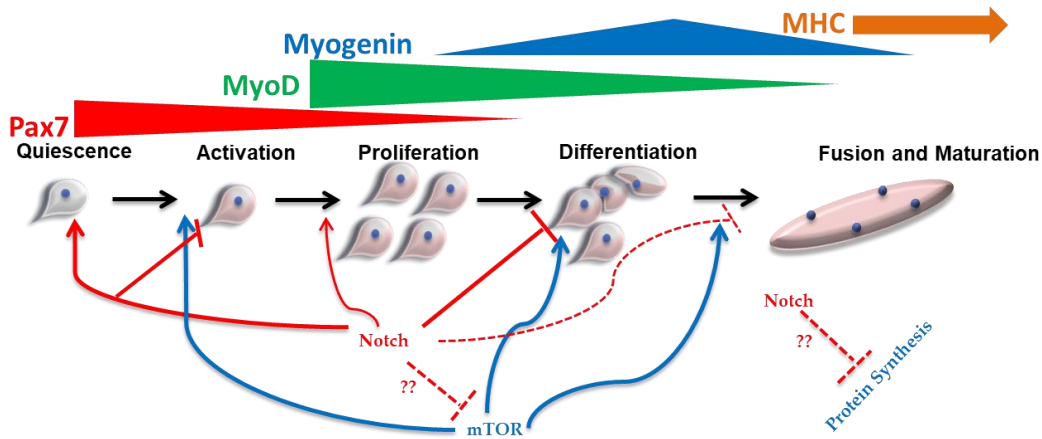


Figure 1.1. Overview of Myogenesis. Notch and mechanistic target of rapamycin (mTOR) signaling during skeletal muscle repair/myogenesis. The process of myogenesis consists of quiescent satellite cells (SCs) (express Paired box 7 (Pax7)), which activate (express MyoD) upon insult. Activated cells will then proliferate, differentiate (express Myogenin), and subsequently fuse to form multinucleated myofibers (express myosin heavy chain (MHC)). Notch (shown in red) negatively regulates the activation of SCs by maintaining quiescence. Some level of Notch signaling may be necessary for proliferation, though this remains a controversial topic. Elevated Notch signaling prevents differentiation and may also prevent fusion and maturation of myofibers, though the latter is an understudied area. mTOR (shown in blue) is necessary for SC activation and has also shown to be pivotal for differentiation and late stage fusion of mature myofibers. We hypothesize that Notch negatively regulates mTOR during myogenesis. Moreover, we hypothesize that Notch also serves as a molecular brake on muscle protein synthesis.

strength and power resulting in slower movement patterns, increases frailty of aging individuals and increases in the risk of injury, primarily by falling [3]. In 2004, there were an estimated 656 million individuals 60 years and older and estimated healthcare costs that attributed to sarcopenia were as high as 18 billion dollars [4] (Census Bureau). By the year 2025 it is expected that 1.2 billion people will be at least 60 years or older, a ~83% increase from 2004 [5]. If the rise in healthcare costs parallels the rise in the aging population, they will reach roughly 33 billion dollars in the year 2025.

Skeletal muscle accounts for nearly 50% of total body mass in young individuals [6] and serves to secrete cytokines that play a pivotal role in other body tissues making muscle mass and function extremely important to the onset of other diseases as aging progresses [7-9]. When muscle mass is lost over time the effects it has on bone mass maintenance and cardiorespiratory fitness also diminishes, increasing the likelihood of osteoporosis, coronary heart disease, and Alzheimer's disease [10-12]. Furthermore, as skeletal muscle mass decreases; basal metabolic rate declines (~30% between age 20 and 70) and the body loses its efficiency in glucose regulation bringing an increased risk for metabolic disorders such as diabetes [10; 13; 14]. Finding countermeasures to combat sarcopenia would serve significant to improving quality of life to the aging population and reducing the financial burden on the healthcare system.

Several mechanisms within skeletal muscle are thought drive the development of sarcopenia. These include, but are not limited to: a decrease in skeletal muscle protein synthesis (MPS), a reduction in hormone levels, a decline in neural functioning, an elevation in fat cell deposits within skeletal muscle, and an increase of cellular senescence and death [10; 15-18]. Another problematic issue and contributor to the

development of sarcopenia is the abrogated myogenic response in aged skeletal muscle [10; 19], which is considered to have a pivotal role in developing sarcopenia. Known interventions are relatively ineffective in resolving this problem, demanding the advancement in our understanding of the myogenic program during aging.

The process of myogenesis is comprised of activation of adult skeletal muscle stem cells (satellite cells (SCs)), proliferation, differentiation, and fusion of these cells leading to formation of multinucleated myotubes [10]. Aging is associated with deleterious modifications to the intrinsic properties of SCs and the signaling pathways that regulate myogenesis. Two regulatory pathways of the myogenic program are Notch and mechanistic target of rapamycin (mTOR), both of which are thought to weaken with age (Figure 1.1) [10; 20; 21].

Notch signaling is a highly conserved cell-to-cell communication pathway and a key determinant of cellular differentiation and fate (including that of skeletal muscle development) [10; 22]. Signaling of the Notch family transmembrane receptors (Notch 1-4) occurs when ligands (Delta-like protein [DDL] 1, DDL 3, DDL 4, Jagged 1, and Jagged 2) bind and initiate a series of cleavages drive by metalloproteases and λ -secretases resulting cleavage of the Notch intracellular domain (NICD). NICD canonically translocates to the nucleus and initiates transcription and suppression of several target genes including hairy and enhancer of split1 (Hes1) Hey1, and avian myelocytomatosis viral oncogene homolog (Myc) [10; 22-25]. In addition to its pivotal roles during development, Notch signaling is also crucial for a successful myogenic response following injury. It is well established that Notch plays a key role in the maintenance of SC quiescence, thus preventing SC activation [10; 26; 27]. Recently,

context-specific roles of Notch during myogenesis have been postulated: Notch signaling will remain elevated in muscle cells serving to replenish the SC population, whereas Notch signaling will be downregulated in cells pushing towards differentiation and fusion [22]. Other research had previously brought context-roles to light for Notch signaling, albeit with different terminology. Brack *et al* demonstrated a temporal switch of Notch and Wnt signaling during myogenesis, while others have demonstrated that constitutively active Notch prevents cells venturing down the myogenic lineage [25; 28; 29]. However, the impact of Notch on other regulators of the myogenic program are not well understood. It is possible that down-regulation of Notch in cells traveling down the myogenic lineage allows for upregulation of other regulators of the myogenic program such as mTOR. Gathering a better understanding of the context-specific roles of Notch signaling during myogenesis and regulation by Notch on other signaling cascades such as mTOR may hold crucial information to resolving sarcopenia and other muscle wasting diseases.

mTOR is a known to be a key regulator of a wide range of biological process including cell growth and metabolism and its regulation of protein synthesis is an attractive topic to muscle physiologists. One area in which the role of mTOR is less understood is its regulation of the myogenic program, though research in this area is expanding. It is currently postulated that mTOR plays a prominent role in regulating the latter stages of myogenesis, specifically the onset of differentiation and maturation of myotubes. It is thought that mTOR regulation of differentiation occurs at two separate stages. First, mTOR may control initiation of myoblast differentiation via regulation of IGF-II [30-32]. Second, mTOR is thought to act in positively regulating follistatin to aid

in late-stage fusion and maturation of myotubes into muscle fibers [33]. Treatment of C2C12 cells with rapamycin (a commonly used inhibitor of mTOR), prevents differentiation of myoblasts into myotubes. Furthermore, use of a rapamycin-resistant mutant of mTOR demonstrated that C2C12 cells properly differentiated in the presence of rapamycin [34]. Additionally, evidence suggests that mTOR may stabilize and maintain MyoD activity, though this mechanism is unknown. The possible mTOR-MyoD regulatory interaction is of interest as Notch signaling and its downstream effectors have shown to inhibit MyoD expression, though this is not fully understood [35; 36]. Though still unclear as to the exact role of mTOR during the earlier stages of myogenesis, there is evidence demonstrating that mTOR signaling is necessary for SC activation [37]. Furthermore, treatment of rapamycin *in vivo* has demonstrated to impair myofiber formation and myofiber growth following injury [34]. Despite what is known about mTOR thus far, its interaction or regulation by or on other pathways (i.e. Notch) during the myogenic program has yet to be examined.

In addition to their regulatory roles during the myogenic program, it is also known that these two pathways are impacted by age. Notch signaling is greatly reduced in aged skeletal muscle repair. This is reflective of reduced Notch receptors (e.g. Notch1) and ligands (e.g. Delta1) expressed in aged SCs of mouse muscle [10; 38]. These reductions in Notch receptors and ligands lead to reductions in the myogenic program and subsequent inability of aged muscle to repair itself compared to young muscle. Increased inhibitors of Notch signaling (e.g. $\text{TNF}\alpha$ & $\text{TGF}\beta$) may also be upregulated in aged skeletal muscle, further reducing the regenerative capabilities of aged muscle [10]. Additionally aged skeletal muscle is known to have blunted anabolic signaling and

heightened catabolic signaling leading to a net loss in muscle protein and a pivotal contributor to the sarcopenic state [39; 40]. One of the main drivers of MPS and anabolic signaling is mTOR. mTOR signaling is weakened in aged skeletal muscle compared to young skeletal muscle. Phosphorylated mTOR and P70S6K (key downstream target of mTOR signaling) have been found to be significantly reduced by 28% and 57% respectively in aged compared to young rodent muscle [20; 21]. These reductions in

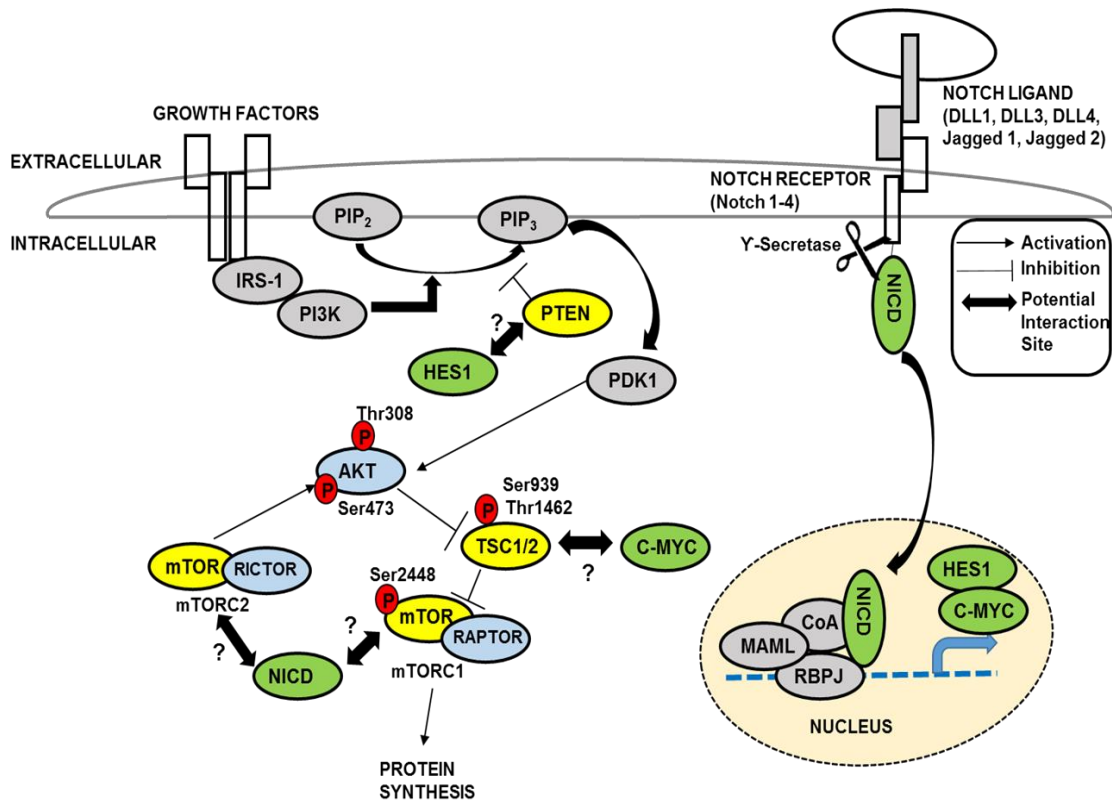


Figure 1.2. Overview of Potential MPS Regulation by Notch. Overview of potential regulation of the phosphatase and tensin homolog (PTEN)/ protein kinase B (AKT)/ mechanistic target of rapamycin (mTOR) [PTEN/AKT/mTOR] signaling cascade by Notch signaling. PTEN is an upstream negative regulator of AKT signaling. PTEN prevents the conversion of Phosphatidylinositol (4,5) -bisphosphate (PIP₂) to Phosphatidylinositol (3,4,5)-trisphosphate (PIP₃), thereby preventing subsequent phosphorylation of AKT on Threonine 308 by Phosphoinositide-dependent kinase-1 (PDK1). Fully activated AKT (via phosphorylation of Serine 473 by mTORC2) phosphorylates tuberous sclerosis complex (TSC1/2) on multiple sites, thus alleviating the inhibitory effect of the TSC complex on mTORC1. Potential cross-talk sites between Notch signaling and this signaling cascade are depicted above and include: hairy and enhancer of split-1 (HES1)-PTEN; avian myelocytomatosis viral oncogene homolog (C-Myc)-TSC; and Notch intracellular domain (NICD)-mTORC1/2.

phosphorylated mTOR and 70S6K likely contribute to the blunted MPS response to exercise seen in aged skeletal muscle further contributing to a sarcopenic state [41].

Despite what is known regarding their myogenic roles, it is not established if Notch and mTOR communicate during the myogenic program, though cancer models suggest that Notch may regulate mTOR in cancer progression [42; 43]. One suggested mechanism (oncogenic and drosophila models) by which Notch precedes mTOR is through regulation of phosphatase and tensin homolog (PTEN), by a downstream target gene of Notch, hairy and enhancer of split1 (Hes1) [42]. PTEN (upstream of mTOR) serves to inhibit the phosphorylation (p) of protein kinase B (AKT) at Threonine (Thr) 308 (see Figure 1.2) [44]. When AKT is phosphorylated on Thr308 it will phosphorylate and inhibit tuberous sclerosis complex 2 (TSC2) (a regulator of mTOR) on multiple sites, resulting in increased mTOR signaling [44]. Thus, elevated PTEN results in inhibition of the AKT/mTOR pathway. If Hes1 regulates PTEN, this would provide a link between Notch and the PTEN/AKT/mTOR pathway. In addition to the Hes1-PTEN interface, there is support for two additional links between Notch and the PTEN/AKT/mTOR pathway. The first is the regulation of TSC2, by the downstream effector of Notch, avian myelocytomatosis viral oncogene homolog (c-Myc) [45]. The second is interaction between Notch intracellular domain (NICD) and mTOR directly as postulated within HeLa cells [46]. Furthermore, research within cardiac muscle has identified signal transducer and activator of transcription 3 (STAT3) as a plausible link between Notch and mTOR [47].

It is plausible that post-injury down regulation of Notch is necessary for both activation of SCs and activation of mTOR leading to cellular fusion and myotube

formation. We postulate that Notch serves as a multifaceted myogenic brake; preventing SC activation, myotube formation, and possibly muscle growth. The latter is evidenced by rescued muscle mass seen in tumor bearing mice treated with γ -secretase inhibitor (GSI) [48]. If Notch does serve as a myogenic brake and if Notch does precede mTOR, discovering the specific interface between these two pathways could possess the key to rejuvenating repair capacity and MPS in aging skeletal muscle. Furthermore, this research has the potential to alleviate skeletal atrophy seen not only in sarcopenia, but other wasting diseases such as cachexia.

1.2 Innovation

This proposal is novel in that this is the first time a research paradigm will be investigated regarding the influence of Notch signaling on muscle injury, repair, and protein synthesis using a physiological modality of injury. Furthermore, despite other fields indicating possible regulation of the PTEN/AKT/mTOR signaling cascade by Notch signaling, it is unknown if this regulation exists during myogenesis or in relation to MPS.

The initial and common injury models used to study skeletal muscle repair utilize artificial techniques (e.g. toxin-induced, freeze-induced) which are focal, lack practicality (to everyday living) and do not incorporate other biological systems. A more practical approach to induce muscle injury is to physiologically stimulate muscle contractions (i.e. exercise), specifically eccentric muscle contractions. In our lab we have established downhill running as a successful model to induce skeletal muscle injury in mice and study the repair process.

One advantage of using a physiological stimulus (i.e. downhill running (DHR)) is its inclusiveness of other biological systems. Artificial and focal models of muscle injury affect a local region of the skeletal muscle, excluding potential immunological, neurological, and systemic responses that are considered via a physiological stimulus [49].

It is understood that the skeletal muscle repair mechanism becomes faulty with age contributing to extreme muscle atrophy and large losses of skeletal muscle function. Additionally, it is recognized that both Notch and mTOR contribute to and are essential for the myogenic program, yet modulation of mTOR by Notch is an uninvestigated area. This will be the first study to examine the potential multi-braking effect that Notch has on skeletal muscle repair and MPS. The results of this project will provide novel insight on potential therapeutic targets towards rescuing skeletal muscle mass in aged and diseased populations.

1.3 Specific Aims

In adult skeletal muscle Notch signaling is known to halt SC activation, yet the specific role of Notch signaling with regards to skeletal muscle repair remains controversial. Some groups have indicated Notch activation is essential for SC activation, proliferation, and successful repair [26; 50; 51]. Furthermore, research suggests that reducing Notch impairs skeletal muscle regeneration of young mice following injury, while activation of Notch is capable of rescuing the impaired ability of aged skeletal muscle to repair itself. Conversely, other findings show that Notch is significantly lowered upon injury and this reduction of Notch is what allows for SCs to

proliferate and subsequently differentiate [22; 29; 52; 53]. These same studies stress the importance of Notch for maintaining SC quiescence and show that with inhibition of Notch, muscle stem cells differentiate early leading to significant hypertrophy. More recently, myogenic stage-specific effects of Notch have been examined revealing differing roles for Notch activation. For example, elevated Notch will dedifferentiate myocytes (committed myogenic cells not yet fused) to increase the SC pool leading to defective myogenesis. In contrast, elevated Notch in post fusion myotubes/myofibers enhances function and repair capacity of skeletal muscle [25; 54]. Dysregulation of Notch during the myogenic program disrupts SC function ultimately impairing the repair response to stimuli: If Notch is inhibited too early following insult SCs prematurely activate and differentiate, do not self-renew, and repair is impaired. If Notch is elevated too early following SC

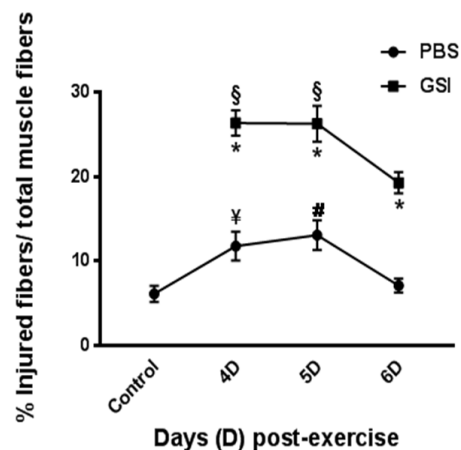


Figure 1.3. Muscle Injury in Aged Mice Following DHR. H&E quantification of muscle injury on cross sections of gastrocnemius muscle in aged mice exposed to downhill running (DHR) and/or Notch inhibition. * $P < 0.01$ vs. all PBS treatment. # $P \leq 0.01$ vs. CT and PBS-treated 6D post-exercise. ¥ $P < 0.05$ vs. CT and PBS-treated 6D post-exercise. § $P < 0.01$ vs. inhibition treated 6D post-exercise (n = 4).

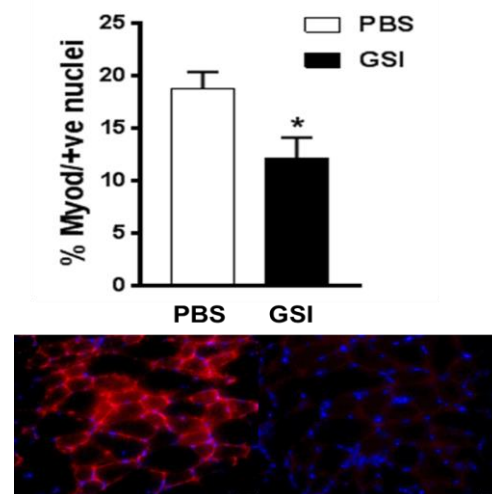
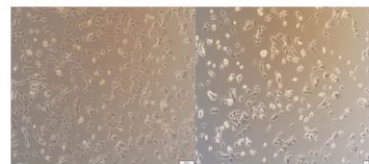
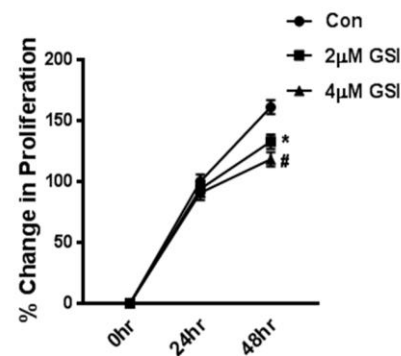


Figure 1.4. MyoD Expression in Aged Mice Following DHR. Quantification of percent (%) MyoD/+ve nuclei sections of aged gastrocnemius 96 hours post downhill running (DHR) treated with either phosphate buffered saline (PBS) or γ -secretase inhibitor (GSI). * $P = 0.05$ vs. PBS (n = 4).

activation self-renewal aberrantly increases, myocyte fusion diminishes, and repair is impaired. The Arthur lab has generated pilot data supporting the former. Our preliminary data demonstrates that Notch inhibition (via GSI) increases gastrocnemius muscle injury in the days following DHR (Figure 1.3). This indicates an impaired resolution of injury. Furthermore, Notch inhibition reduces the amount of MyoD⁺ nuclei 96-hours following DHR (Figure 1.4) indicating an early (likely premature) myogenic response. It is plausible that knockdown of Notch in skeletal muscle induces a faulty myogenic response in response to exercise, but these studies have yet to be carried out.

It has been previously postulated that Notch may have context-specific roles with regard to muscle cells. The Arthur lab has data indicating differential effects of Notch



Con (48hrs) 2µM GSI (48hrs)

Figure 1.5. Percent Change in Myoblast Proliferation. Percent change from control in 3-(4,5-dimethylthiazol-2-yl)-2,5-diphenyl tetrazolium bromide (MTT; Sigma) proliferation assay of proliferating C2C12 cells at 24 and 48 hours treated with or without γ -secretase inhibitor (GSI). * $P < 0.05$ vs. Control (Con); # $P < 0.01$ vs. Con (n = 3).

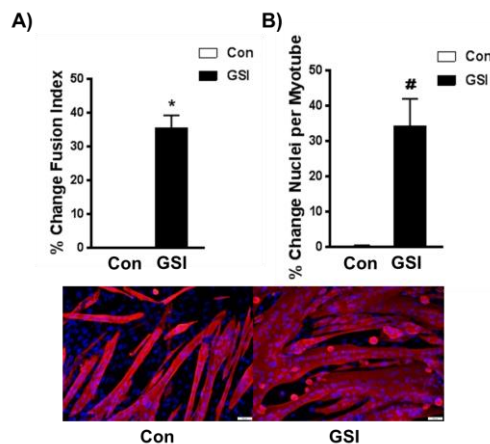


Figure 1.6. Percent Change in Fusion Indices of Day 4 Myotubes. A)

Percent change in fusion index (nuclei fused into myotubes/total nuclei) in 96 hour myotubes treated with or without γ -secretase inhibitor (GSI). B) Percent change in nuclei per myotube in 96 hour myotubes treated with or without GSI. * $P < 0.001$ vs. Control (Con); # $P < 0.05$ vs. Con (n = 3).

inhibition on myoblasts and myotubes: Where Notch inhibition via GSI treatment lowers proliferation of C2C12 myoblasts (Figure 1.5) while enhancing the fusion of C2C12s into myotubes (Figure 1.6). It is currently unknown to what extent key myogenic factors and MPS pathways interact during the myogenic response. It could be true that Notch has context-specific interactions with other signaling pathways, like mTOR.

In fact, given our differing results on myoblast proliferation and myotube fusion, our lab had initially postulated that Notch and mTOR may have a context-specific interaction. We thought it plausible that mTOR signaling would be reduced in proliferating C2C12 cells given the negative impact that GSI treatment has shown on proliferation. However, recent data from our lab indicates otherwise. We now have data indicating that Notch inhibition enhances p-mTORser228 (Figure 1.7) and elevates protein synthesis (Figure

1.8) in proliferating C2C12 cells, despite lowering proliferation. Furthermore, our data indicates that GSI treatment also increases p-mTORSer2448 in C2C12 myotubes (Figure

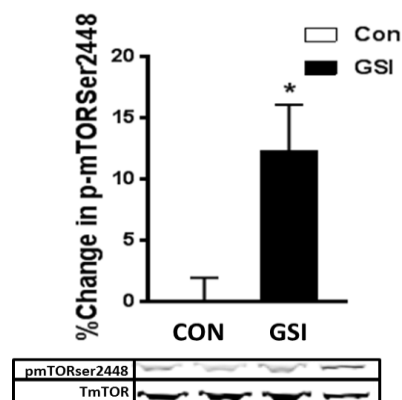


Figure 1.7. Percent Change of mTOR in C2C12 Myoblasts. Percent change in phosphorylated (p)-mTOR (Ser2448) expression relative to total (t)-mTOR in 48 hour myoblasts treated with or without γ -secretase inhibitor (GSI). * P < 0.05 vs. Control (Con) (n = 2).

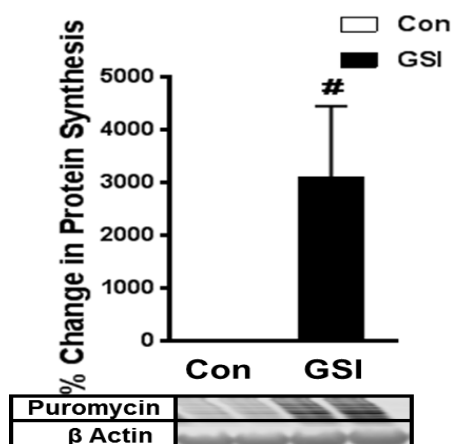


Figure 1.8. Percent Change of Protein Synthesis in C2C12 Myoblasts. Percent change in Puromycin expression relative to β Actin in 48 hour myoblasts treated with or without γ -secretase inhibitor (GSI) # P = 0.05 vs. Control (Con) (n = 2).

1.9), though the mechanism by which Notch may modulate mTOR remains to be elucidated.

However, findings from our laboratory and interactions between Notch and mTOR pathways indicated by other fields, strongly suggest that Notch and mTOR communicate, and may even physically interact in skeletal muscle [42; 45; 46]. Despite what is known, research has not been carried out that investigates the regulation of Notch on mTOR and muscle growth. Thus the present study addressed the following aims:

Specific Aim 1: To examine the effect of Notch

signaling on skeletal muscle injury and repair following physiological insult.

Hypothesis 1: Knocking down Notch1 using lentiviral shRNA will result in increased skeletal muscle injury and abrogate muscle repair in young male mice following injurious downhill running.

Specific Aim 2a: To examine the effect of Notch signaling on mTOR and protein synthesis in proliferating and differentiating C2C12 cells.

Hypothesis 2a: Inhibition of Notch signaling via GSI-treatment will elevate mTOR signaling and protein synthesis in both proliferating and differentiating C2C12 cells.

Specific Aim 2b: To determine if Notch acts through mTOR to influence protein synthesis and hypertrophy in C2C12 myotubes.

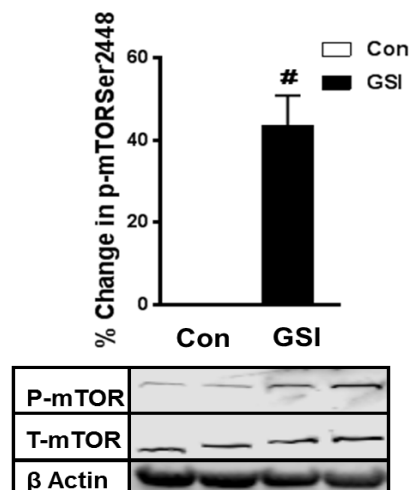


Figure 1.9. Percent Change of mTOR in C2C12 Myotubes. Percent change in phosphorylated (p)-mTOR (Ser2448) expression relative to total (t)-mTOR in 96 hour myotubes treated with or without γ -secretase inhibitor (GSI). # $P < 0.05$ vs. Control (Con) (n = 3).

Hypothesis 2b: Inhibition of Notch signaling via GSI-treatment will elevate C2C12 protein synthesis and hypertrophy in a mTOR-dependent manner.

1.4 Approach

We performed a myriad of experiments in order to test Specific Aims 1 and 2. In the first experimental set (Chapter 2) we intramuscularly injected an empty lentiviral vector (pLKO.1-puro-CMV-tGFP, right hindlimb) or

Notch1shRNA lentiviral vector (pLKO.1-puro-Notch1shRNA-CMV-tGFP, left hindlimb) into the gastrocnemius prior to a bout of downhill running and examined the subsequent muscle remodeling response. In the second set of experiments (Chapter 3) we treated proliferating (myoblasts) and differentiating (myotubes) C2C12 cells with a GSI to determine if Notch signaling regulates mTOR signaling during the

myogenic program. In a third set of experiments (Chapter 4) we introduced both GSI and rapamycin (an mTOR inhibitor) to C2C12 myotubes in order to determine if Notch signaling acts through mTOR in its regulation of the myogenic program. We completed pilot experiments for *in vivo* knockdown of Notch1. Our preliminary work demonstrated that intramuscular injection of Notch1 shRNA was sufficient to reduce Notch1 expression (Figure 1.10).

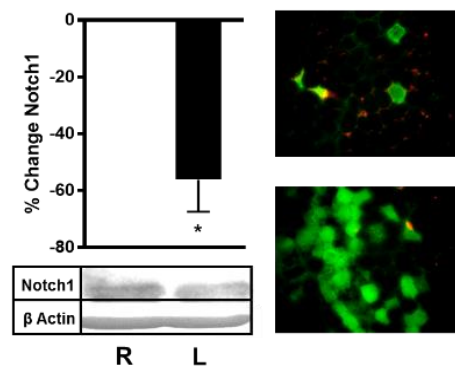


Figure 1.10. Knockdown of Notch1 Receptor. (Left) Percent change in Notch1 protein expression relative to β Actin expression in gastrocnemius muscles injected with lentiviral (LV) green fluorescent protein (GFP) vector (right [R] limb) or LV GFP Notch1shRNA (left [L] limb). (Right) Two representative images from the same left gastrocnemius (LV GFP Notch1shRNA injected) co-stained for GFP/green and Notch1/red. The area lacking LV incorporation shows higher Notch1 compared to the area expressing GFP. * $P < 0.05$ vs. R limb ($n = 4$).

CHAPTER 2: EFFECTS OF NOTCH1 KNOCKDOWN ON SKELETAL MUSCLE REMODELING FOLLOWING DOWNHILL RUNNING

2.1 Introduction

The age-induced loss of skeletal muscle mass (i.e. sarcopenia) and function significantly impedes quality of life of elderly individuals, resulting in heightened susceptibility to injury, morbidity, and mortality [1; 2; 5; 55-59]. The onset of sarcopenic muscle has several prognosticators including anabolic and insulin resistance, mitochondrial dysfunction, elevated pro-inflammatory cytokines, and dysfunctional satellite cell (SC) mediated remodeling of aged muscle upon insult [10; 58; 60-68]. Known interventions are relatively ineffective at combatting the multifaceted development of sarcopenia, however physical activity may provide an inexpensive relief and a practical model to examine sarcopenia, in particular the muscle remodeling response following activity.

Aged skeletal muscle displays an impaired regenerative response following injury, however, a majority of these studies utilize artificial models (such as cardiotoxin injection and freeze injury) to induce extensive muscle injury, while simultaneously ignoring other biological systems which may influence the regenerative response [19; 26; 28; 69-71]. Physiological stimulus models (i.e. aerobic and resistance exercise) are inclusive of other biological systems and are ideal in determining SC dynamics and the regenerative response to insult.

Our laboratory has previously established downhill running (DHR) as an effective model to stimulate and examine the muscle regeneration response [10; 49; 72]. In particular, we have demonstrated that DHR induces changes in key signaling pathways that influence SC fate and subsequent regeneration, including Notch and Wnt. The role of Notch signaling with respect to muscle regeneration remains controversial. With evidence of both inhibitory and stimulatory roles of Notch regulation of muscle regeneration, further research of this fascinating cell to cell communicating pathway is necessary [19; 22; 26; 27; 29; 35; 50; 52].

Interestingly, a majority of the studies examining Notch signaling's role to the regenerative capacity or response to insult of skeletal muscle utilize the artificial models mentioned above. Few studies outside of our lab have utilized physiological models to examine Notch signaling in skeletal muscle [73-78]. Furthermore, manipulation of Notch signaling to examine muscle regeneration following insult is constrained to artificial models. To better understand how Notch impacts muscle regeneration, studies using both physiological models of insult and manipulation (knockdown, knockout, knock-in) of Notch need to be conducted. In the present study we examined the effect of Notch1 knockdown on skeletal muscle remodeling following a bout of DHR. Here we show that reduced Notch signaling elevates muscle regeneration and remodeling.

2.2 Experimental Design and Methods

2.2.1 Experimental Animals

Young (2-4 months) male C57BL/6 mice ($n = 6/\text{group}$, 30 total) were purchased from Charles River Laboratories (Wilmington, MA), randomly allocated into exercising or non-exercising (CT) groups (Figure 2.5.1) and group housed in the vivarium at the

University of North Carolina at Charlotte, an AAALAC accredited facility. The mice were kept on a reverse 12-hour light cycle, with room temperatures set to 18-22°C and relative humidity set at 20-40%. Mice were allowed to consume food and water *ad libitum*. All procedures were approved by the University of North Carolina at Charlotte Animal Care and Use Committee.

2.2.2 Lentiviral Knockdown

Notch1 shRNA (Knockdown) and control (Vector) Lentiviral particles (pLKO.1-puro-CMV-tGFP) were purchased from Sigma (Sigma Mission™ shRNA). Per the manufacturers' recommendation, four separate clones against Notch1 were obtained in order to optimize knockdown. The four clones (GCAGATGATCTTCCCGTACTA; GCCCTTTGAGTCTTCATACAT; GCCAGGTTATGAAGGTGTATA; CCCACATTCCAGAGGCATTTA) were pooled together summing 100,000 transducing units (TUs) (25,000 TUs/clone/injection) and injected (50µls) into the left gastrocnemius on five consecutive days (modified from Carlson et al) [79]. Control (Vector) particles totaling 100,000 TUs were injected (50µls) into the right gastrocnemius on five consecutive days. Injections were administered using a 27-gauge syringe needle and evenly distributed along the longitudinal axis of the gastrocnemius while slowly withdrawing the syringe [80].

2.2.3 Treadmill Familiarization and Downhill Run Exercise Bout

Animals randomly allocated to the exercise groups underwent 5 days of treadmill familiarization (Table 2.6.1) as to optimize exercise behavior for the downhill bout. The exercise bout consisted of running downhill (-15% grade) at a speed of 22 m min⁻¹ (modified from Boppart *et al* 2006 and Tsivitse *et al* 2009) until exhaustion (Columbus

Instruments, 6 lane treadmill, 33 x 50.8 x 50.8cm) [72; 81]. The exercise bout took place on the same day as the last lentiviral injection. Animals were encouraged to run using an electrical shock grid (1.0mA at 163V) and all treadmill exposure was conducted in the dark.

2.2.4 SUnSET Technique and Muscle Tissue Harvesting

Mice were euthanized 24, 48, 72, and 96 hours following the downhill running bout. CT animals were euthanized on the same day as the exercise bout. All animals were fasted 5 hours prior to terminal surgery as to remove any potential feeding influence over MPS. Animals underwent anesthesia with 2-4% inhaled isoflurane supplemented with oxygen. 30 minutes prior to euthanasia and while under anesthesia, mice received an intraperitoneal injection of 0.040 μmol puromycin/g body weight dissolved in PBS [82]. At exactly 30 minutes post-injection, the left (Knockdown) and right (Vector) gastrocnemius muscles were immediately harvested, trimmed of any fat and connective tissue, weighed, and subsequently frozen in one of two fashions: 1) the top third of the muscle was cut and snap frozen in liquid N_2 for western blot analyses. 2) The remaining muscle was frozen in liquid N_2 -chilled isopentane for immunohistochemistry. All samples were stored at -80°C until analyses were performed.

2.2.5 Tissue Homogenization and Protein Concentration Assay

Homogenization was performed as previously described [83]. Briefly, the gastrocnemius muscles were bead blast homogenized (BeadBlasterTM 24 Microtube, Sigma) in 10 volumes of ice-cold Radioimmunoprecipitation assay (RIPA) buffer (sc-24948; Santa Cruz, supplemented with 1% Triton-x, 2% SDS, protease cocktail inhibitor). Bead blast homogenization consisted of two separate rounds of 2-30 second cycles at a speed of 6

meters/second with a 1-minute rest interval between cycles. Samples were removed from the bead blaster, put on ice for 5 minutes, and then underwent the second round of homogenization. Following the second round of homogenization, samples were transferred to a clean ice-cold tube and placed on ice for 30 minutes with periodic vortexing. Protein concentration was determined by Pierce BCA kit (23225; ThermoFisher).

2.2.6 SDS-Page and Western Blotting

30ug of protein/sample was loaded onto a 4-12% Bis-Tris gel (3450125; Bio-Rad) and run (XT MES running buffer; 1610789; Bio-Rad) at 125V for 2 hours. Following electrophoresis, proteins were transferred (Towbin Buffer; 10% methanol) onto a .22uM Polyvinylidene difluoride (PVDF) membrane for 1 hour at 100V. Membranes were washed 1x in Tris-buffered saline (TBS) and blocked for 1 hour in Odyssey blocking buffer 1:1 in TBS. Following blocking, membranes were incubated overnight (16 hours) in primary antibodies (Table 2.6.2). The next day membranes were washed 3 x 5 minutes in TBST (TBS: 0.1% Tween 20) and then incubated in secondary antibodies directed to primary antibodies (1:10,000 in TBST) for 1 hour. Following 3 x 5 minute washes in TBST and 1 x 5 min wash in TBS, membranes were imaged and bands were quantified using the Odyssey® Licor CLx System. Integrated optical density (IOD) was then finalized by normalizing phosphorylated proteins (p-mTORSer 2448) to respective total proteins (total mTOR) and total proteins (Notch1, Hes1, Pax7, MyoD, Myogenin, mTOR, Puromycin) to β -actin.

2.2.7 Immunofluorescent Staining

In preparation for immunofluorescent staining, the gastrocnemius muscle was cross-sectioned at 10- μ m beginning at the mid-belly on a cryostat (Microm HM505E). Upon sectioning, samples were left out to air-dry for 1 hour and then stored in -80°C until staining. Immunofluorescent staining was carried out as previously described in modified fashion [49; 72; 84]. Sections were fixed in 4% paraformaldehyde for 10 minutes, serially washed with phosphate buffered saline (PBS), blocked for endogenous peroxidase activity with 3% hydrogen peroxide in PBS for 7 minutes, and again serially washed in PBS. Epitope retrieval was then performed using sodium citrate (2.94g/L, pH 6.8 in deionized water) at 92°C for 11 minutes. Following epitope retrieval, sections were serially washed in PBS, and underwent a 45-minute blocking step in Mouse-on-Mouse Blocking Reagent (#MKB-2213, Vector laboratories) in PBS and an additional 1-hour blocking step in 1% bovine serum albumin (BSA) in PBS. Primary antibodies for GFP, Laminin, embryonic Myosin Heavy Chain (eMHC), Pax7, MyoD, and Myogenin (in 1% BSA in PBS) (Table 2.6.3) were incubated at room temperature for 1 hour followed by an overnight incubation (16 hours) at 4°C . The next day, signal amplification was performed in order to visualize Pax7, MyoD, and Myogenin. Briefly, sections were serially washed in PBS, incubated with a biotin-conjugated secondary antibody (#115-065-205, Jackson ImmunoResearch) for 70 minutes, serially washed in PBS and incubated in streptavidin-HRP (#B40935, ThermoFisher) for 1 hour all at room temperature. Secondary antibodies (Table 2.6.3) for Laminin, GFP, and eMHC were applied in concert during the streptavidin-HRP incubation as well as 4',6-Diamidino-2-Phenylindole, Dihydrochloride (DAPI: 10nM). TSA-Alexa Fluor 594 (#B40935,

ThermoFisher) was used to visualize antibody binding for Pax7, MyoD, and Myogenin. Sections were again serially washed in PBS and mounted with Vectashield fluorescent mounting media (#H-1000, Vector Labs).

2.2.8 Immunofluorescent Quantification

For immunofluorescence, images were captured as previously done by our lab [49; 72]. Briefly, sections were captured in their entirety with 10x (GFP and eMHC quantification) and 20x (Pax7, MyoD, Myogenin quantification) images using a IX71 inverted fluorescence microscope (Olympus™). For GFP and eMHC, entire cross sections were formulated using Microsoft's Image Composite Editor. Total fiber number as well as GFP+ and eMHC+ fibers were manually counted by 2 blinded individuals using ImageJ software (cell counter plugin). Pax7+ cells were determined using ImageJ software (particle analyzer) excluding Pax7+ staining outside of nuclei. MyoD and Myogenin staining was analyzed using FIJI software (COLOC2) and the Pearson r value was used for data reporting.

2.2.9 Hematoxylin and Eosin Staining and Quantification

Hematoxylin and eosin (H&E) staining was performed for muscle injury and cross-sectional area quantification following Mayer's protocol (Sigma). Muscle sections were imaged in their entirety at 10x under standard light microscopy and images were stitched together using Microsoft's Image Composite Editor. For muscle injury quantification, 2 blinded individuals quantified the number injured fibers (pale cytoplasm, centrally located nuclei, and infiltrated muscle fibers) and total fiber number using ImageJ software (cell counter plugin). 500 random fibers throughout each muscle sample were manually traced using ImageJ software (freehand tool) to determine cross-sectional area.

2.2.10 Statistical Analysis

A two-way analysis of variance was used (Experimental Group x Limb (Knockdown vs Vector), with repeated measures between contralateral limbs). Post-hoc comparisons were accomplished via a Tukey's test, with statistical significance set *a priori* at $p \leq 0.05$. All statistical analyses and graphs were made using Graphpad Prism 7.03 (GraphPad, San Diego, CA, USA). All data are presented as means \pm SD.

2.3 Results

2.3.1 Lentiviral incorporation and knockdown of Notch1 receptor and signaling

Lentiviral percent incorporation as measured by GFP staining was $\sim 20\%$ across all animals with no significant differences in incorporation by limb ($p > 0.05$) or group ($p > 0.05$) (Figure 2.5.2 A&B). There was a main effect in concentration of Notch1 receptor expression ($p \leq 0.05$) with Knockdown reduced compared Vector (Figure 2.5.3).

Additionally, within the 96-hour group Notch1 expression was significantly reduced in Knockdown compared to Vector ($p \leq 0.05$). There was no change in Notch1 expression between experimental groups: CT, 24, 48, 72, 96 ($p > 0.05$). There was also a main effect of Knockdown ($p \leq 0.05$) in Hes1 expression compared to Vector (Figure 2.5.4). Just as in Notch1 expression, there was significant reduction in Hes1 expression within the 96-hour group in Knockdown compared to Vector ($p \leq 0.05$). There were no significant differences in Hes1 expression between experimental groups ($p > 0.05$).

2.3.2 Skeletal muscle injury

Muscle injury of the gastrocnemius quantified via hematoxylin and eosin staining was reduced with Knockdown compared to Vector (main effect; $p \leq 0.05$). There were no significant differences ($p > 0.05$) between or within any of the experimental groups,

although within the 24-hour group Knockdown was trending down compared to Vector ($p = 0.07$).

2.3.3 Pax7 expression

Western blot analysis revealed a significant reduction in Pax7 expression in Knockdown compared to Vector (main effect; $p \leq 0.05$) (Figure 2.5.6) independent of group. Pax7 expression also differed between experimental groups (main effect, $p \leq 0.05$). Within Vector, Pax7 expression was significantly elevated at 96-hours compared to both 24 ($p \leq 0.05$) and 48-hours ($p \leq 0.05$). Within Knockdown, Pax7 expression was significantly elevated at 96-hours compared to 24-hours ($p \leq 0.05$). Immunofluorescence staining demonstrated similar changes in Pax7/Fiber. Pax7/Fiber was significantly reduced in Knockdown (main effect, $p \leq 0.05$) independent of group (Figure 2.5.7). Pax7/Fiber differed significantly between experimental groups (main effect, $p \leq 0.05$). Within Vector, Pax7/Fiber was significantly elevated at 96-hours compared to 24 ($p \leq 0.05$) and 48-hours ($p \leq 0.05$). Within Knockdown, Pax7/Fiber was significantly elevated at 96-hours compared to 24-hours ($p \leq 0.05$).

2.3.4 MyoD expression

MyoD expression (as determined by western blot) was significantly elevated in Knockdown compared to Vector (main effect, $p \leq 0.05$) (Figure 2.5.8). MyoD expression was also significantly increased ($p \leq 0.05$) in Knockdown within the 24-hour group.

There were no significant differences within Vector between any experimental groups ($p > 0.05$). However within Knockdown, MyoD expression at 24-hours was significantly elevated compared to both the 72 ($p \leq 0.05$) and 96-hour ($p \leq 0.05$) group.

Colocalization analysis revealed significant elevations in MyoD+/DAPI+ in Knockdown

compared to Vector (main effect, $p \leq 0.05$) (Figure 2.5.9). There was also a significant elevation in MyoD+/DAPI+ in Knockdown compared to Vector within the 24-hour group. There were no significant differences within the Vector between experimental groups ($p > 0.05$). Within Knockdown, MyoD+/DAPI+ was significantly elevated at 24-hours compared to the 96-hour group ($p \leq 0.05$).

2.3.5 Myogenin expression

Myogenin expression (as determined by western blot) was significantly elevated in Knockdown compared to Vector (main effect, $p \leq 0.05$) (Figure 2.5.10). Within the 24-hour group there was also a significant elevation of Myogenin expression in Knockdown compared to Vector ($p \leq 0.05$). There were no significant differences between experimental groups in either Knockdown or Vector ($p > 0.05$). Colocalization analysis revealed significantly increased Myogenin+/DAPI+ in Knockdown compared to Vector (main effect, $p \leq 0.05$) (Figure 2.5.11). Within the 24-hour group, there was a significant increase of Myogenin+/DAPI+ in Knockdown compared to Vector ($p \leq 0.05$). Within Vector, there was no significant differences between any experimental groups ($p > 0.05$). Within Knockdown, Myogenin+/DAPI+ was significantly elevated at 24-hours compared to CT.

2.3.6 eMHC fibers

eMHC stained fibers were significantly elevated in Knockdown following DHR (interaction, $p \leq 0.05$) (Figure 2.5.12). Within the 96-hour group there was a significant increase in the percentage of eMHC fibers in Knockdown compared to Vector ($p \leq 0.05$). There were no differences in the percentage of eMHC fibers between experimental groups within Vector ($p > 0.05$). Within Knockdown, the percentage of eMHC fibers

was significantly elevated in the 96-hour group compared to both CT ($p \leq 0.05$) and 24-hours ($p \leq 0.05$).

2.3.7 Muscle wet weight and cross-sectional area

There was no significant difference in muscle wet weight in Knockdown compared to Vector ($p > 0.05$) (Table 2.6.4). Interestingly, there was a significant difference between experimental groups (main effect, $p \leq 0.05$). Within Vector, muscle wet weight was elevated 24-hours following DHR compared to the 72 ($p \leq 0.05$) and 96-hour ($p \leq 0.05$) groups. Within Knockdown, muscle wet weight was elevated in the control group compared to 96-hours following DHR ($p \leq 0.05$). There were no significant differences ($p > 0.05$) in cross-sectional area (CSA) frequency distribution between Knockdown and Vector within in any of the experimental groups (Figure 2.5.13A-E). Similar to muscle wet weight, average CSA was elevated within Vector at 24-hours compared to 96-hours ($p \leq 0.05$; Figure 2.5.14). There were no other significant differences ($p > 0.05$) in average CSA, however within Vector, 24-hour vs 72-hour was trending ($p = 0.09$). Additionally within Knockdown, 24-hour vs 96-hour was trending ($p = 0.08$).

2.3.8 Phosphorylation and total mTOR expression

Phosphorylation of mTOR on Ser 2448 was significantly elevated in Knockdown compared to Vector (main effect, $p \leq 0.05$) independent of experimental group (Figure 2.5.15A). Phosphorylation on Ser2448 did not differ between experimental groups ($p > 0.05$). Total mTOR expression did not differ between Knockdown and Vector or between experimental groups ($p > 0.05$) (Figure 2.5.15B).

2.3.9 Mixed muscle protein synthesis

Mixed MPS was determined using the non-radioactive SUnSET method as indicated above [82; 85]. MPS was significantly increased in Knockdown compared Vector (main effect, $p \leq 0.05$) (Figure 2.5.16). Additionally, Knockdown increased MPS within both the CT ($p \leq 0.05$) and 72- hour groups ($p \leq 0.05$). There was no significant difference in MPS between experimental groups ($p > 0.05$).

2.4 Discussion and Conclusion

Notch signaling has been widely characterized during skeletal muscle regeneration, however, most of these studies have neglected to use physiological models [19; 26-28]. Additionally, of the studies in which physiological models were employed, none have yet to manipulate Notch signaling in order to examine its impact of muscle remodeling [73-78]. In this study, using both manipulation of Notch signaling and a physiological model, we demonstrated that knockdown of Notch1 elevates skeletal muscle regeneration, remodeling, and MPS.

Upon insult, skeletal muscle undergoes a tightly regulated and dynamic remodeling response which is tied directly to the function of SCs. In young healthy muscle, SCs will activate upon injury, and choose a fate of proliferating myoblasts. Myoblasts will then begin to differentiate (termed myocytes), ultimately aligning and fusing together to form immature muscle fibers (termed myotubes). These myotubes will ultimately mature into myofibers, thus resolving the remodeling response [59; 86]. At the forefront of the regenerative response is Notch, a widely studied, yet controversial signaling pathway whose regenerative role requires further interrogation.

Notch signaling occurs when one of its transmembrane receptors (Notch1-4) binds to a ligand (Delta-like protein (DLL) 1, DLL 3, DLL4, Jagged1, and Jagged2) on an adjacent cell. The receptor-ligand interface initiates a series of cleavages by metalloproteinases and γ -secretases, thereby releasing Notch intracellular domain (NICD). NICD canonically translocates to the nucleus where it will induce expression of target genes including Hes1, hairy/enhancer-of-split related with YRPW motif protein 1 (Hey1), and avian myelocytomatosis viral oncogene homolog (Myc) [10; 22]. In the present study our model was sufficient to reduce both the Notch1 receptor as well as Hes1 expression indicating a reduction in Notch signaling (Figures 2.5.3 & 2.5.4).

The early studies examining Notch in skeletal muscle demonstrated its extreme importance in regulating the early stages of myogenesis thereby determining the outcome of regeneration. In particular, inhibition of Notch signaling in young muscle was shown to impair regeneration while activation of Notch signaling in aged muscle was shown to rescue regeneration [26; 27]. In fact, our lab has unpublished preliminary data (Figure 1.4, Chapter 1) demonstrating that Notch inhibition reduces MyoD expression 96-hours following DHR in aged mice, which was foundational to our hypothesis that Notch1 knockdown would abrogate muscle regeneration following DHR. In contrast to the earlier findings, and in opposition to our hypothesis, the present study shows that Notch1 knockdown elevates muscle regeneration following DHR. The differing overall impact could be due in part to a variety of factors including: model of insult, mode of Notch manipulation, and timepoint of measurement.

Essentially all of the early studies examining the effects of Notch on skeletal muscle used artificial modalities to stimulate the regenerative response including

cardiotoxin injection, needle injury, and freeze injury [26-28]. Though these models are a good means of administering injury, they lack the physiological inclusiveness of using exercise. Skeletal muscle is often viewed solely as a locomotive organ system, however, in recent years it has been demonstrated that skeletal muscle also serves as a prominent secretory organ. Furthermore, the secretory functions of skeletal muscle appear to be either enhanced in response to exercise or are exercise (i.e. contraction) dependent [87-89]. The molecules secreted from skeletal muscle, termed myokines, are efficacious in the treatment and prevention of a wide variety of diseases, including the regeneration response. Some of the myokines impacting regeneration that are secreted with exercise include interleukin-15 (IL-15), leukemia inhibitory factor (LIF), brain-derived neurotrophic factor (BDNF), and Irisin [90-98]. Irisin has been identified as a myokine that stimulates SC activation, while LIF promotes proliferation of activated SCs [99-104]. IL-15 stimulates and elevates differentiation of myogenic cells while knockout of BDNF delays the myogenic response [105-107]. Notch down regulation is required for SC activation so it is entirely possible that these pro-myogenic myokines are working in concert with Notch1 knockdown to elevate the regeneration response. In absence of exercise and without the secretion of myokines, it is possible that inhibition of Notch signaling leads to aggressive pre-mature differentiation of myogenic cells and ultimately an impaired regeneration response.

Another contributor to the controversy of Notch with respect to regeneration is the way in which Notch is manipulated, particularly via the use of γ -secretase inhibitors (GSIs). As mentioned above, the release of NICD (the active component of the Notch receptor) is mediated by a series of cleavages including the terminal γ -secretase cleavage

site. Treatment with GSIs have demonstrated to lower Notch signaling, including work from our own lab (Chapter 3). Furthermore, use of GSI treatment has shown to impair the regenerative response, opposing our current finding that Notch1 knockdown elevates regeneration (Figures 2.5.8-2.5.12) [28]. However, GSI treatment is not specific to a particular Notch receptor, and as mentioned already there are 4 Notch receptors, three of which are expressed on SCs [27; 108; 109]. It has recently been revealed that the different Notch receptors may have distinct roles within skeletal muscle. For example Notch1 overexpression and deletion of Notch3 both lead to an increase in quiescent SCs demonstrating that Notch receptors may have differing roles on SC fate [29; 110]. In contrast, others have demonstrated comparable roles for Notch1 and Notch3. In particular when activated by DLL4, Notch3 may promote SC quiescence [111]. If this is the case, it sheds light that specific ligand-receptor interactions may have differing effects on SC fate, further complicating the issue. More recently, it was demonstrated that Notch1 and Notch2 may be required for successful coordination of SC self-renewal. Furthermore, this same study demonstrated that knockout of both Notch1 and Notch2 completely ablated the regenerative response, a similar result seen in the earlier studies using GSIs [112]. In the studies using GSIs it is likely that the disruption of regeneration response was due to global muscle reductions in the Notch1, Notch2, and Notch3 receptors. It is possible that just knocking down the Notch1 receptor is sufficient to elevate the regeneration response without derailing proper SC dynamics following insult.

Given the temporal dynamics of SCs during regeneration and the myriad of cell surface markers that provide information on SC fate, measurement time of MRFs appears to be critical. In our own preliminary data we found reductions of MyoD+ Nuclei in aged

mice 96hours following DHR with exposure to GSI treatment (Figure 1.4). Though GSI treatment has shown to impair regeneration, it is possible that MyoD expression would have been elevated in response to GSI treatment at an earlier time point (24hr, 48hr, 72hr) following DHR similar to our studies present findings of elevated MyoD in the Notch1 knockdown limb 24 hours after DHR (Figure 2.5.8 & 2.5.9). The timing of the Notch manipulation itself also appears to have an impact to the regenerative outcome. In the earlier studies, Notch manipulation was implemented days following injury, disrupting and impairing the regenerative response [26; 28]. This is also true of our preliminary data in which GSI was administered days following DHR. In the present study, Notch1 knockdown was performed prior to the exercise bout. It is possible that this method of Notch manipulation pre-activated and readied SCs for a more robust regenerative response. Additionally, though the studies examining regeneration with Notch manipulation have examined some MRFs *in vitro*, they have done a poor job characterizing MRFs within their *in vivo* work. To our knowledge this is the only study to characterize a multitude of MRFs over the course of four days using Notch manipulation. As previously mentioned this is also the only study to our knowledge in which a physiological model of insult is used in conjunction with Notch manipulation.

SCs are tightly regulated muscle stem cells, whose fate can be identified by expression several MRFs including paired box 7 (Pax7) and MyoD. MyoD is pivotal MRF which can provide insight along with Pax7 on the state and fate of a SC. More specifically, Pax7+/MyoD- represent quiescent SCs, Pax7+/MyoD+ activated SCs and Pax7-/MyoD+ cells that are committed to differentiation and subsequent myofiber contribution [113-116]. Notch has previously been shown to positively regulate Pax7

and thus maintain SC quiescence, likely through the interaction of NICD with RBPJ, which binds upstream of Pax7 [29]. Furthermore, overexpressed NICD also leads to dedifferentiation of late stage myocytes back to their quiescent state [54]. Our findings support the notion that Notch positively regulates Pax7 expression as the Notch1 knockdown displayed reduced Pax7 protein expression and a reduced number of Pax7+ cells per fiber (Figure 2.5.6 & 2.5.7). Interestingly, the SC pool is maintained in the co-presence of NICD activation and Pax7 deletion indicating that Notch may also function independently of Pax7 [117]. In recent years, PW1+ interstitial cells (PICs) have been identified as muscle resident stem cells. PICs do not express Pax7, and interestingly in Pax7 knockout mice, the number of PICs increases [118; 119]. Given the regulatory role of Notch over Pax7 and its ability to maintain the SC pool in the absence of Pax7, it is possible that Notch may also regulate the SC pool and muscle regeneration via PICs. It is important to note that the maintained SCs with Notch activation and Pax7 depletion are unable to increase MyoD expression [117]. This is concert with several other findings that over expression of Notch signaling prevents myogenic progression, particularly differentiation. In particular, NICD has shown to repress MyoD in both frog and chick embryos, as well as C2C12 cells [120-122]. In support of this, here we show that knockdown of Notch1 elevates MyoD expression and MyoD:DAPI 24hrs following DHR (Figure 2.5.8 & 2.5.9). These findings fall in line with data indicating that nearly all SCs express MyoD (activated) 24hrs following an adequate stimulus [123]. In this particular case Notch1 knockdown was an adequate stimulus. Despite this, the exact mechanism by which Notch acts to prevent regeneration (or by which Notch inhibition elevates regeneration) needs to be better defined as several Notch targets (including Hes1, Hey1,

Musculin (MyoR)) inhibit the regenerative response [35; 36]. Interestingly, DHR itself was not sufficient to increase MyoD expression or MyoD:DAPI (Figure 2.5.8 & 2.5.9). This finding is in concert with previous research conducted in rats following DHR in which MyoD + cells were unchanged with exercise [124; 125]. It appears that Notch knockdown primes SCs for activation following an exercise bout leading to a heightened regenerative response. Resistance exercise, unlike DHR is sufficient to increase MyoD protein expression in rats [126]. It would be interesting to apply this Notch1 knockdown approach in conjunction with resistance exercise to determine if there is a positive impact on MyoD expression.

As mentioned above, there are several MRFs that are expressed throughout the regeneration process. A majority of the research investigating Notch signaling's role to the regenerative response focus on the previously discussed surface markers, Pax7 and MyoD. This is likely due to extreme importance that Notch has in regulating SC self-renewal and fate. However, Pax7 and MyoD only tell half of the regenerative story. In order to obtain a full regeneration picture it is imperative to measure MRFs that are expressed in the later stages of myogenesis (late differentiation and myotube formation) including Myogenin and myosin heavy chain (MHC), particularly embryonic MHC (eMHC). As was discussed previously, a majority of studies neglect to measure multiple MRFs throughout the regenerative response, particularly within their respective *in vivo* models. In fact, to our knowledge none of the previously discussed studies measured the late MRFs myogenic or eMHC following Notch manipulation [19; 26; 28; 77; 111; 112]. This is likely a result of the assumption that there is subsequent upregulation of Myogenin and fiber formation following MyoD expression [127; 128]. The present

findings reveal an elevation in Myogenin expression and Myogenin:DAPI 24hrs following DHR with Notch1 knockdown (Figure 2.5.10 & 2.5.11). Given the elevation we saw in MyoD in the knockdown hindlimb, it was expected that Myogenin would too be elevated. However, the timing of the Myogenin increase is interesting. Regeneration is known to be a temporal process with elevation of MyoD followed by elevation of Myogenin [129]. However in this case we saw co-elevation of MyoD and Myogenin simultaneously at 24hr following DHR, likely do to pre-mature differentiation of SC in the knockdown hindlimb [122; 130; 131]. Resolving the heightened regenerative response in the knockdown limb, there was elevated eMHC+ fiber % 96hrs following DHR (Figure 2.5.12). Several *in vitro* studies have shown elevations in MHC expression and increased myotube formation attributed to Notch inhibition [24; 127], including work out of our own lab (Figure 1.6). Moreover, in recent years Notch has resurfaced as a negative regulator of regeneration with *in vivo* studies showing increased regenerative capacity attributed to lowered Notch signaling [23; 132; 133]. However, none of these studies were examining regeneration or Notch signaling following physiological stimuli. Furthermore, none of these studies utilized eMHC staining as a regeneration measurement.

Since Notch has been identified as a negative regulator of regeneration and myotube formation (whereby reduced Notch signaling elevates regeneration and myotube formation) it is reasonable to assume that Notch may also serve as a regulator of muscle hypertrophy in adult skeletal muscle. In fact, several studies have implicated Notch as a mediator of muscle size. For example deletion of Protein O-fucosyltransferase1 (Pofut1), which is necessary for regular Notch activation, leads to reduced Notch signaling and

muscle hypertrophy [23]. Moreover, in instances of cachexia Notch signaling has been identified as a mediator of cachexic (atrophic) muscle which can be resolved by GSI treatment [48]. Our present study did not align with these previous findings as we saw no change in either muscle wet weight (Table 2.6.4) or CSA (2.5.13 A-E) with knockdown of Notch1. Recent *in vitro* findings demonstrated that GSI treatment elevated myotube hypertrophy but specific reductions of Notch1 did not [136]. With implications that Notch may regulate hypertrophy, but confounding results indicating that Notch1 on its own does not, it is plausible that Notch receptors coordinate together to mediate hypertrophy just as they have been implicated in SC self-renewal [112]. This would better explain the phenotype changes seen with the differing modes of Notch manipulation. There were differences in muscle weight and average CSA following DHR independent of hindlimb. For example, within Vector wet weight was increased at 24hrs compared to 72 and 96hrs (Table 2.6.4). Additionally, average CSA was elevated at 24hrs compared to 96hrs within Vector (Figure 2.5.14). These increases (wet weight and CSA) are likely due to inflammation that would normally follow a bout of exercise. Interestingly, the only difference within the knockdown hindlimb was between the non-exercising group (CT) and 96hr post-DHR, likely due to inflammation stemming from the intramuscular injections. In response to exercise, it is possible that Notch1 knockdown serves a protective effect against inflammation. Recently, Notch has shown to mediate inflammation in a positive fashion (whereby reducing Notch has lowered inflammation and improved wound healing/repair) in models of diabetes, liver inflammation and angiogenesis [137-141].

In line with this notion is the fact that Notch1 knockdown appeared to have a protective effect on skeletal muscle injury compared to Vector (Figure 2.5.5). Interestingly, DHR was not sufficient to induce muscle injury compared to CT mice. This differs from our lab's previous work demonstrating that DHR is a sufficient model to increase muscle injury in young mice compared to non-exercising mice [49; 72]. The likely rationale for this difference is the incorporation of intramuscular injections, or needle induced injury. The muscle injury from the injections likely diluted out the difference of DHR induced injury. In our prior work, DHR led to approximately a 1-2% increase in muscle injury compared to non-exercising mice (~0.3% injury). In the present study, CT-Vector mice had an average injury of 5.7% and by 48 hours it increased to 8.8%. The 3% increase observed in the present study, though not significant, is larger than we have previously seen. It would be interesting to conditionally knockdown Notch1, thereby removing any influence of injection-induced muscle injury and study the injury and repair response following DHR. Moreover, given the apparent protective effect Notch1 knockdown has on injury (and possibly inflammation) it would be interesting to examine any changes in immune cells.

In contrast to the lack of change in hypertrophy (muscle wet weight/CSA), we did see an increase in MPS as measured by puromycin incorporation into muscle (Figure 2.5.16). This is in concert with our preliminary *in vitro* findings showing that Notch inhibition elevates MPS in C2C12 myoblasts (Figure 1.8). To our knowledge no other studies have examined the regulation of MPS by Notch signaling either *in vitro* or *in vivo*. With the observed increase in MPS it is interesting that we did not observe any changes in hypertrophy. However, this is likely due to both the model and the timeframe.

Though a bout of exercise has the capacity to stimulate MPS, the stimulus it provides does not compare to other models used to induce growth. Models such as synergistic ablation, tenotomy, stretch hypertrophy, and unloading are able to simulate significant muscle growth [84; 142-147]. Prolonged treadmill training has shown to elevate skeletal muscle mass, however in the present study only an acute bout was used [146].

Additionally, in most of the studies just referenced the time at which hypertrophy occurs is outside the timeframe of the current study. For example, peak hypertrophy with ablation models of overload occurs between 12 and 15 days, whereby stretch hypertrophy peaks at 7 days [146; 148]. It is plausible that we would have seen indices of hypertrophy had the timeline of the study been carried out longer. In conjunction with the increase in MPS, we also observed an effect of Notch1 knockdown on phosphorylation of mTOR at Ser 2448 with no changes seen in total mTOR protein concentration (Figures 2.5.15A&B). This is in concert with our preliminary findings that Notch inhibition leads to elevations in mTOR phosphorylation in both C2C12 myoblasts and myotubes (Figures 1.7 & 1.9). Despite contrasting roles of Notch and mTOR on muscle regeneration few studies have examined potential cross-talk or interaction of these two signaling pathways [32; 34; 37]. Some studies have recently shown possible links between the two pathways in particular PTEN and LKB1 (negative upstream regulators of mTOR) [149; 150], however studies have not examined the effects of Notch on mTOR.

In summary, we have demonstrated that Notch1 knockdown elevates the early (MyoD) and late (Myogenin and eMHC) MRFs of the regenerative response in skeletal muscle. The elevations seen in regeneration may be due to summation of exercise and

Notch1 knockdown. Despite increasing MPS and phosphorylation of mTOR, Notch1 knockdown failed to induce indices of muscle hypertrophy, though this is likely due to the model used as well as the timeframe of the study. Overall, these results indicate that Notch has a braking effect on skeletal muscle regeneration and MPS. Alleviating the braking effect of Notch may serve as a therapeutic approach to combatting muscle wasting conditions. These findings warrant further investigation to the impact that Notch signaling has on skeletal muscle regeneration and growth within exercise models.

2.5 Figures

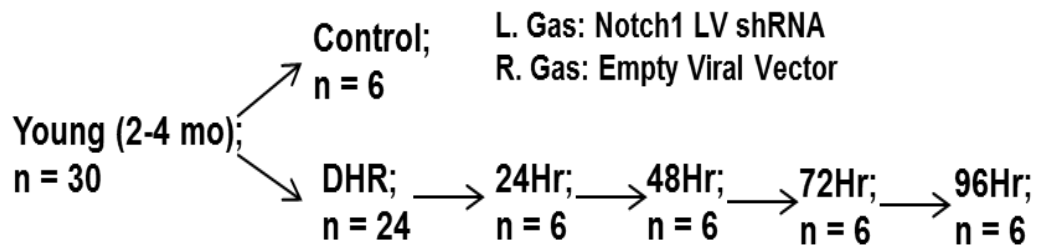


Figure 2.5.1. Experimental Design of Young Mice (n = 30). Left (L) gastrocnemius (Gas) of all mice was injected with Lentiviral (LV) shRNA against Notch1 (Knockdown) while the right (R) Gas was injected with an empty LV vector. Injections were administered on 5 consecutive days. Control mice simulated a sedentary lifestyle. On the last day of LV injections exercising mice underwent downhill running (DHR) to induce insult and study the subsequent regeneration response.

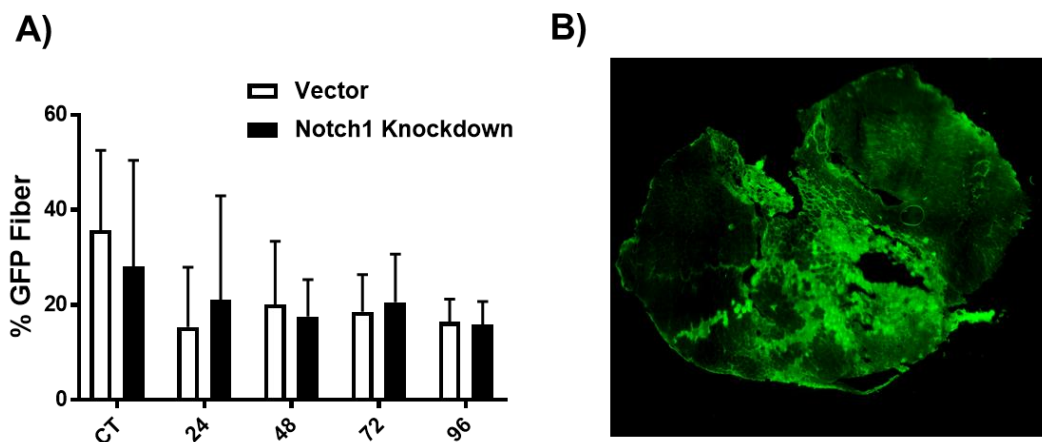


Figure 2.5.2. Lentiviral Incorporation. A) Gastrocnemius (GAS) green fluorescent protein (GFP) percentage of total fiber number in young (2-4 mo.) C57BL/6 mice injected with shRNA against Notch1 (Notch1 knockdown) or an empty vector (Vector) on 5 consecutive days in the left and right GAS, respectively. On day 5 of injection, animals were either euthanized (CT) or underwent a bout of downhill running (DHR) to exhaustion and were subsequently euthanized over the next 4 days (24hr, 48hr, 72hr, 96hr). 30 minutes prior to tissue harvest, all animals received 0.040 μmol puromycin/g body weight. B) Representative image (stitched from 10x images) of GFP stained GAS from 24hr Notch1 knockdown limb. Data were analyzed using a two-way repeated measures ANOVA ($n = 6$ per group). Data are mean \pm SD.

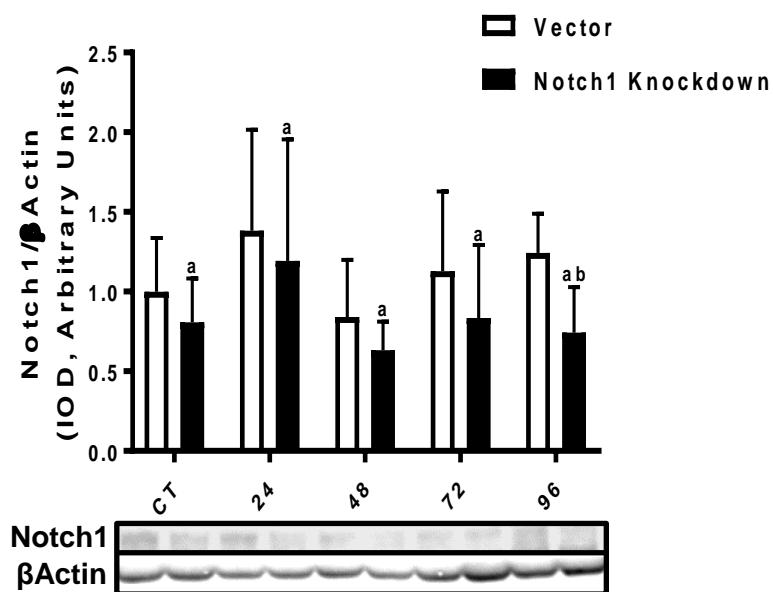


Figure 2.5.3. Notch1 Expression in Gastrocnemius Muscle. Gastrocnemius (GAS) Notch1/ β -Actin expression (Integrated optical density, IOD) in young (2-4 mo.) C57BL/6 mice injected with shRNA against Notch1 (Notch1 knockdown) or an empty vector (Vector) on 5 consecutive days in the left and right GAS, respectively. On day 5 of injection, animals were either euthanized (CT) or underwent a bout of downhill running (DHR) to exhaustion and were subsequently euthanized over the next 4 days (24hr, 48hr, 72hr, 96hr). 30 minutes prior to tissue harvest, all animals received 0.040 μ mol puromycin/g body weight. Data were analyzed using a two-way repeated measures ANOVA. a: significant ($p \leq 0.05$) main effect of limb; b: significantly different within timepoint ($n = 6$ per group). Data are mean \pm SD.

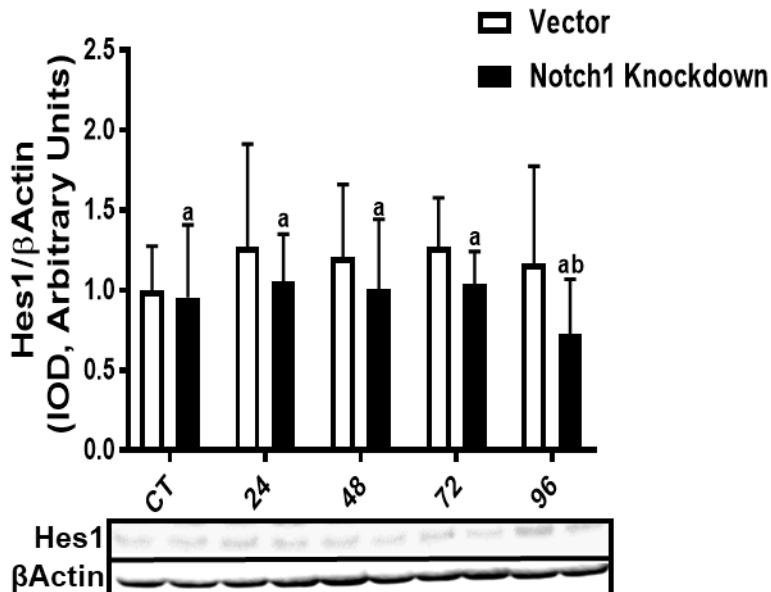


Figure 2.5.4. Hes1 Expression in Gastrocnemius Muscle. Gastrocnemius (GAS) hairy/enhancer of split-1 (Hes1)/ β -Actin expression (Integrated optical density, IOD) in young (2-4 mo.) C57BL/6 mice injected with shRNA against Notch1 (Notch1 knockdown) or an empty vector (Vector) on 5 consecutive days in the left and right GAS, respectively. On day 5 of injection, animals were either euthanized (CT) or underwent a bout of downhill running (DHR) to exhaustion and were subsequently euthanized over the next 4 days (24hr, 48hr, 72hr, 96hr). 30 minutes prior to tissue harvest, all animals received 0.040 μ mol puromycin/g body weight. Data were analyzed using a two-way repeated measures ANOVA. a: significant ($p \leq 0.05$) main effect of limb; b: significantly different within timepoint ($n = 6$ per group). Data are mean \pm SD.

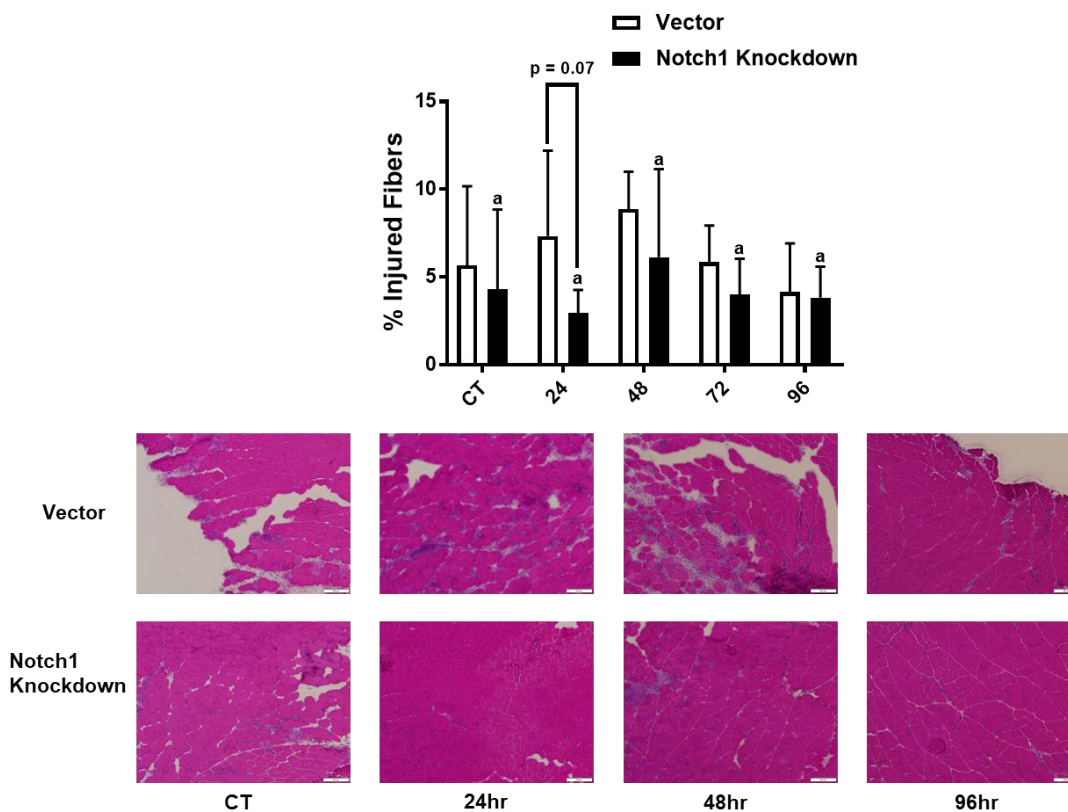


Figure 2.5.5. Muscle Injury in Gastrocnemius. Gastrocnemius (GAS) muscle injury percentage in young (2-4 mo.) C57BL/6 mice injected with shRNA against Notch1 (Notch1 knockdown) or an empty vector (Vector) on 5 consecutive days in the left and right GAS, respectively. On day 5 of injection, animals were either euthanized (CT) or underwent a bout of downhill running (DHR) to exhaustion and were subsequently euthanized over the next 4 days (24hr, 48hr, 72hr, 96hr). 30 minutes prior to tissue harvest, all animals received 0.040 μmol puromycin/g body weight. Representative hematoxylin and eosin images are taken at 10x. Data were analyzed using a two-way repeated measures ANOVA. a: significant ($p \leq 0.05$) main effect of limb ($n = 6$ per group). Data are mean \pm SD.

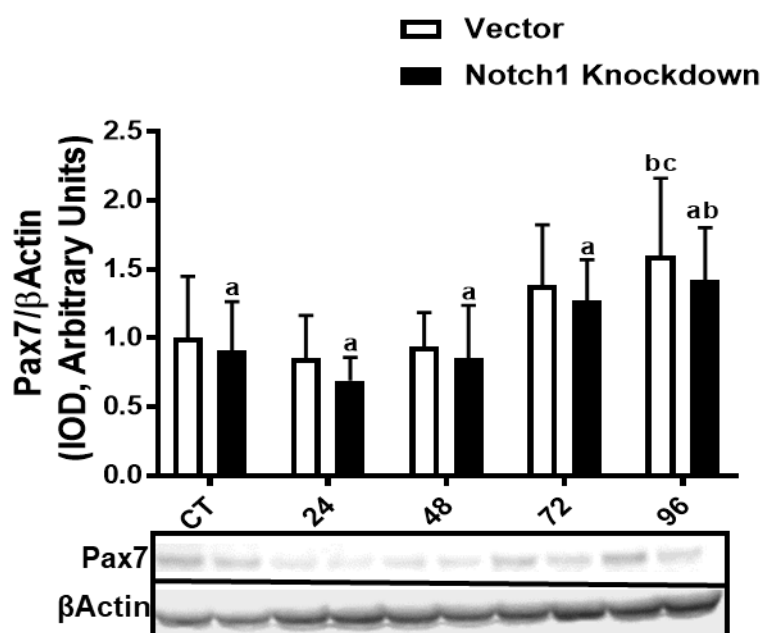


Figure 2.5.6. Pax7 expression in gastrocnemius muscle. Gastrocnemius (GAS) paired box 7 (Pax7)/ β -Actin expression (Integrated optical density, IOD) in young (2-4 mo.) C57BL/6 mice injected with shRNA against Notch1 (Notch1 knockdown) or an empty vector (Vector) on 5 consecutive days in the left and right GAS, respectively. On day 5 of injection, animals were either euthanized (CT) or underwent a bout of downhill running (DHR) to exhaustion and were subsequently euthanized over the next 4 days (24hr, 48hr, 72hr, 96hr). 30 minutes prior to tissue harvest, all animals received 0.040 μ mol puromycin/g body weight. Data were analyzed using a two-way repeated measures ANOVA. a: significant ($p \leq 0.05$) main effect of limb; b: significantly different within limb from 24; c: significantly different within limb from 48 ($n = 6$ per group). Data are mean \pm SD.

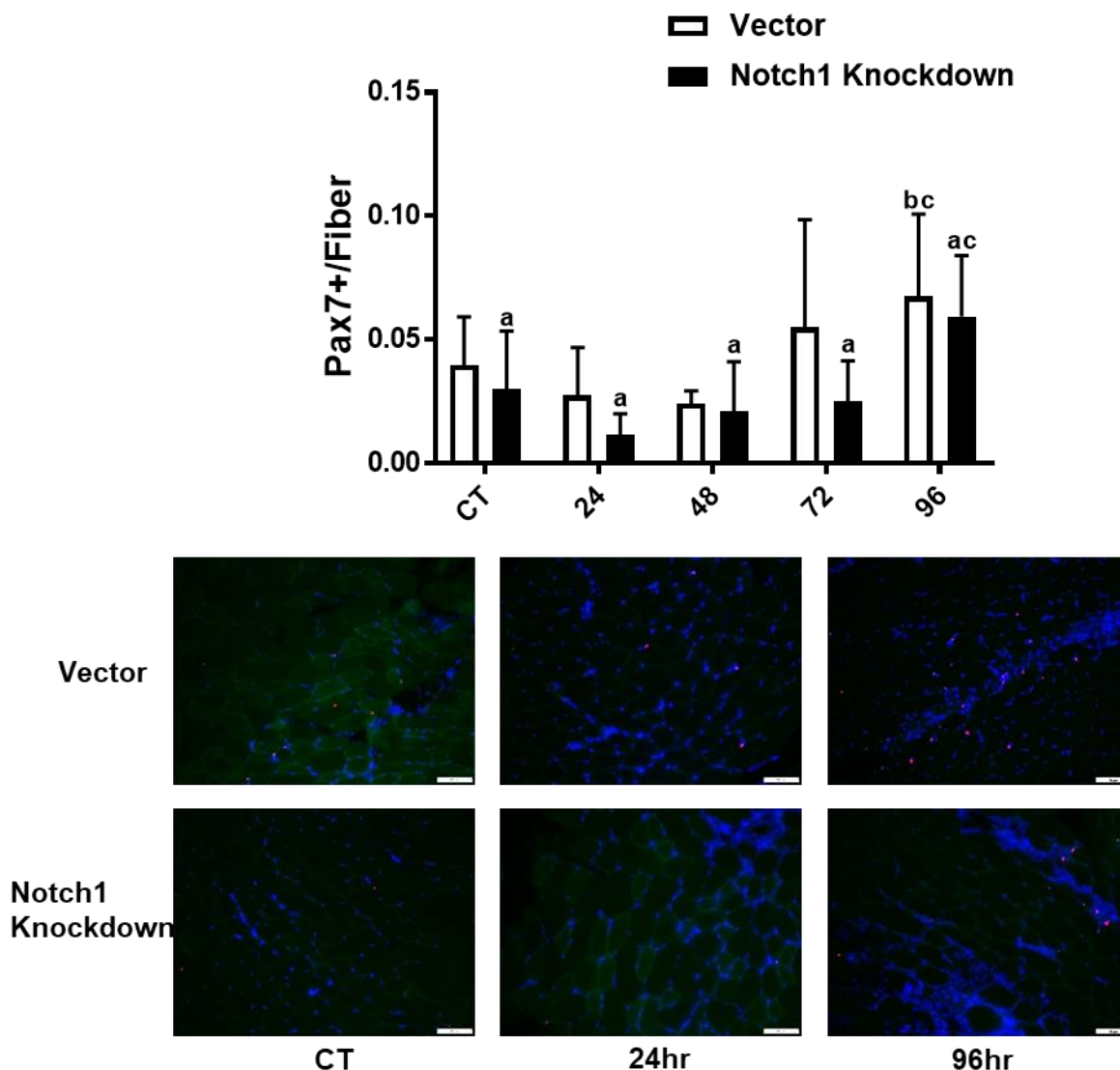


Figure 2.5.7. Pax7/fiber in Gastrocnemius Muscle. Gastrocnemius (GAS) paired box 7 (Pax7) + cells per fiber in young (2-4 mo.) C57BL/6 mice injected with shRNA against Notch1 (Notch1 knockdown) or an empty vector (Vector) on 5 consecutive days in the left and right GAS, respectively. On day 5 of injection, animals were either euthanized (CT) or underwent a bout of downhill running (DHR) to exhaustion and were subsequently euthanized over the next 4 days (24hr, 48hr, 72hr, 96hr). 30 minutes prior to tissue harvest, all animals received 0.040 μ mol puromycin/g body weight. Representative images are taken at 20x: Blue- 4',6-Diamidino-2-Phenylindole, Dihydrochloride (DAPI); Green-Laminin; Red-Pax7. Data were analyzed using a two-way repeated measures ANOVA. a: significant ($p \leq 0.05$) main effect of limb; b: significantly different within limb from 24; c: significantly different within limb from 48 (n = 6 per group). Data are mean \pm SD.

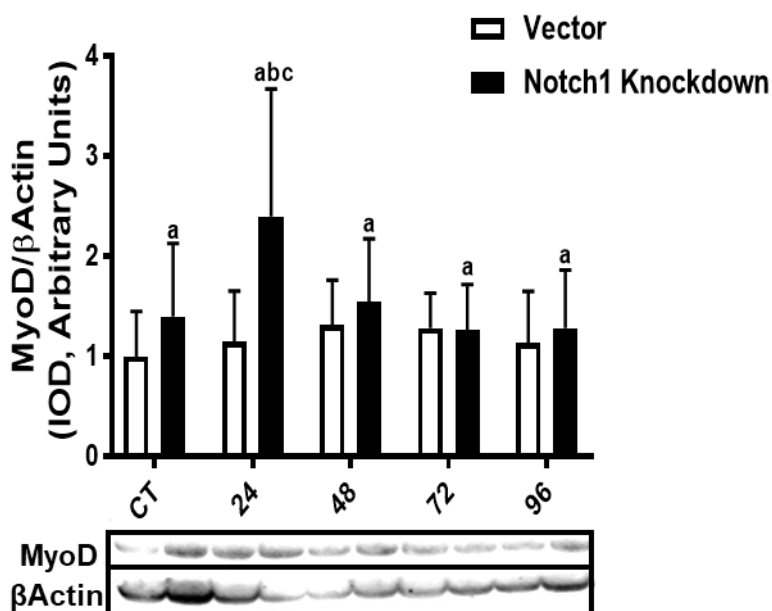


Figure 2.5.8. MyoD expression in gastrocnemius muscle. Gastrocnemius (GAS) myogenic differentiation 1 (MyoD)/ β -Actin expression (Integrated optical density, IOD) in young (2-4 mo.) C57BL/6 mice injected with shRNA against Notch1 (Notch1 knockdown) or an empty vector (Vector) on 5 consecutive days in the left and right GAS, respectively. On day 5 of injection, animals were either euthanized (CT) or underwent a bout of downhill running (DHR) to exhaustion and were subsequently euthanized over the next 4 days (24hr, 48hr, 72hr, 96hr). 30 minutes prior to tissue harvest, all animals received 0.040 μ mol puromycin/g body weight. Data were analyzed using a two-way repeated measures ANOVA. a: significant ($p \leq 0.05$) main effect of limb; b: significantly different within timepoint; c: significantly different within limb from 72 and 96 ($n = 6$ per group). Data are mean \pm SD.

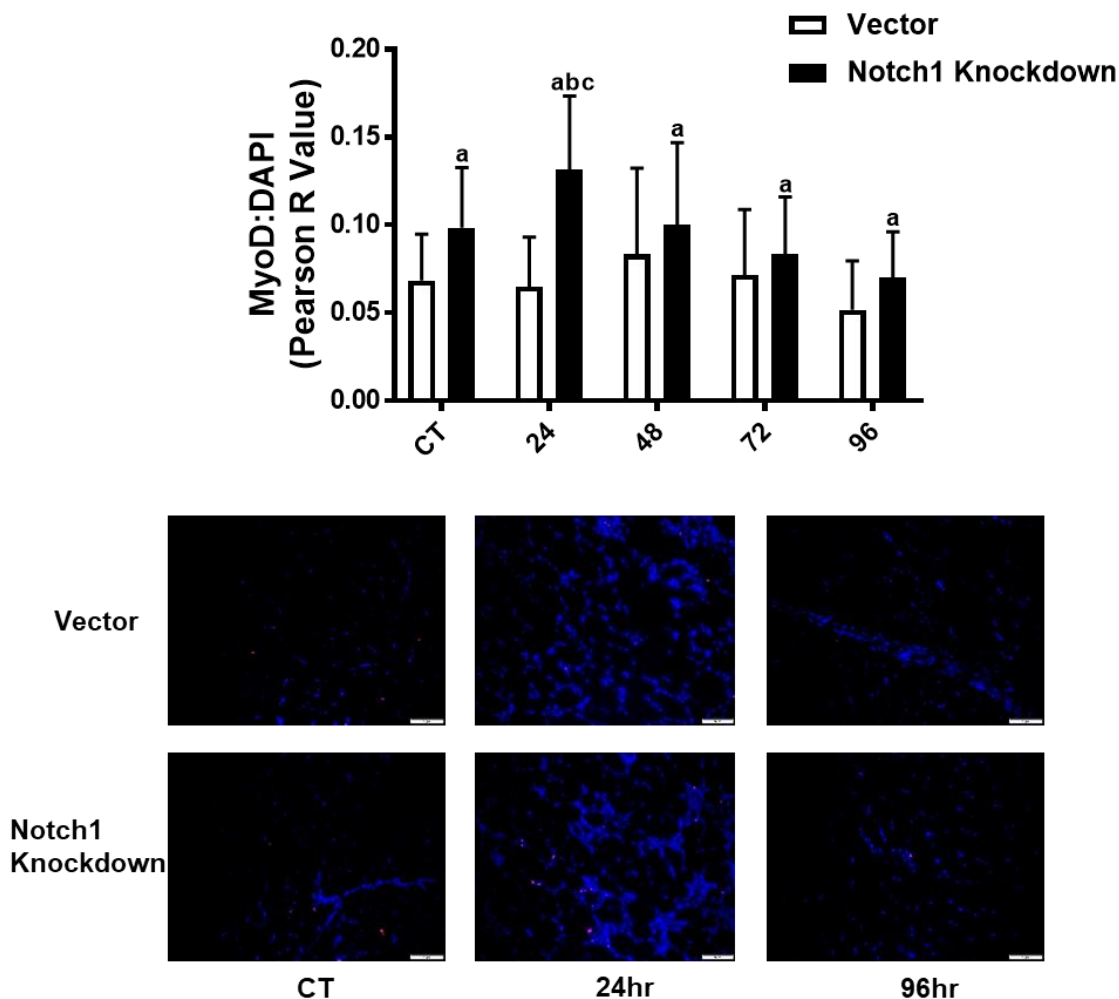


Figure 2.5.9. MyoD+/DAPI+ Colocalization in Gastrocnemius Muscle.

Gastrocnemius (GAS) myogenic differentiation 1 (MyoD): 4',6-Diamidino-2-Phenylindole, Dihydrochloride (DAPI) colocalization in young (2-4 mo.) C57BL/6 mice injected with shRNA against Notch1 (Notch1 knockdown) or an empty vector (Vector) on 5 consecutive days in the left and right GAS, respectively. On day 5 of injection, animals were either euthanized (CT) or underwent a bout of downhill running (DHR) to exhaustion and were subsequently euthanized over the next 4 days (24hr, 48hr, 72hr, 96hr). 30 minutes prior to tissue harvest, all animals received 0.040 μmol puromycin/g body weight. Representative images are taken at 20x: Blue-DAPI; Green-Laminin; Red-MyoD. Data were analyzed using a two-way repeated measures ANOVA. a: significant ($p \leq 0.05$) main effect of limb; b: significantly different within timepoint; c: significantly different within limb from 96 ($n = 6$ per group). Data are mean \pm SD.

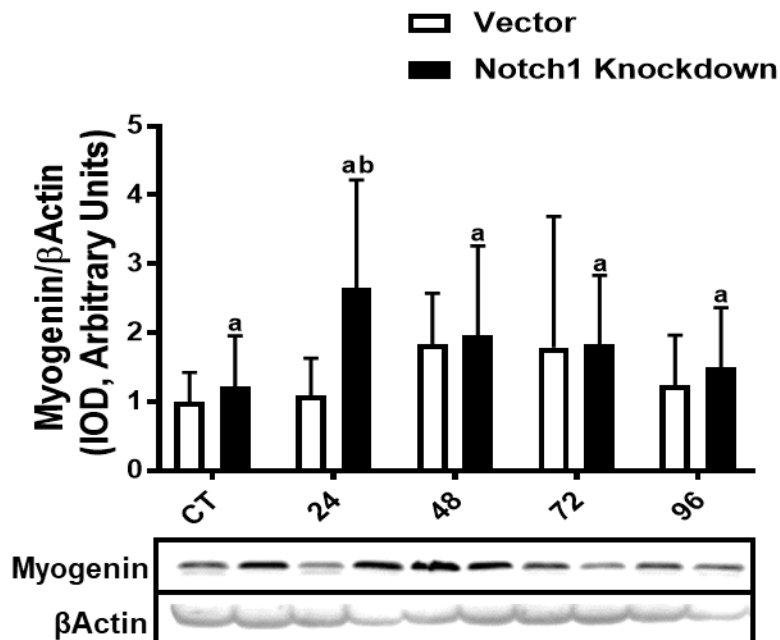


Figure 2.5.10. Myogenin Expression in Gastrocnemius Muscle. Gastrocnemius (GAS) Myogenin/ β -Actin expression (Integrated optical density, IOD) in young (2-4 mo.) C57BL/6 mice injected with shRNA against Notch1 (Notch1 knockdown) or an empty vector (Vector) on 5 consecutive days in the left and right GAS, respectively. On day 5 of injection, animals were either euthanized (CT) or underwent a bout of downhill running (DHR) to exhaustion and were subsequently euthanized over the next 4 days (24hr, 48hr, 72hr, 96hr). 30 minutes prior to tissue harvest, all animals received 0.040 μ mol puromycin/g body weight. Data were analyzed using a two-way repeated measures ANOVA. a: significant ($p \leq 0.05$) main effect of limb; b: significantly different within timepoint ($n = 6$ per group). Data are mean \pm SD.

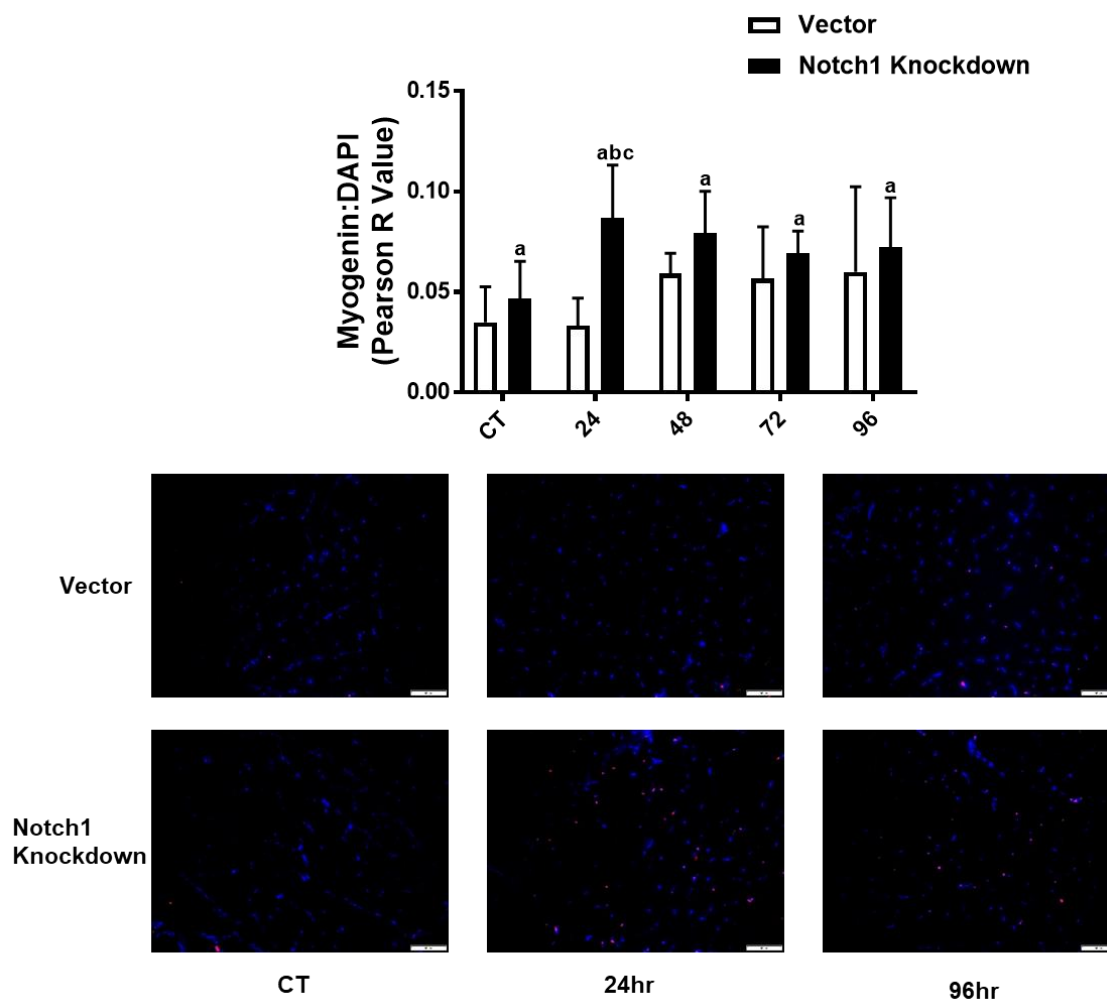


Figure 2.5.11. Myogenin+/DAPI+ Colocalization in Gastrocnemius Muscle.

Gastrocnemius (GAS) Myogenin: 4',6-Diamidino-2-Phenylindole, Dihydrochloride (DAPI) colocalization in young (2-4 mo.) C57BL/6 mice injected with shRNA against Notch1 (Notch1 knockdown) or an empty vector (Vector) on 5 consecutive days in the left and right GAS, respectively. On day 5 of injection, animals were either euthanized (CT) or underwent a bout of downhill running (DHR) to exhaustion and were subsequently euthanized over the next 4 days (24hr, 48hr, 72hr, 96hr). 30 minutes prior to tissue harvest, all animals received 0.040 μmol puromycin/g body weight. Representative images are taken at 20x: Blue-DAPI; Green-Laminin; Red-Myogenin. Data were analyzed using a two-way repeated measures ANOVA. a: significant ($p \leq 0.05$) main effect of limb; b: significantly different within timepoint; c: significantly different within limb from CT (n = 6 per group). Data are mean \pm SD.

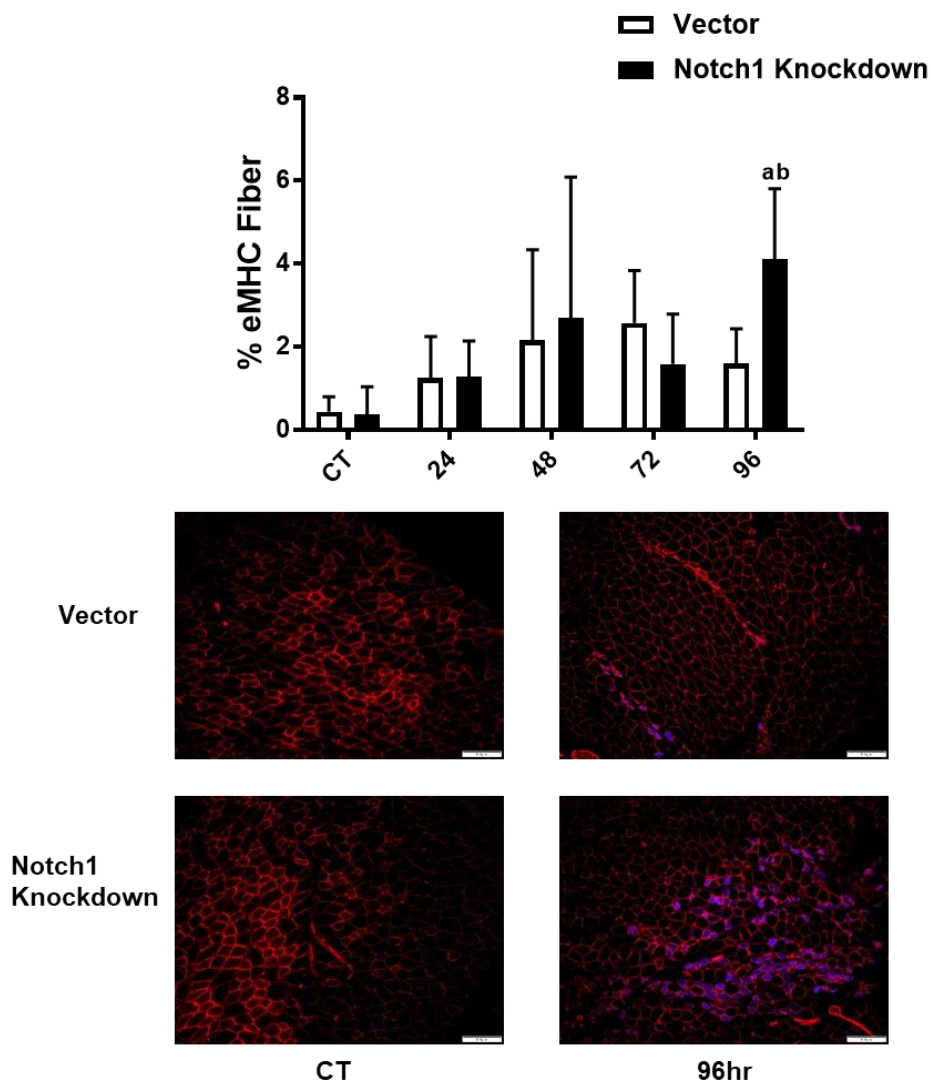


Figure 2.5.12. Percentage of Embryonic Myosin Heavy Chain Fibers in Gastrocnemius Muscle. Gastrocnemius (GAS) embryonic myosin heavy chain (eMHC) percentage of total fiber number in young (2-4 mo.) C57BL/6 mice injected with shRNA against Notch1 (Notch1 knockdown) or an empty vector (Vector) on 5 consecutive days in the left and right GAS, respectively. On day 5 of injection, animals were either euthanized (CT) or underwent a bout of downhill running (DHR) to exhaustion and were subsequently euthanized over the next 4 days (24hr, 48hr, 72hr, 96hr). 30 minutes prior to tissue harvest, all animals received 0.040 μmol puromycin/g body weight. Representative images are taken at 10x: Blue-EMHC; Red-Laminin. Data were analyzed using a two-way repeated measures ANOVA. a: significant ($p \leq 0.05$) main effect of limb; b: significantly different within timepoint; c: significantly different within limb from CT (n = 6 per group). Data are mean \pm SD.

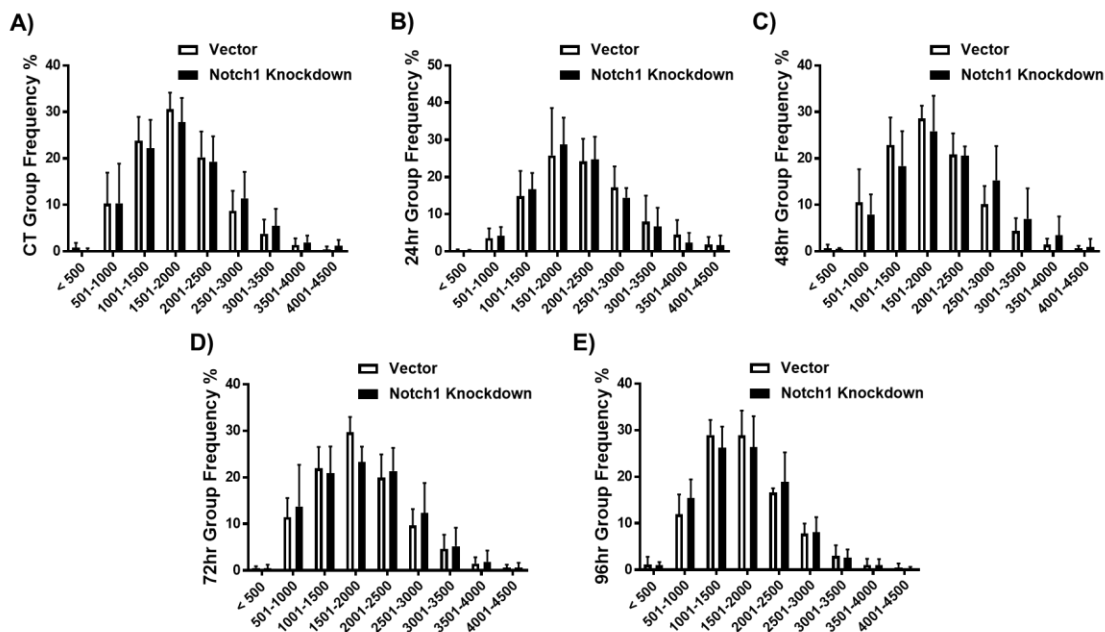


Figure 2.5.13. CSA Frequency Distribution in Gastrocnemius Muscle. A) Control (CT) non exercising group frequency distribution; B) 24 hour (hr) group frequency distribution; C) 48hr group frequency distribution; D) 72hr group frequency distribution; E) 96hr group frequency distribution percentage of cross-sectional area (CSA) of Gastrocnemius (GAS) muscles of young (2-4 mo.) C57BL/6 mice injected with shRNA against Notch1 (Notch1 knockdown) or an empty vector (Vector) on 5 consecutive days in the left and right GAS, respectively. On day 5 of injection, animals were either euthanized (CT) or underwent a bout of downhill running (DHR) to exhaustion and were subsequently euthanized over the next 4 days (24hr, 48hr, 72hr, 96hr). 30 minutes prior to tissue harvest, all animals received 0.040 μmol puromycin/g body weight. Data were analyzed using a two-way repeated measures ANOVA. Grouping sizes are in microns; 500 fibers were traced per section ($n = 6$ per group). Data are mean \pm SD.

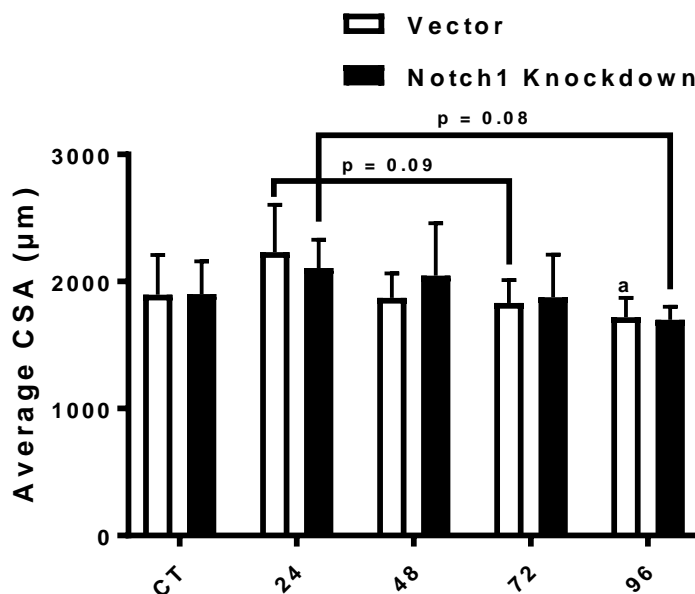


Figure 2.5.14. Average CSA in Gastrocnemius Muscle. Average cross-sectional area (CSA) of Gastrocnemius (GAS) muscles of young (2-4 mo.) C57BL/6 mice injected with shRNA against Notch1 (Notch1 knockdown) or an empty vector (Vector) on 5 consecutive days in the left and right GAS, respectively. On day 5 of injection, animals were either euthanized (CT) or underwent a bout of downhill running (DHR) to exhaustion and were subsequently euthanized over the next 4 days (24hr, 48hr, 72hr, 96hr). 30 minutes prior to tissue harvest, all animals received 0.040 μmol puromycin/g body weight. Data were analyzed using a two-way repeated measures ANOVA. 500 fibers were traced per section. a: significantly ($p \leq 0.05$) different within limb from 24 ($n = 6$ per group). Data are mean \pm SD.

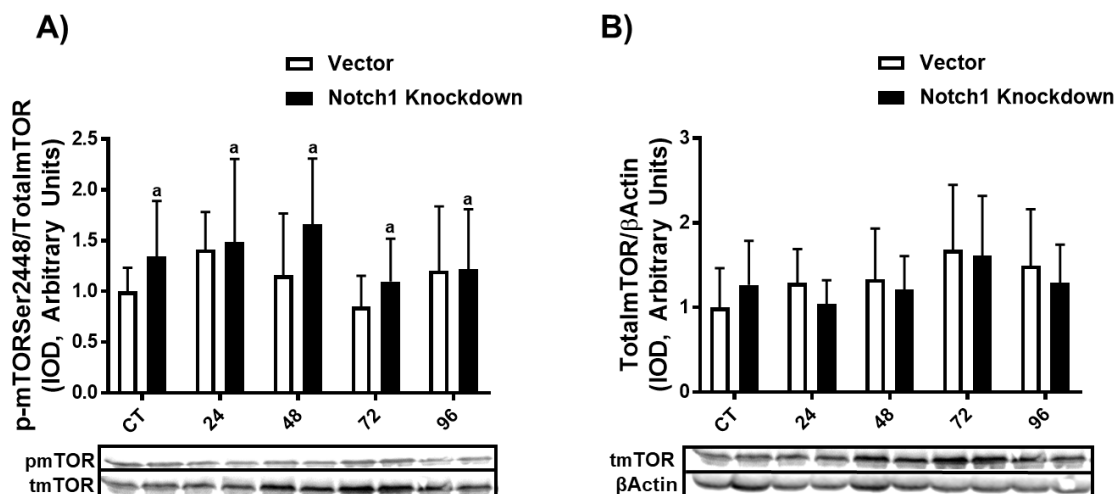


Figure 2.5.15. Phosphorylated and Total mTOR in Gastrocnemius Muscle. A) Gastrocnemius (GAS) phospho (p)-mechanistic target of rapamycin (mTOR) Ser2448/Total mTOR; B) Total mTOR/ β -Actin expression (Integrated optical density, IOD) in young (2-4 mo.) C57BL/6 mice injected with shRNA against Notch1 (Notch1 knockdown) or an empty vector (Vector) on 5 consecutive days in the left and right GAS, respectively. On day 5 of injection, animals were either euthanized (CT) or underwent a bout of downhill running (DHR) to exhaustion and were subsequently euthanized over the next 4 days (24hr, 48hr, 72hr, 96hr). 30 minutes prior to tissue harvest, all animals received 0.040 μ mol puromycin/g body weight. Data were analyzed using a two-way repeated measures ANOVA. a: significant ($p \leq 0.05$) main effect of limb ($n = 6$ per group). Data are mean \pm SD.

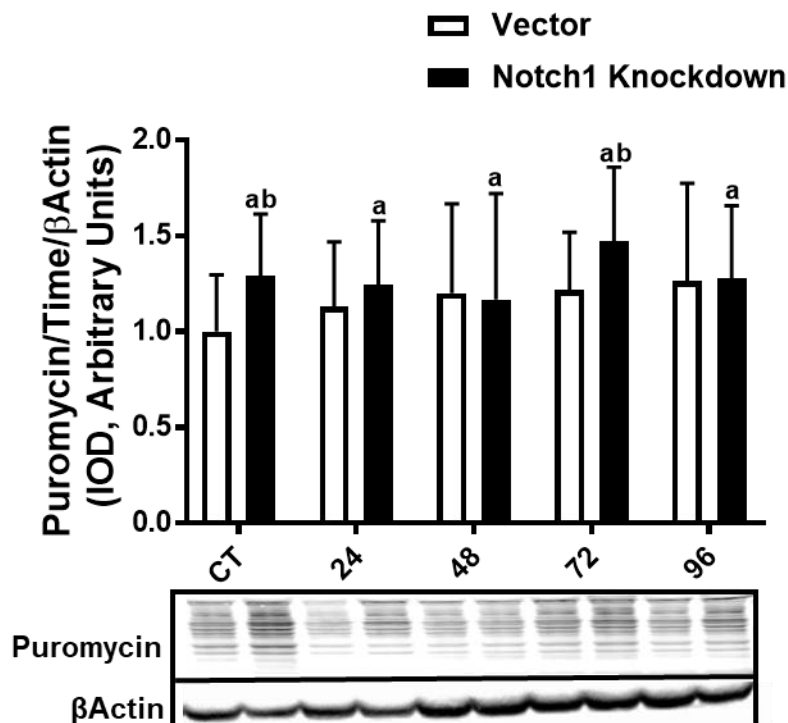


Figure 2.5.16. Muscle Protein Synthesis Rate in Gastrocnemius Muscle.

Gastrocnemius (GAS) Puromycin/ β -Actin expression (Integrated optical density, IOD) in young (2-4 mo.) C57BL/6 mice injected with shRNA against Notch1 (Notch1 knockdown) or an empty vector (Vector) on 5 consecutive days in the left and right GAS, respectively. On day 5 of injection, animals were either euthanized (CT) or underwent a bout of downhill running (DHR) to exhaustion and were subsequently euthanized over the next 4 days (24hr, 48hr, 72hr, 96hr). 30 minutes prior to tissue harvest, all animals received 0.040 μ mol puromycin/g body weight. Data were analyzed using a two-way repeated measures ANOVA. a: significant ($p \leq 0.05$) main effect of limb; b: significantly different within timepoint ($n = 6$ per group). Data are mean \pm SD.

2.6 Tables

Table 2.6.1 *Treadmill Familiarization Protocol.*

| Day | Protocol | Minutes | Belt Speed (m/min) | Percent Grade | Shock Grid |
|------------|---------------------|----------------|---------------------------|----------------------|-------------------|
| 1 | Place mice in lanes | 5 | 0 | 0 | on |
| 2 | Place mice in lanes | 2 | 0 | 0 | on |
| | Let mice run | 2 | 7 | 0 | on |
| 3 | Place mice in lanes | 2 | 0 | 0 | on |
| | Let mice run | 2 | 7 | 0 | on |
| | Let mice run | 2 | 9 | 0 | on |
| 4 | Place mice in lanes | 2 | 0 | 0 | on |
| | Let mice run | 3 | 7 | 0 | on |
| | Let mice run | 3 | 9 | 0 | on |
| 5 | Place mice in lanes | 2 | 0 | 0 | on |
| | Let mice run | 3 | 7 | 0 | on |
| | Let mice run | 3 | 9 | 0 | on |
| | Let mice run | 2 | 11 | 0 | on |

m: meters

Table 2.6.2 *Primary Antibodies used for Western Blot Analysis.*

| <u>Antibody</u> | <u>Catalog #, Company</u> | <u>Dilution</u> |
|-----------------|---------------------------|------------------------|
| Notch1 | (#3608, CS) | 1:500 |
| Hes1 | (#11988, CS) | 1:500 |
| P-mTOR Ser2448 | (#5536, CS) | 1:500 |
| Total mTOR | (#4517, CS) | 1:1000 |
| MyoD | (#13812, CS) | 1:500 |
| Pax7 | (Supernatant, DSHB) | 1:50 (1:1 in glycerol) |
| Myogenin | (82843, ABcam) | 1:500 |
| Puromycin | (#MABE343EMD Millipore) | 1:5000 |
| Beta Actin | (#A2228, Sigma Aldrich) | 1:10000 |

Hes1: hairy/enhancer of split 1; mTOR: mechanistic target of rapamycin; MyoD: myogenic differentiation 1; Pax7: paired box 7; CS: Cell signaling; DSHB: Developmental Studies Hybridoma Bank.

Table 2.6.3 *Primary and Secondary Antibodies used for Immunohistochemistry.*

| <u>Antibody</u> | <u>Catalog #, Company</u> | <u>Dilution</u> |
|---------------------|----------------------------|------------------------|
| GFP | (12A6 Supernatant, DSHB) | 1:50 |
| Pax7 | (Supernatant, DSHB) | 1:50 (1:1 in glycerol) |
| Myogenin | (F5D Supernatant, DSHB) | 1:50 (1:1 in glycerol) |
| eMHC | (F1.652, Supernatant DSHB) | Neat |
| MyoD | (#MA5-12902, ThermoFisher) | 1:100 |
| Laminin | (#05-206, Sigma Aldrich) | 1:200 |
| GT-Anti MS IgG1 488 | (#A21121, ThermoFisher) | 1:200 |
| GT-Anti MS IgG1 350 | (#A21120, ThermoFisher) | 1:200 |
| GT-Anti Rat IgG 488 | (#A11006, ThermoFisher) | 1:200 |
| GT-Anti Rat IgG 555 | (#A21434, ThermoFisher) | 1:200 |

GFP: green fluorescent protein; Pax7: paired box 7; eMHC: embryonic myosin heavy chain; MyoD: myogenic differentiation 1; GT: goat; MS: mouse; IgG: immunoglobulin G; DSHB: Developmental Studies Hybridoma Bank

Table 2.6.4 *Muscle Wet Weights of Young C57BL/6 Mice.*

| | CT (n = 6) | 24 (n = 6) | 48 (n = 6) | 72 (n = 6) | 96 (n = 6) |
|----------------------------|-------------|-------------|-------------|--------------------------|--------------------------|
| Muscle wet weight, mg/g BW | | | | | |
| Vector | 5.92 ± 0.63 | 6.38 ± 0.52 | 5.95 ± 0.51 | 5.42 ± 0.21 ^a | 5.39 ± 0.48 ^a |
| Knockdown | 6.11 ± 0.59 | 5.95 ± 0.39 | 5.83 ± 0.63 | 5.61 ± 0.22 | 5.26 ± 0.34 ^b |

Values are means ± SD. a: significantly different within same limb from the 24-hour group. B: significantly different within same limb from CT group.

CHAPTER 3: EFFECTS OF NOTCH INHIBITION ON THE MYOGENIC PROGRAM AND PROTEIN SYNTHESIS IN C2C12 CELLS

3.1 Introduction

Aging and skeletal muscle-associated diseases (e.g. diabetes, cancer cachexia), can lead to significant reductions in skeletal muscle mass, which impedes quality of life and the ability for individuals to perform daily activities of living [1; 2; 10]. The reductions in skeletal muscle mass in these debilitating conditions are due in part to dysfunction in the muscle repair process (myogenesis: activation and subsequent fusion of satellite cells (SCs)) and blunted muscle protein synthesis (MPS). Proper myogenic processing of SC and muscle protein turnover are critical to maintaining skeletal muscle vigor yet are complex processes regulated by the orchestration of cell signaling pathways. Notch signaling is a highly conserved cell-to-cell communication pathway and a key determinant of cell fate during embryogenesis, including skeletal muscle. In addition to its pivotal roles during development, Notch signaling is crucial for a successful myogenic response following injury [26; 28]. Notch signaling may be dysfunctional in aged skeletal muscle, resulting in a weakened myogenic response. Dysfunctional Notch signaling has been identified as a contributor to the development of insulin resistance and cachexic muscle [48; 151; 152]. However, whether Notch signaling has a regulatory role regarding MPS has yet to be determined. Understanding the role of Notch on MPS will shed light to its contribution to aging and disease.

It is established that Notch plays a key role in SC activation and commitment to enter a proliferative state. Specifically, high levels of Notch signaling will maintain SC quiescence, essentially serving as a myogenic brake [29; 52; 53]. Furthermore, constitutively active Notch signaling is known to prevent muscle cell differentiation, while knocked-down Notch signaling leads to increased differentiation and fusion of myoblasts, enhancing myotube formation [29]. Enhanced myotube formation could be considered a mode of hypertrophy. With its inhibitory role on myotube formation and size, Notch could also be considered a negative regulator, or a brake on hypertrophy. In support of this, it was recently demonstrated that Notch signaling drives skeletal muscle atrophy seen in cancer cachexia [48]. Despite Notch's regulation of myogenesis and its impact on muscle mass, it is unknown whether Notch has a regulatory or braking role over protein synthesis. In addition, the interaction of Notch with other signaling pathways during the myogenic response and protein synthesis is not well studied.

Mechanistic target of rapamycin (mTOR) is an established regulator of protein synthesis [44; 153]. It is currently postulated that mTOR regulates the latter stages of myogenesis, specifically differentiation and maturation of myotubes [30-32]. With Notch's inhibitory impact on differentiation, and mTOR's necessity for differentiation, it is intriguing to consider that Notch and mTOR interact to regulate differentiation. If Notch signaling impacts mTOR, it would be logical that Notch has an effect on protein synthesis. T-cell leukemia (T-ALL) cell lines and *Drosophila melanogaster* models of Notch induced tumorigenesis have demonstrated that Notch and Phosphatidylinositol-4,5-bisphosphate 3-kinase (PI3K) (upstream of mTOR) are linked via phosphatase and tensin homolog (PTEN), an upstream negative regulator of protein kinase B

(AKT)/mTOR [154]. Specifically, it has been postulated that hairy and enhancer of split-1 (Hes1) (downstream Notch effector) regulates PTEN expression [154]. However, it is unknown whether Notch signaling impacts the PTEN/AKT/mTOR pathway in skeletal muscle thereby influencing protein synthesis. Here we demonstrate that Notch inhibition in C2C12 mouse muscle cells, elevates protein synthesis potentially through the PTEN/AKT/mTOR pathway.

3.2 Experimental Design and Methods

3.2.1 Cell Culture

The C3H murine cell line C2C12 (ATCC p3-p8) was used for all experiments. For myoblast experiments, cells were seeded in growth media (GM: Dulbecco's Modified Eagles Medium [DMEM], 10% fetal bovine serum (FBS), 10% horse serum (HS), and 1% penicillin/streptomycin (P/S)) in 12-well plates at a density of 10,000 cells/well. 24 hours following seeding (~30% confluence), cells were washed 1x with phosphate buffered saline (PBS), and serum-starved (DMEM: 1% P/S) for 12 hours to induce cell-cycle arrest. Cells were then treated with either 2 μ M γ -secretase inhibitor (GSI: L-685,458; Millipore Sigma- dimethyl sulfoxide [DMSO]), 4 μ M-GSI, or control (DMSO equal volume to 4 μ M-GSI) for 48 hours (every 12 hours). Following GSI treatment, myoblasts were assessed for proliferation and protein expression as detailed below. For myotube experiments, cells were seeded in GM in 6-well plates at a density of 75,000 cells/well, grown to ~100% confluence, washed 2x with PBS, and differentiated for 96 hours in differentiation media (DM: DMEM: 2% HS, 1% P/S) with or without 4 μ M-GSI every 12 hours. Myotubes were analyzed for indices of fusion, protein expression, and protein synthesis as detailed below. For late-stage myotube experiments, cells were

seeded, grown to ~100% confluence, washed 2x with PBS, and differentiated for 120 hours in DM. At 120 hours, wells were treated with or without 4 μ M-GSI every 12 hours for 24 hours. 144-hour (Day 6) myotubes were analyzed for indices of fusion and protein synthesis as detailed below.

3.2.2 MTT Proliferation Assay on Myoblasts

Following 20 and 144-hours of treatment (Control or GSI), media was changed and myoblasts were treated with 1ng/ml of 3-(4,5-Dimethylthiazol-2-yl)-2,5-Diphenyltetrazolium Bromide) (MTT) reagent in GM for 4 hours as previously described [155] to obtain cell proliferation at 24 and 48 hours. Following the 4 hour incubation, residual GM was pulled off and the MTT reagent-cell formed crystals were dissolved in DMSO, pipette titrated ~ 10 times, and incubated for 30 minutes in the dark. Triplicates of each well were loaded into a 96-well plate and absorbance was read at 560 nm with a 592nm reference reading.

3.2.3 Myosin Heavy Chain Staining

Following 96 (and 144) hours of differentiation, myotubes were labeled with myosin heavy chain (MHC) to determine properties of fusion and area. Briefly, cells were fixed with 70% Acetone/30% Methanol for 10 minutes at room temperature (RT). Following fixation cells were washed 2x with PBS, blocked for 1 hour with 10% normal goat serum (NGS) in PBS, and incubated overnight in MHC. Following overnight incubation (16 hours), cells were washed 3x with PBS, and counter stained with a secondary antibody (1:500) specific to the MHC primary and 4',6-Diamidino-2-Phenylindole, Dihydrochloride (DAPI 1:1000) in PBS for 60 minutes. Wells were mounted with Vectashield and a coverslip.

3.2.4 Myotube Fusion and Myotube Area

Following MHC labeling, myotubes were imaged with an Olympus iX inverted microscope at 20x. Images from wells were all taken in the same fashion: 1) the top left of the well was imaged, 2) the stage was moved over three fields of view to the right and imaged, 3) the stage was moved down three fields of view and imaged, 4) the stage was moved over three fields of view to the left and imaged, 5) the stage was moved down three fields of view and imaged, 6) the stage was moved three fields of view to the right and imaged. 6 fields of view per well were captured. Myotube fusion was determined by counting the total nuclei, total myotubes, and nuclei fusing into myotubes, by 2 blinded individuals using ImageJ software (cell counter plugin). A myotube was defined as a MHC labeled cell containing two or more nuclei. All myosegments (MHC labeled without two or more nuclei) were ignored as myotubes in the fusion index and area quantification. Fusion index was calculated by nuclei within myotubes/total nuclei. Myotube area was determined from the same images used to calculate fusion, using Adobe Photoshop as previously described [156]. Briefly, three random control and three random GSI images were used to set a color range (accepted tones of red (MHC)). The established color range was then applied to all experiment images, a measurement scale was set (pixels to microns) and measurements were obtained for total myotube area, area per myotube, and myotube area per fused nuclei.

3.2.5 Protein Synthesis

For protein synthesis measurements, the SUnSET method using puromycin was used as previously described [82; 85]. Briefly, 30 minutes prior to collection, C2C12 cells were

treated with 1 μ M puromycin (P-1033, A.G. Scientific). Puromycin incorporation was determined via western blot analysis as described below.

3.2.6 Western Blot

Collection and preparation of C2C12s was done as previously described for western blot analysis [155]. Briefly, C2C12s myoblasts and myotubes were washed 2x with ice cold PBS followed by addition of ice cold Radioimmunoprecipitation assay buffer (sc-24948; Santa Cruz, supplemented with 1% Triton-x, 2% SDS, protease cocktail inhibitor) for 5 minutes. Wells were scraped, mechanically lysed (using a 25 gauge-needle-syringe), and centrifuged for 20 minutes at 20,000G (4°C). Protein concentration of the supernatant was determined by Pierce BCA kit (23225; ThermoFisher). 20ug of sample was loaded onto a 4-12% Bis-Tris gel (3450125; Bio-Rad) and run (XT MES running buffer; 1610789; Bio-Rad) at 125V for 2 hours. Following electrophoresis, proteins were transferred (Towbin Buffer; 10% methanol) onto a .22uM Polyvinylidene difluoride (PVDF) membrane for 1 hour at 100V. Membranes were washed 1x in Tris-buffered saline (TBS) and blocked for 1 hour in Odyssey blocking buffer 1:1 with TBS. Following blocking, membranes were incubated overnight (16 hours) in primary antibodies (Table 3.6.1). The next day membranes were washed 3 x 5 minutes in TBST (TBS: 0.1% Tween 20) and then incubated in secondary antibodies (1:10,000 in TBST) for 1 hour. Following 3 x 5 minute washes in TBST and 1 x 5 min wash in TBS, membranes were imaged and bands were quantified using the Odyssey® Licor CLx System.

3.2.7 Statistical Analysis

T-tests were used to determine differences between control and GSI groups for myoblast and myotube protein expression levels as well as properties of myotube formation (Fusion/Area). A two-way ANOVA (Time x Treatment) with a Tukey's post-hoc test was used to determine differences for the MTT proliferation assay. Significance was set at an alpha level of 0.05. All statistics were performed using GraphPad Prism 7.03 and all data are presented as means \pm SD.

3.3 Results

3.3.1 GSI reduces Notch signaling and blunts proliferation in C2C12 myoblasts

C2C12 myoblasts were treated over the course of 48hours with two concentrations of GSI (2 μ M or 4 μ M) or control (DMSO). There was no effect on myoblast proliferation at 24hours, however, at 48hours both 2 μ M and 4 μ M-treated cells displayed reduced proliferation (marked by cell viability) compared to control (2 μ M: $p < 0.001$; 4 μ M: $p < 0.0001$; Figure 3.5.1A). As a result of a more significant effect on proliferation, 4 μ M was selected for all subsequent experiments. Relative to control, 4 μ M GSI treatment reduced Hes1 expression by ~35% ($p \leq 0.01$) in C2C12 myoblasts (Figure 3.5.1B).

3.3.2 GSI elevates myotube formation in differentiating C2C12 myotubes

GSI treatment reduced Hes1 expression by ~38% ($p \leq 0.0001$) and Notch intracellular domain (NICD/A.Notch) by ~40% ($p \leq 0.001$) in C2C12 myotubes (Figure 3.5.2A&B). To determine the impact that GSI treatment had on myotube formation, C2C12 cells were treated over the course (every 12 hours) of 96hours with or without 4 μ M of GSI. As anticipated, GSI treatment lead to significant increases in myotube formation. All fusion markers were enhanced with GSI treatment including: fused nuclei ($p \leq 0.05$), non-fused

($p < 0.001$), nuclei per myotube ($p \leq 0.05$), and fusion index (nuclei fusing/total nuclei) ($p < 0.01$) (Figure 3.5.3A-F). There were no significant differences ($p > 0.05$) in total nuclei or myotube number with GSI treatment. In addition to increasing myotube fusion, GSI treatment augmented total myotube area ($p < 0.01$), area per myotube ($p \leq 0.05$), and myonuclear domain (myotube area per fusing nuclei; $p \leq 0.05$) (Figure 3.5.4A-D). In support of these findings, Myogenin ($p < 0.001$) and Myosin heavy chain ($p \leq 0.05$) protein levels were elevated following GSI treatment (Figure 3.5.5A&B).

3.3.3 GSI elevates protein synthesis and mTOR in C2C12 myoblasts and myotubes

In contrast to blunting proliferation in C2C12 myoblasts, GSI treatment elevated protein synthesis ($p \leq 0.05$; Figure 3.5.6A). These same experiments revealed increases in phosphorylation of the crucial modulator of protein synthesis, mTOR at Ser 2448 ($p \leq 0.05$) and Ser2481 ($p \leq 0.01$) (Figure 3.5.6B&C), and its downstream effector: 4EBP1 (Thr37/46; $p \leq 0.05$) (Figure 3.5.6D). Interestingly, there was no significant difference in either p70S6K (Thr389; $p > 0.05$) (Figure 3.5.6E) or eEF2 (Thr56; $p > 0.05$) (Figure 3.5.6F). Coinciding with its hypertrophic effect on myotubes, GSI treatment also elevated protein synthesis in 96 hour-myotubes ($p < 0.0001$) (Figure 3.5.7A). Mirroring its effect in myoblasts, GSI treatment increased phosphorylation (Ser 2448; $p \leq 0.05$ & Ser2481; $p \leq 0.05$) in mTOR (Figure 3.5.7B&C) and its downstream effector: 4EBP1 (Thr37/46; $p < 0.0001$) (Figure 3.5.7D) in 96-hour myotubes. While phosphorylation of p70S6K (Thr389) and eEF2 (Thr56) were unchanged in myoblasts, they were interestingly decreased ($p < 0.01$) and increased ($p \leq 0.05$) respectively in myotubes (Figure 3.5.7E&F).

3.3.4 GSI modulates signaling upstream of mTOR in C2C12 myoblasts and myotubes

To identify if Notch regulates protein synthesis upstream of mTOR in myoblasts and myotubes we measured PTEN, AKT, and TSC2 protein expression levels. 4 μ M GSI-treatment reduced PTEN expression in myoblasts ($p < 0.001$; Figure 3.5.8A).

Additionally, GSI treatment increased phosphorylation of AKT (Thr 308; $p < 0.001$ & Ser473; $p < 0.001$) and TSC2 (Ser939; $p \leq 0.05$ & Thr1462; $p \leq 0.05$) (Figure 3.5.8B-E).

Mimicking its effect in myoblasts, GSI treatment reduced PTEN ($p \leq 0.05$; Figure 3.5.9A) expression and increased phosphorylation of AKT (Thr 308; $p < 0.001$ & Ser473; $p < 0.01$) and TSC2 (Ser939; $p < 0.001$ & Thr1462; $p < 0.0001$) (Figure 3.5.9B-E) in 96-hour myotubes.

3.3.5 GSI elevates protein synthesis and myotube hypertrophy in day 6 myotubes

To verify the hypertrophic impact of GSI-treated differentiating C2C12 cells, we measured protein synthesis along with indices of fusion and hypertrophy (as described above) in day 6 myotubes which were treated over 24-hours (120-144hrs). GSI treatment elevated protein synthesis in day 6 myotubes ($p < 0.001$; Figure 3.5.10). GSI treatment did not significantly change ($p > 0.05$) several indices of fusion in day 6 myotubes including fused nuclei, non-fused nuclei, total nuclei, or fusion index (Figure 3.5.11A-C; F). Though myotube number was not significantly different, it was trending downward with GSI treatment ($p = 0.09$) and nuclei per myotube was significantly elevated ($p \leq 0.05$) with GSI treatment (Figure 3.5.11 D&E). Neither total myotube area or myotube area per nuclei were increased ($p > 0.05$) with GSI treatment (Figure 3.5.12 A;C). However, area per myotube was significantly increased ($p \leq 0.05$) with GSI treatment in day 6 myotubes (Figure 3.5.12B).

3.4 Discussion and Conclusion

Though Notch signaling has been widely studied within skeletal muscle, a majority of this research focused on Notch's role in the regulation of SC activity. Previous findings demonstrated that inhibition of Notch signaling induced muscle cell differentiation, enhanced myotube formation and, led to hypertrophy [48; 136]. However, despite its influence on myotube hypertrophy or rescue of atrophy, none of the prior studies have investigated Notch's influence over protein synthesis or anabolic signaling. We are the first to show that Notch inhibition (via GSI treatment) not only increased myotube hypertrophy, but also increased protein synthesis, possibly through modulation of the PTEN-AKT-mTOR signaling pathway.

Signaling of the Notch family transmembrane receptors (Notch1-4) occurs when ligands (Delta-like protein (DLL) 1, DLL 3, DLL4, Jagged1, and Jagged2) bind and initiate a series of cleavages driven by metalloproteases and γ -secretases, ending with release and subsequent translocation of NICD to the nucleus. The translocated NICD induces expression of several target genes including Hes1, hairy/enhancer-of-split related with YRPW motif protein 1 (Hey1), and avian myelocytomatosis viral oncogene homolog (Myc) [10; 22]. Notch signaling's influence over SC activation and myoblast proliferation via regulation of myogenic regulatory factors has been widely studied [52; 131]. However, specific roles for Notch downstream effectors within other skeletal muscle processes are still largely unknown.

A widely used method of inhibiting Notch signaling is by treating cells with a GSI. Here we demonstrated that GSI treatment reduced Hes1 and blunted proliferation of C2C12 myoblasts compared to control (Figures 3.5.1 & 3.5.2), likely due to premature

differentiation and fusion. This is in agreement with prior studies demonstrating that the Notch ligand DLL1 enhanced proliferation of SCs, while inhibition of Notch signaling prevented SC self-renewal and led to premature differentiation of cells [26; 122; 131]. Our data also supports prior findings that Notch signaling has an inhibitory effect on myotube formation and expression of late-stage myogenic regulatory factors (Figures 3.5.3-3.5.5). However, the exact mechanism by which Notch inhibition elevates myotube formation is unknown as several Notch effectors (Hes1/MyoD, Hey, MyoR (Musculin)) have shown to suppress the myogenic response [35; 36]. Despite evidence of mTOR's roles in SC activation, differentiation, and fusion and Notch's known ability to halt differentiation and fusion, interplay between these two signaling pathways within skeletal muscle has not been elucidated [32; 34; 37]. Here for the first time we demonstrated significantly increased myotube fusion (e.g. fusion index, nuclei/myotube) with GSI treatment along with increased mTOR signaling (Figures 3.5.3 & 3.5.7). These findings suggest that mTOR signaling may be an additional mechanism by which Notch mediates myoblast differentiation and fusion.

Maintaining or increasing skeletal muscle mass (hypertrophy) is extremely important for sustaining quality of life in aging and diseased populations. Post-natal hypertrophy is achieved by increasing cellular fusion (myonuclear accretion) or by increasing protein synthesis (expansion of myonuclear domain) [157-159]. Given what is known about Notch's braking regulation over SCs and prevention of differentiation, it is no surprise that Notch mediated myotube hypertrophy by elevating cellular fusion (Figure 3.5.3). In addition to an increase in myonuclear accretion we also show expanded myonuclear domain, by which myotube area per fused nuclei increased with

GSI treatment (Figure 3.5.4). Our findings are in concert with previous literature showing that mutations in Notch associated proteins (Protein O-Fucosyltransferase 1 (Pofut1)) induced *in vitro* and *in vivo* muscle hypertrophy [23; 127]. Our findings however, revealed for the first time that Notch may serve as a molecular brake on muscle hypertrophy through regulation of both myonuclear accretion (fusion) and expansion of myonuclear domain (protein synthesis). It is plausible that the increased cellular fusion was the primary driver myotube hypertrophy. However, we believe that Notch warrants further investigation in its role on expansion of myonuclear domain. We wanted to further examine if GSI could have similar effects on already formed myotubes. The effect of GSI on already formed myotubes was not as robust compared to when C2C12 cells were treated from the onset of differentiation. However, area per myotube and nuclei per myotube were elevated (Figures 3.5.10 & 3.5.11). Both of these changes coincide with the slight non-significant reduction in myotube number. It is likely that the myotubes were increasing in size ultimately fusing together to form larger myotubes. These three findings, suggest that even in formed myotubes, GSI treatment may be able to augment hypertrophy.

Augmenting protein synthesis is pivotal to maintaining lean body mass in aged and diseased populations. The known driver of protein synthesis, mTOR, is under vast regulation by upstream proteins including AKT and PTEN [44]. However, whether or not Notch signaling modulates MPS has yet to be elucidated. We have for the first time demonstrated that Notch may modulate protein synthesis in C2C12 skeletal muscle cells (Figures 3.5.6A & 3.5.7A). In both proliferating myoblasts and differentiating myotubes GSI treatment significantly elevated protein synthesis. This elevation of protein synthesis

is in concert with our findings of increased myonuclear domain in C2C12 myotubes (myotube area/ fusing nuclei). Interestingly, with all the evidence of Notch modulation over differentiation and fusion leading to hypertrophy, this was the first study investigating Notch modulation of protein synthesis. Furthermore, we were also able to demonstrate that GSI treatment significantly elevates protein synthesis in formed C2C12 myotubes (Figure 3.5.10).

In addition to showing elevations in mTOR signaling and protein synthesis, we demonstrated for the first time that GSI treatment may act on mTOR via modulation of the PTEN/AKT/mTOR cascade (Figures 3.5.8 & 3.5.9). PTEN is a negative upstream regulator of AKT and mTOR. It does so by dephosphorylating Phosphatidylinositol (3,4,5)-trisphosphate (PIP3) to Phosphatidylinositol 4,5-bisphosphate (PIP2) [44]. Here we revealed that in both myoblasts and myotubes, PTEN expression is significantly reduced following GSI treatment. Following suit, we demonstrated increased phosphorylated AKT (Thr308 and Ser473) and phosphorylated TSC2 (Ser939 and Thr1462) with GSI treatment. Research outside of skeletal muscle supports that notion that Notch may regulate the PTEN/AKT/mTOR cascade. Within T-cell acute lymphoblastic leukemia (T-ALL) Notch signaling has demonstrated modulation over phosphatidylinositol 3-kinase (PI3K), AKT, and mTOR [42; 154; 160; 161]. Both Hes1 and c-Myc have shown to target PTEN expression [154], while c-Myc has also been identified to regulate gene expression of TSC2 [45]. These findings along with the results presented here, support that Notch may modulate the PI3K/AKT/mTOR cascade. One interesting finding was that 4EBP1 was the only downstream target of mTOR that was changed in a pro protein synthesis manner with GSI treatment. Given our findings

that GSI treatment modulated PTEN/AKT, it is plausible that Notch may actually act through ATK as opposed to mTOR, though further studies need to be carried out in order to determine this.

In addition, our data revealed elevations in P-AKT Ser473, which indicates activity in the mTORC2 complex. In support of this, we also showed elevations of P-mTOR Ser2481, which has been implicated as a biomarker for mTORC2 activity [162]. Interestingly, non-canonical roles for NICD have been identified in which NICD integrates with mTORC2 to regulate AKT-mediated (P-AKTSer473) antiapoptotic effects. It is clear that there are several sites of potential interplay between Notch and the PI3K/AKT/mTOR cascade. Given the present findings, further investigation as to the specific interactions between these signaling pathways in skeletal muscle is warranted. Especially given that Notch (and its downstream targets) may have distinct roles regarding SC self-renewal and protein synthesis. Identifying these distinct roles may allow us to develop targeted therapeutics aimed at elevating hypertrophy while maintaining the SC population.

This study further elucidated the molecular braking effect that Notch signaling has on skeletal muscle. We demonstrated that GSI treatment increases protein synthesis in C2C12 myoblasts and C2C12 myotubes, potentially through modulation of the PTEN/AKT/mTOR signaling cascade. The increased protein synthesis, increased myonuclear domain, and increased myonuclear accretion, indicate that Notch may modulate skeletal muscle hypertrophy via multiple avenues. Future research should focus on further elucidating the regulation of protein synthesis by Notch signaling.

3.5 Figures

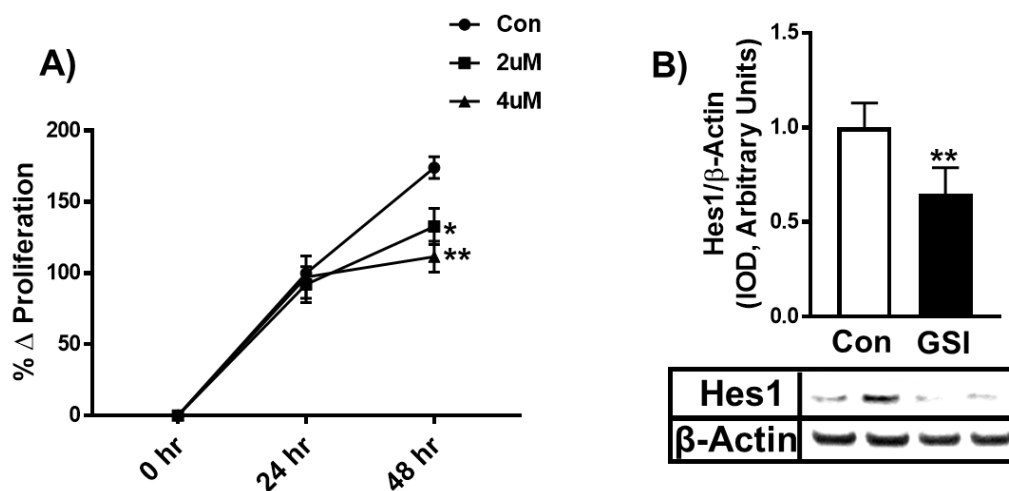


Figure 3.5.1. GSI Reduces Notch Signaling and Blunts Proliferation in C2C12 Myoblasts. A) Percent change from control (Con) in proliferation in 24 and 48-hour myoblasts treated with or without γ -secretase inhibitor (GSI- 4 μ M) every 12 hours. Data were analyzed using a two-way ANOVA followed by Tukey's multiple comparison test. B) Hes1/ β -Actin expression (Integrated optical density, IOD) in 48-hour myoblasts treated with or without 4 μ M GSI every 12 hours. 30 minutes prior to collection all cells were treated with 1 μ M puromycin (For B only). Data were analyzed using a Student's T-test. * $p \leq 0.05$ vs. Con. ** $p < 0.01$ vs. Con (n = 3 experiments). Data are mean \pm SD.

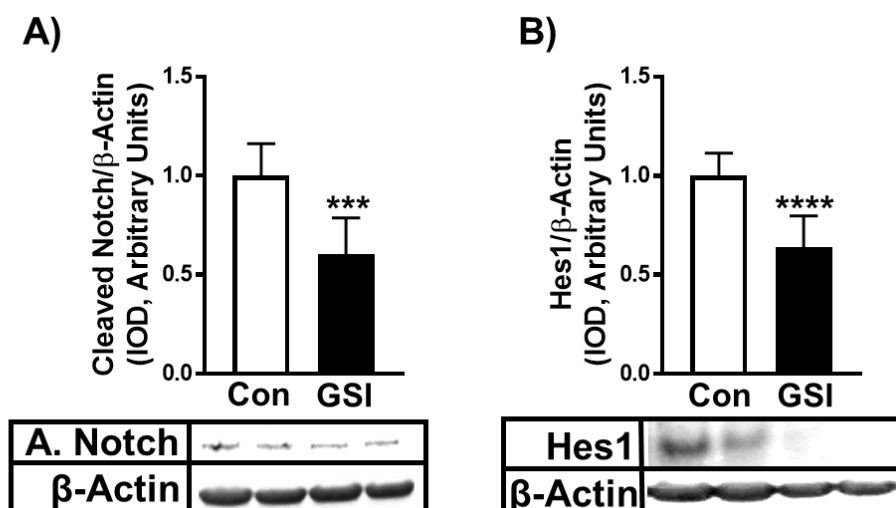


Figure 3.5.2. GSI Reduces Notch Signaling C2C12 Myotubes. A) Cleaved Notch (A.Notch)/ β -Actin; B) Hairy/enhancer of split-1(Hes1)/ β -Actin expression (Integrated optical density, IOD) in 96-hour myotubes treated with or without 4 μ M γ -secretase inhibitor (GSI) every 12 hours. 30 minutes prior to collection all cells were treated with 1 μ M puromycin. Data were analyzed using a Student's T-test. *** $p < 0.001$ vs. Control (Con). **** $p < 0.0001$ vs. Con ($n = 3$ experiments). Data are mean \pm SD.

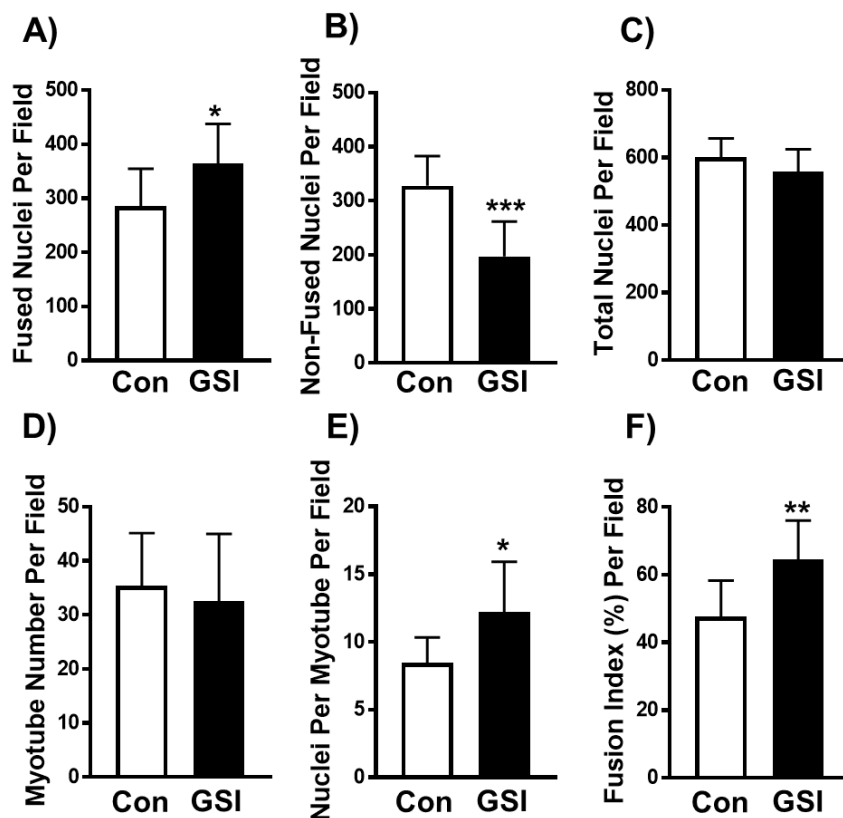


Figure 3.5.3. GSI Treatment Increases Indices of Myotube Fusion in C2C12 Myotubes. A) Fused nuclei per field; B) Non-fused nuclei per field; C) Total nuclei per field; D) Myotube number per field; E) Nuclei per myotube per field; F) Fusion index per field in 96-hour cultured myotubes. At the onset of differentiation C2C12 cells were treated every 12 hours with either control (Con) or 4 μ M Υ -secretase inhibitor (GSI). Data were analyzed using a Student's T-test. * $P \leq 0.05$ vs. Con. ** $P < 0.01$ vs. Con; *** $P < 0.001$ vs. Con (n = 3 experiments). Data are mean \pm SD.

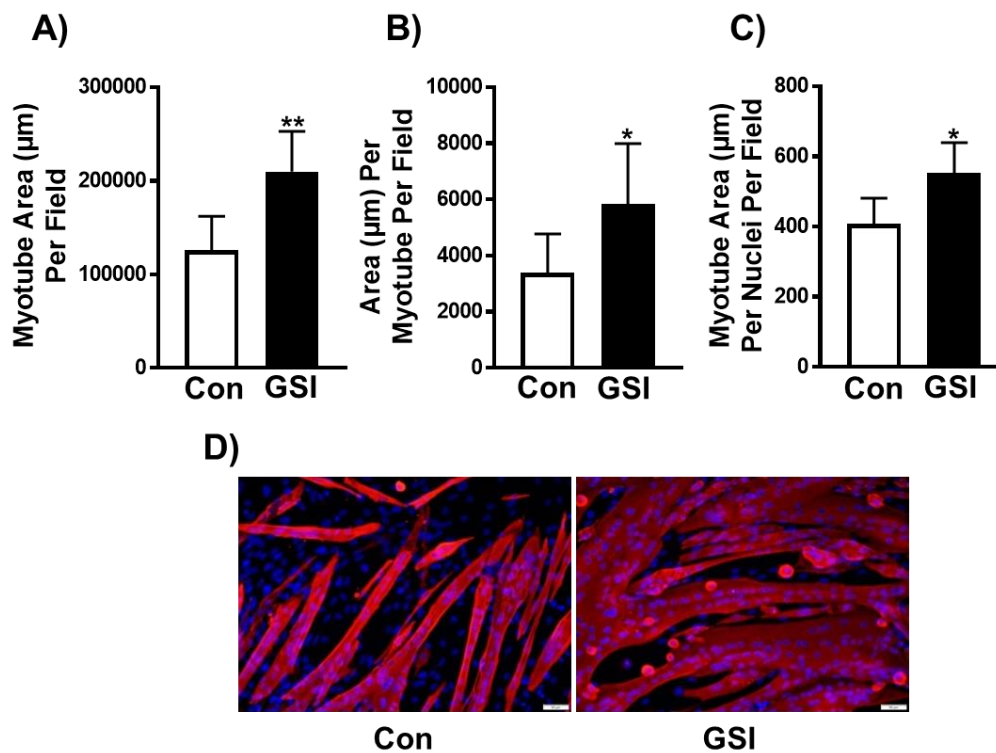


Figure 3.5.4. GSI Treatment Increases Indices of Myotube Hypertrophy in C2C12 Myotubes. A) Myotube area (μm) per field; B) Area (μm) per myotube per field; C) Myotube area (μm) per nuclei per field; D) Representative images of 96-hour cultured myotubes. At the onset of differentiation C2C12 cells were treated every 12 hours with either control (Con) or $4\mu\text{M}$ γ -secretase inhibitor (GSI). Representative images are taken at 20x. Data were analyzed using a Student's T-test. * $P \leq 0.05$ vs. Con. ** $P < 0.01$ vs. Con (n = 3 experiments). Data are mean \pm SD.

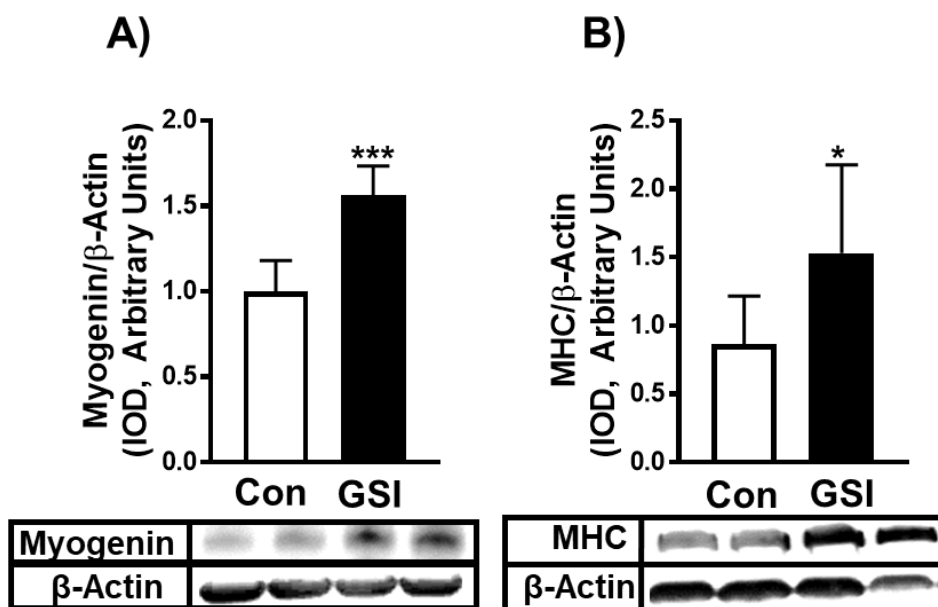


Figure 3.5.5. GSI Treatment Increases Markers of Differentiation in C2C12 Myotubes. A) Myogenin/ β -Actin; B) Myosin heavy chain (MHC)/ β -Actin expression (Integrated optical density, IOD) in 96-hour myotubes treated with or without $4\mu\text{M}$ γ -secretase inhibitor (GSI) every 12 hours. 30 minutes prior to collection all cells were treated with $1\mu\text{M}$ puromycin. Data were analyzed using a Student's T-test. * $P \leq 0.05$ vs. Control (Con); *** $p < 0.001$ vs. Con ($n = 3$ experiments). Data are mean \pm SD.

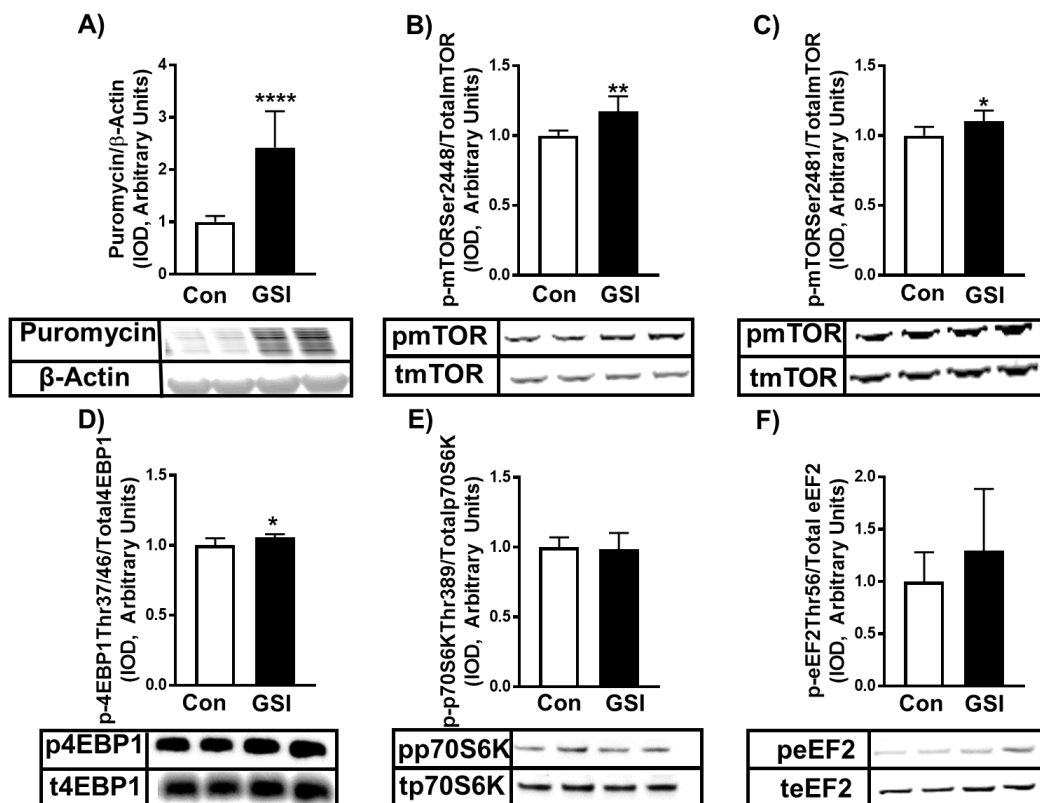


Figure 3.5.6. GSI Treatment Elevates Protein Synthesis in C2C12 Myoblasts. A) Puromycin/ β -Actin; B) Phospho (p)-mechanistic target of rapamycin (mTOR) Ser2448/Total mTOR; C) p-mTOR Ser2481/Total mTOR; D) p-eukaryotic initiation factor 4E binding protein (4EBP1) Thr37/46/Total 4EBP1; E) p-70 kDa ribosomal protein S6 kinase (p70S6K) Thr389/Total p70S6K; F) p-eukaryotic elongation factor 2 (eEF2) Thr56/Total eEF2 expression (Integrated optical density, IOD) in 48-hour myoblasts treated with or without 4 μ M γ -secretase inhibitor (GSI) every 12 hours. 30 minutes prior to collection all cells were treated with 1 μ M puromycin. Data were analyzed using a Student's T-test. * $p \leq 0.05$ vs. Control (Con); ** $p < 0.01$ vs. Con; **** $p < 0.0001$ vs. Con (n = 3 experiments). Data are mean \pm SD.

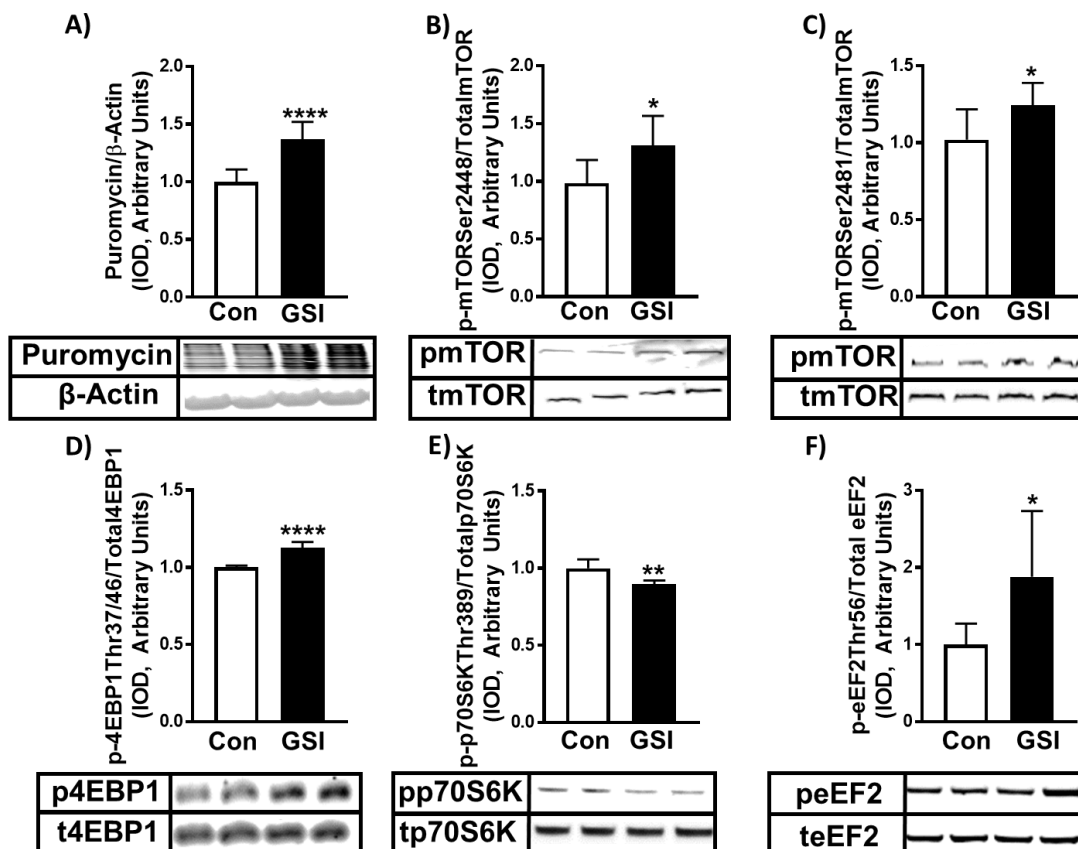


Figure 3.5.7. GSI Treatment Elevates Protein Synthesis in C2C12 Myotubes. A) Puromycin/ β -Actin; B) Phospho (p)-mechanistic target of rapamycin (mTOR) Ser2448/Total mTOR; C) p-mTOR Ser2481/Total mTOR; D) p-eukaryotic initiation factor 4E binding protein (4EBP1) Thr37/46/Total 4EBP1; E) p-70 kDa ribosomal protein S6 kinase (p70S6K) Thr389/Total p70S6K; F) p-eukaryotic elongation factor 2 (eEF2) Thr56/Total eEF2 expression (Integrated optical density, IOD) in 96-hour myotubes treated with or without 4 μ M γ -secretase inhibitor (GSI) every 12 hours. 30 minutes prior to collection all cells were treated with 1 μ M puromycin. Data were analyzed using a Student's T-test. * $p \leq 0.05$ vs. Control (Con); ** $p < 0.01$ vs. Con; **** $p < 0.0001$ vs. Con ($n = 3$ experiments). Data are mean \pm SD.

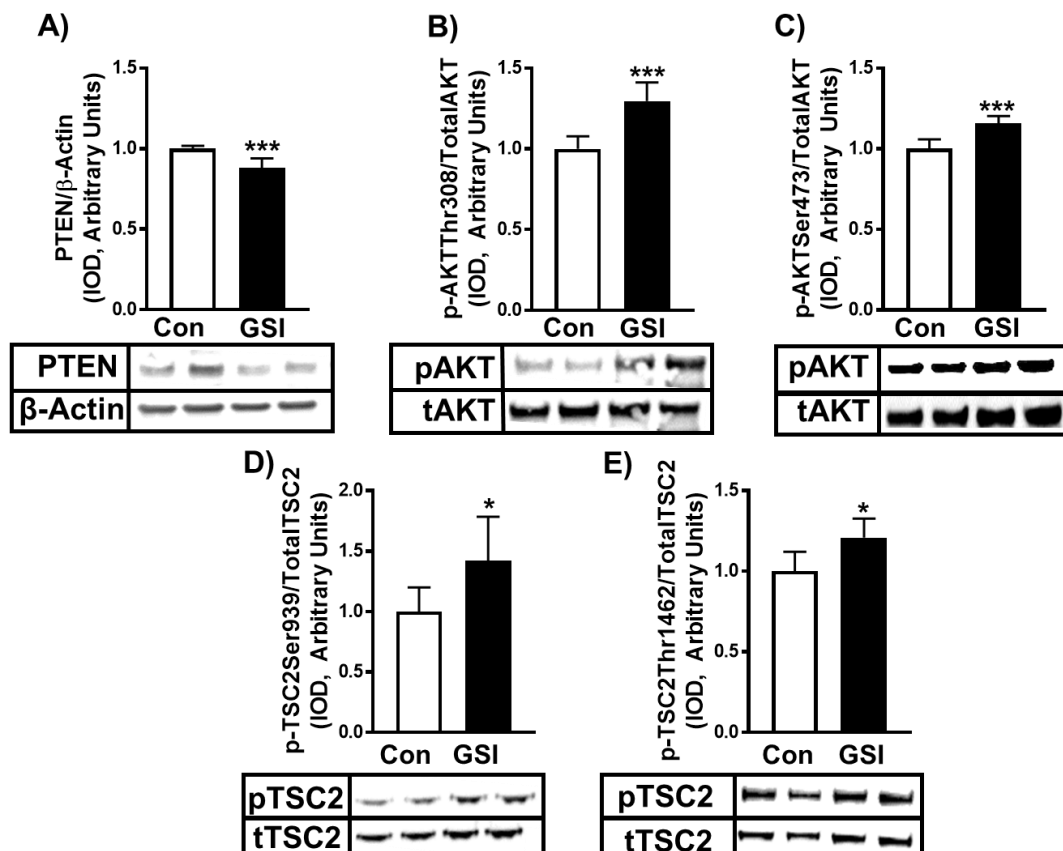


Figure 3.5.8. GSI Treatment Elevates Upstream mTOR Signaling in C2C12 Myoblasts. A) Phosphatase and tensin homolog (PTEN)/ β -Actin; B) Phospho (p)-protein kinase B (AKT) Thr308/Total AKT; C) p-AKT Ser473/Total AKT; D) p-tuberous sclerosis complex 2 (TSC2) Ser939/Total TSC2; E) p-TSC2 Thr1462/Total TSC2 expression (Integrated optical density, IOD) in 48-hour myoblasts treated with or without 4 μ M γ -secretase inhibitor (GSI) every 12 hours. 30 minutes prior to collection all cells were treated with 1 μ M puromycin. Data were analyzed using a Student's T-test. * $p \leq 0.05$ vs. Control (Con); *** $p < 0.001$ vs. Con (n = 3 experiments). Data are mean \pm SD.

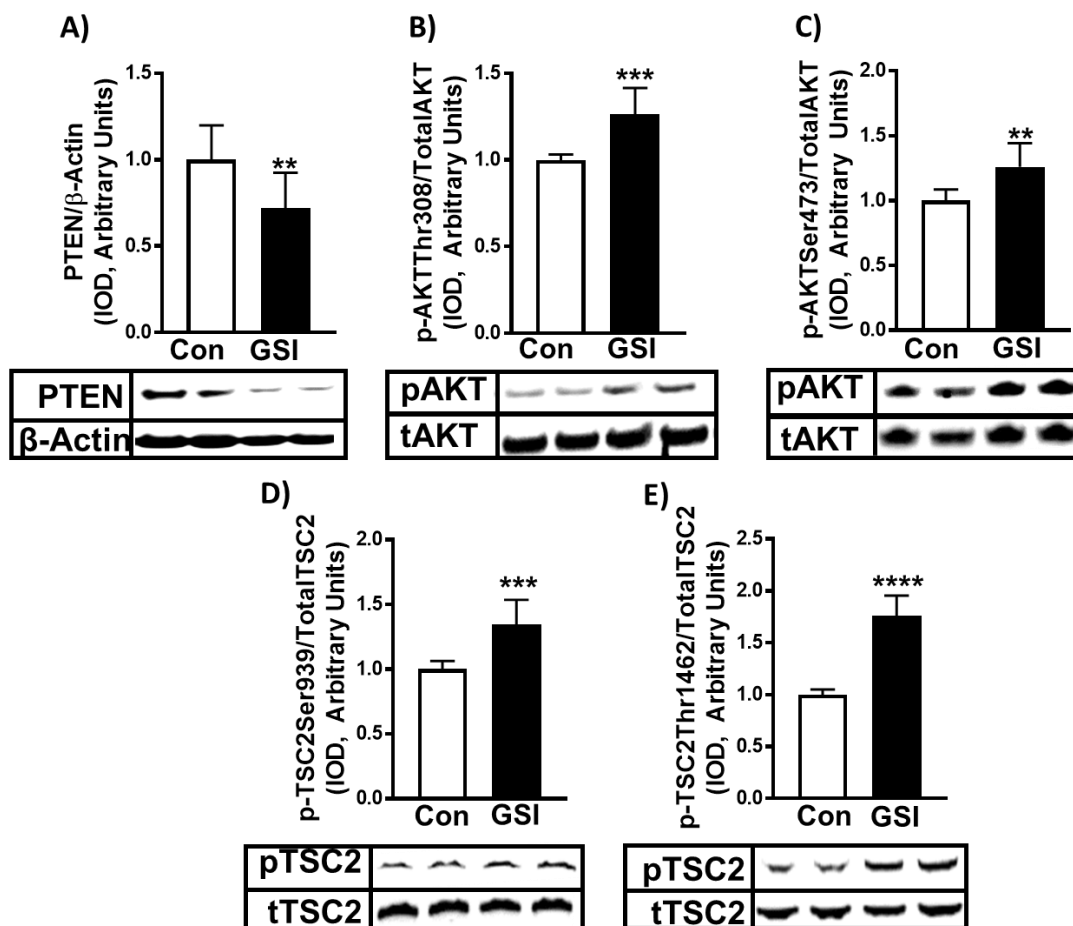


Figure 3.5.9. GSI Treatment Elevates Upstream mTOR Signaling in C2C12 Myotubes. A) Phosphatase and tensin homolog (PTEN)/ β -Actin; B) Phospho (p)-protein kinase B (AKT) Thr308/Total AKT; C) p-AKT Ser473/Total AKT; D) p-tuberous sclerosis complex 2 (TSC2) Ser939/Total TSC2; E) p-TSC2 Thr1462/Total TSC2 expression (Integrated optical density, IOD) in 96-hour myoblasts treated with or without 4 μ M γ -secretase inhibitor (GSI) every 12 hours. 30 minutes prior to collection all cells were treated with 1 μ M puromycin. Data were analyzed using a Student's T-test. ** $p < 0.01$ vs. Control (Con); *** $p < 0.001$ vs. Con; **** $p < 0.0001$ ($n = 3$ experiments). Data are mean \pm SD.

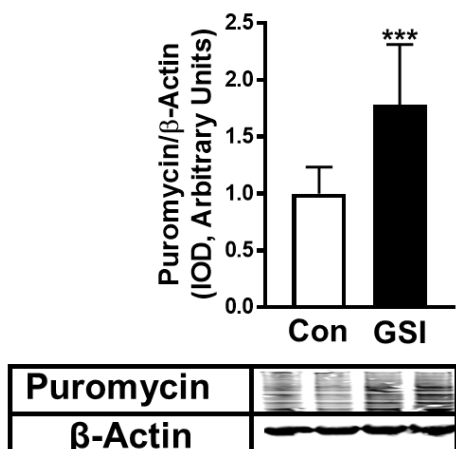


Figure 3.5.10. GSI Treatment Elevates Protein Synthesis in Formed C2C12 Myotubes. Puromycin/β-Actin expression (Integrated optical density, IOD) in 144-hour cultured myotubes. 120-hours post differentiation C2C12 cells were treated every 12 hours with either control (Con) or 4μM γ-secretase inhibitor (GSI). Data were analyzed using a Student's T-test. *** P < 0.001 vs. Con. (n = 2 experiments). Data are mean ± SD.

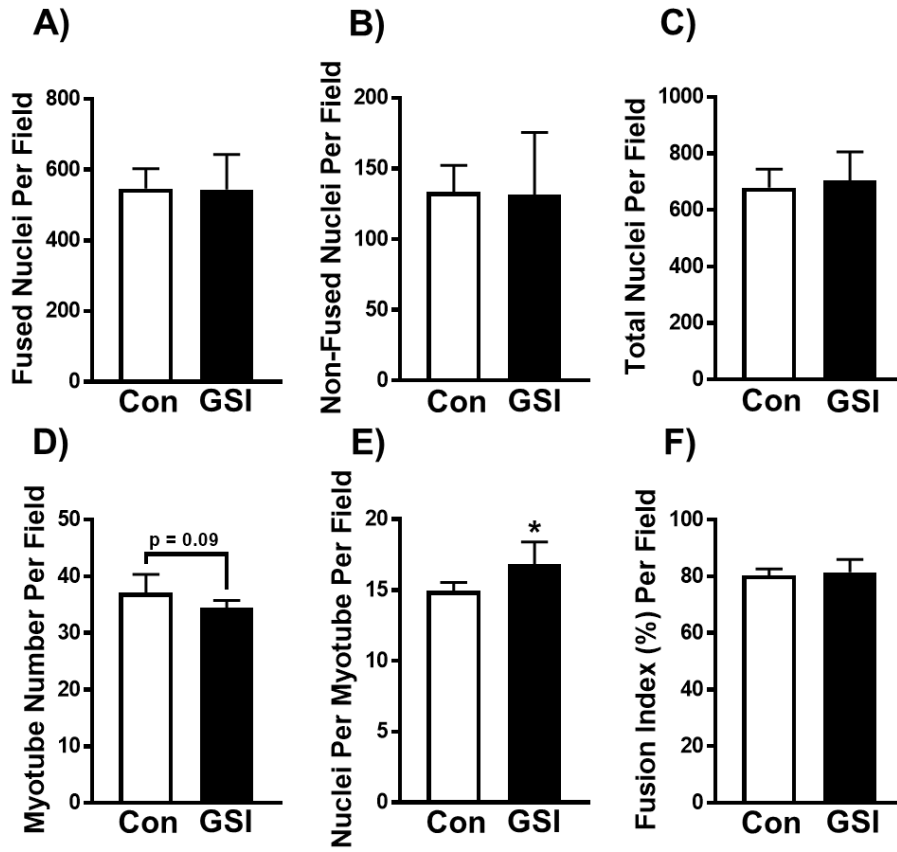


Figure 3.5.11. Effect of GSI Treatment on Indices of Myotube Fusion in Formed C2C12 Myotubes. A) Fused nuclei per field; B) Non-fused nuclei per field; C) Total nuclei per field; D) Myotube number per field; E) Nuclei per myotube per field; F) Fusion index per field in 144-hour cultured myotubes. 120-hours post differentiation C2C12 cells were treated every 12 hours with either control (Con) or 4 μ M γ -secretase inhibitor (GSI). Data were analyzed using a Student's T-test. * $P \leq 0.05$ vs. Con. (n = 2 experiments). Data are mean \pm SD.

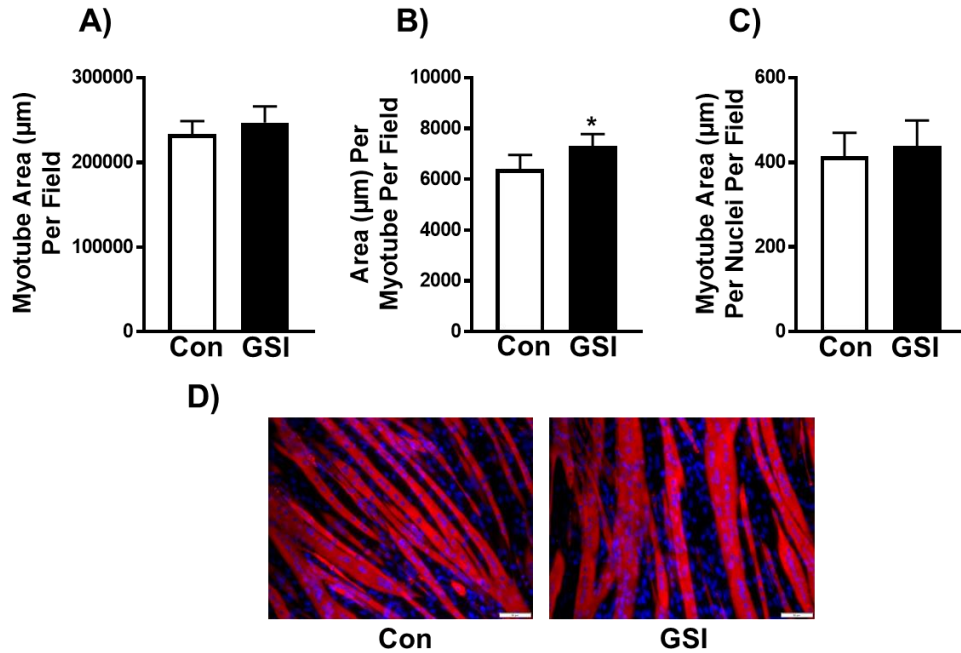


Figure 3.5.12. Effect of GSI Treatment on Indices of Myotube Hypertrophy in Formed C2C12 Myotubes. A) Myotube area (μm) per field; B) Area (μm) per myotube per field; C) Myotube area (μm) per nuclei per field; D) Representative images of 144-hour cultured myotubes. 120-hours post differentiation C2C12 cells were treated every 12 hours with either control (Con) or $4\mu\text{M}$ γ -secretase inhibitor (GSI). Data were analyzed using a Student's T-test. * $P \leq 0.05$ vs. Con. (n = 2 experiments). Data are mean \pm SD.

3.6 Tables

Table 3.6.1 *Antibodies used for Western Blot Analysis.*

| <u>Antibody</u> | <u>Catalog #, Company</u> | <u>Dilution</u> |
|------------------------|----------------------------------|------------------------|
| Hes1 | (#11988, CS) | 1:500 |
| Cleaved Notch | (#4147, CS) | 1:500 |
| PTEN | (#9188, CS) | 1:1000 |
| p-AKT Thr308 | (#13038, CS) | 1:500 |
| p-AKT Ser473 | (#4060, CS) | 1:500 |
| Total AKT | (#2920, CS) | 1:1000 |
| p-TSC2 Ser939 | (#3615, CS) | 1:500 |
| p-TSC2 Thr1462 | (#3617, CS) | 1:500 |
| Total TSC2 | (#4308, CS) | 1:1000 |
| p-mTOR Ser2448 | (#5536, CS) | 1:500 |
| p-mTOR Ser2481 | (#2974, CS) | 1:500 |
| Total mTOR | (#4517, CS) | 1:1000 |
| p-4EBP1 Thr37/46 | (#2855, CS) | 1:500 |
| Total 4EBP1 | (#9644, CS) | 1:1000 |
| p-eEF2 Thr56 | (#2331, CS) | 1:500 |
| Total eEF2 | (#2332, CS) | 1:500 |
| p-p70S6K Thr389 | (#9234, CS) | 1:500 |
| Total p70S6K | (#2708, CS) | 1:1000 |
| Myosin Heavy Chain | (#MF 20, DSHB) | 1:50 |
| Myogenin | (82843, ABcam) | 1:500 |
| Puromycin | (#MABE343EMD Millipore) | 1:5000 |
| Beta Actin | (#A2228, Sigma Aldrich) | 1:10000 |

Hes1: hairy/enhancer of split 1; PTEN: phosphatase and tensin homolog; p: phosphorylated; AKT: protein kinase B; TSC: tuberous sclerosis complex; mTOR: mechanistic target of rapamycin; 4EBP1: eukaryotic initiation factor 4E binding protein; eEF2: eukaryotic elongation factor 2; p70S6K: 70 kDa ribosomal protein S6 kinase; CS: Cell signaling; DSHB: Developmental Studies Hybridoma Bank.

CHAPTER 4: GSI-MEDIATED ELEVATIONS IN PROTEIN SYNTHESIS INDEPENDENT OF AKT AND MTOR

4.1 Introduction

Mechanistic target of rapamycin (mTOR) is essential in a myriad of biological process including cellular differentiation, metabolism, survival and autophagy [44; 163]. mTOR is also critical in the maintenance of skeletal muscle mass, particularly through its pivotal mediation of muscle protein synthesis (MPS) [44; 98; 153]. In recent years mTOR has been identified as a primary antagonist of lifespan with administration of rapamycin (a potent inhibitor of mTOR) increasing lifespan, improving aging, and combatting age-related disease development [164-169]. However, reduced mTOR in skeletal muscle diminishes myogenic potential along with increasing anabolic resistance to exercise and nutrients [170; 171]. This poses an interesting dilemma for skeletal muscle researchers, in particular those seeking to maintain muscle mass in diseased and aged populations.

One tactic to circumvent the mTOR dilemma (MPS and muscle mass vs. longevity) would be to identify signaling pathways that modulate MPS independent of mTOR. One example of this is protein kinase B (AKT), which has been implicated in mediating MPS independent of mTOR via glycogen synthase kinase 3 beta (GSK3B) [172-174]. Interestingly, our lab recently demonstrated that Notch inhibition via γ -secretase inhibitor (GSI) treatment elevates MPS in C2C12 myoblasts and myotubes by modulation of phosphatase and tensin homolog (PTEN)/AKT/mTOR (Chapter 3).

However, it is not known if this mechanism is reliant on mTOR or if Notch is mediating MPS in an AKT-dependent manner. Here we demonstrate that Notch inhibition via GSI treatment mediates MPS independent of both mTOR and AKT.

4.2 Experimental Design and Methods

4.2.1 Cell Culture

The C3H murine cell line C2C12 (ATCC p3-p8) was used for all experiments. For fusion experiments, cells were seeded in growth media (GM: Dulbecco's Modified Eagles Medium [DMEM], 10% fetal bovine serum (FBS), 10% horse serum (HS), and 1% penicillin/streptomycin (P/S)) in 12-well plates at a density of 50,000 cells/well. Cells were grown to ~100% confluence, washed 2x with phosphate buffered saline (PBS), and differentiated for 96 hours in differentiation media (DM: DMEM: 2% HS, 1% P/S) with one of the following experimental treatment setups: 1) 4 μ M γ -secretase inhibitor (GSI: L-685,458; Millipore Sigma- dimethyl sulfoxide [DMSO]), 100nM rapamycin (RAP: 13346; Cayman Chemicals in DMSO), GSI + RAP, or control (Con: DMSO). 2) GSI, 10 μ M 4-Amino-5,8-dihydro-5-oxo-8-b-D-ribofuranosyl-pyrido[2,3-d]pyrimidine-6-carboxamide (API-1: SML1342; Millipore Sigma in DMSO), GSI + API-1, or Con. Cells were treated every 12 hours throughout the 96-hour differentiating period and analyzed for indices of fusion as outlined below. In separate experiments intended for protein expression analysis, cells were seeded in GM into 12-well plates at a density of 50,000 cells/well. Cells were then grown to ~100% confluence, washed 2x with PBS, and differentiated for 72 hours in DM. At 72 hours, cells were treated every 12 hours for 24 hours with one of the following experimental treatment setups: 1) GSI, RAP, GSI + RAP, or Con. 2) GSI, API-1, GSI + API-1, or Con. 3) GSI, RAP+API-1,

GSI+RAP+API-1, or Con. Myotubes were analyzed for protein expression and protein synthesis as detailed below. In separate experiments, cells were seeded into p60 culture dishes and were grown in one of two ways: C2C12 myoblasts (proliferated for 48-hours in GM) and myotubes (96-hours) were collected for protein-protein interactions as outlined below.

4.2.2 Myosin Heavy Chain Staining

Following 96 hours of differentiation, myotubes were labeled with myosin heavy chain (MHC) to determine properties of fusion and area. Briefly, cells were fixed with 70% Acetone/30% Methanol for 10 minutes at room temperature (RT). Following fixation cells were washed 2x with PBS, blocked for 1 hour with 10% normal goat serum (NGS) in PBS, and incubated overnight in MHC. Following overnight incubation (16 hours), cells were washed 3x with PBS, and counter stained with a secondary antibody (1:200) specific to the MHC primary and 4',6-Diamidino-2-Phenylindole, Dihydrochloride (DAPI 1:1000) in PBS for 60 minutes. Wells were mounted with vectashield and a coverslip.

4.2.3 Myotube Fusion and Myotube Area

Following MHC labeling, myotubes were imaged with an Olympus iX inverted microscope at 20x. Images from wells were all taken in the same fashion: 1) the top left of the well was imaged, 2) the stage was moved over three fields of view to the right and imaged, 3) the stage was moved down three fields of view and imaged, 4) the stage was moved over three fields of view to the left and imaged, 5) the stage was moved down three fields of view and imaged, 6) the stage was moved three fields of view to the right and imaged. 6 fields of view per well were captured. Myotube Fusion was determined

by counting the total nuclei, total myotubes, and nuclei fusing into myotubes, by 2 blinded individuals using ImageJ software (cell counter plugin). A myotube was defined as a MHC labeled cell containing two or more nuclei. All myosegments (MHC labeled without two or more nuclei) were ignored as myotubes in the fusion index and area quantification. Fusion index was calculated by nuclei within myotubes/total nuclei. Myotube area was determined from the same images used to calculate fusion, using Adobe Photoshop as previously described [156]. Briefly, three random images from each group (Con, GSI, RAP, GSI+RAP or Con, GSI, API-1, GSI+API-1) were used to set a color range (accepted tones of red (for MHC) and blue (for DAPI)). The established color range was then applied to all experiment images, a measurement scale was set (pixels to microns) and measurements were obtained for total myotube area, area per myotube, and myotube area per fused nuclei.

4.2.4 Protein Synthesis

For protein synthesis measurements, the SUnSET method using puromycin was used as previously described [82; 85]. Briefly, 30 minutes prior to collection, C2C12 cells were treated with 1 μ M puromycin (P-1033, A.G. Scientific). Puromycin incorporation was determined via western blot analysis as described below.

4.2.5 Western Blot

Collection and preparation of C2C12s was done as previously described for western blot analysis [155]. Briefly, C2C12 myotubes were washed 2x with ice cold PBS followed by addition of ice cold Radioimmunoprecipitation assay buffer (sc-24948; Santa Cruz, supplemented with 1% Triton-x, 2% SDS, protease cocktail inhibitor) for 5 minutes. Wells were scraped, mechanically lysed (using a 25 gauge-needle-syringe), and

centrifuged for 20 minutes at 20,000G (4°C). Protein concentration of the supernatant was determined by Pierce BCA kit (23225; ThermoFisher). 20ug of sample was loaded onto a 4-12% Bis-Tris gel (3450125; Bio-Rad) and run (XT MES running buffer; 1610789; Bio-Rad) at 125V for 2 hours. Following electrophoresis, proteins were transferred (Towbin Buffer; 10% methanol) onto a .22uM Polyvinylidene difluoride (PVDF) membrane for 1 hour at 100V. Membranes were washed 1x in Tris-buffered saline (TBS) and blocked for 1 hour in Odyssey blocking buffer 1:1 with TBS. Following blocking, membranes were incubated overnight (16 hours) in primary antibodies (Table 4.6.1). The next day membranes were washed 3 x 5 minutes in TBST (TBS: 0.1% Tween 20) and then incubated in secondary antibodies (1:10,000 in TBST) for 1 hour. Following 3 x 5 minute washes in TBST and 1 x 5 min wash in TBS, membranes were imaged and bands were quantified using the Odyssey® Licor CLx System.

4.2.6 Co-immunoprecipitation

Co-immunoprecipitation was performed using both the Dynabeads® Protein A (10006D, ThermoFisher Scientific) and Dynabeads® M-270 Epoxy (14321D, ThermoFisher Scientific) kits to test for protein-protein interactions between hairy/enhancer of split-1 (Hes1)-PTEN, notch intracellular domain (NICD)-mTOR, and avian myelocytomatosis viral oncogene homolog (c-Myc)-tuberous sclerosis complex (TSC). For co-immunoprecipitation with Dynabeads® Protein A samples were washed twice with ice-cold PBS and collected on ice in NP40 lysis buffer (FNN0021, Invitrogen) supplemented with protease and phosphatase inhibitors followed by periodic pipetting during a 20 minute incubation on ice. Samples were then lightly spun (500G) for 5 minutes at 4°C,

transferred to a clean ice-cold tube, and were immediately used for co-immunoprecipitation. Samples were incubated (on roller) with antibodies (Table 4.6.2) overnight for 16 hours at 4°C. The next day, 100µL of dynabeads were washed twice with NP40 lysis buffer, added to the sample-ab complex, and incubated (on roller) for 4 hours at 4°C. Following the 4 hour incubation, the dynabeads-sample-ab complex was placed on a magnet, and underwent a series of washes, ended by eluting the antibody bound sample from the beads. SDS-Polyacrylamide gel electrophoresis and western blot analysis for co-immunoprecipitation of proteins was done as previously described above. For co-immunoprecipitation with Dynabeads® M-270 Epoxy cells were washed twice with ice-cold PBS, gently scraped (on ice) and transferred to a pre-chilled tube. The cells were then centrifuged (4°C) at 200G for 5 minutes and the supernatant was discarded. 9 volumes of extraction buffer (Nanopure H₂O: 1X IP Buffer from kit; 100mM NaCl; 2mM MgCl₂; 1mM DTT) supplemented with protease and phosphatase inhibitors was added to the pellet. Samples were then incubated on ice for 20 minutes with periodic pipetting, followed by centrifugation (4°C) at 500G for 5 minutes. The supernatant was then transferred to a pre-chilled tube and immediately used for co-immunoprecipitation. Samples were added to 1.5mg of antibody-coupled Dynabeads® M-270. For antibody coupling, the beads were incubated (rolling) with the appropriate antibody (Table 4.6.2) for 24 hours at 37°C. The sample-antibody-beads complex was incubated (rolling) for 1 hour at 4°C. Following the incubation the samples were placed on a magnet and underwent a series of washes, ending with elution of the antibody bound sample. Samples then underwent SDS-Polyacrylamide gel electrophoresis and western blot as previously described to assess interactions.

4.2.7 Statistical Analysis

One-way analysis of variance (ANOVA) tests were performed to determine difference between experimental groups (1) GSI, RAP, GSI + RAP, or Con. 2) GSI, API-1, GSI + API-1, or Con. 3) GSI, RAP+API-1, GSI+RAP+API-1, or Con). Post-hoc comparisons were accomplished via a Tukey's test, with statistical significance set *a priori* at $p \leq 0.05$. All statistical analyses and graphs were made using Graphpad Prism 7.03 (GraphPad, San Diego, CA, USA). All data are presented as means \pm SD.

4.3 Results

4.3.1 A lack of protein-protein interactions between Notch and mTOR signaling

There was no protein-protein interaction found between any of the postulated cross-talk sites including Hes1-PTEN, c-Myc-TSC, or NICD-mTOR in either C2C12 myoblasts or myotubes (Figure 4.5.1).

4.3.2 Rapamycin ablates GSI-mediated elevations in myotube formation

GSI treatment significantly increased ($p \leq 0.05$) several indices of myotube formation compared to all groups (Con, RAP, GSI+RAP) including fused nuclei per field, nuclei per myotube per field, and fusion index per field (Figure 4.5.2A-F). GSI treatment also resulted in significantly reduced ($p \leq 0.05$) non-fused nuclei compared to all other groups. RAP significantly reduced ($p \leq 0.05$) fused nuclei, nuclei per myotube, and fusion index compared to Con, but did not differ ($p > 0.05$) from GSI+RAP in any of these measures. Both RAP and GSI+RAP had significantly elevated ($p \leq 0.05$) non-fused nuclei compared to Con, but did not differ from each other. Total nuclei per field was significantly increased in RAP and GSI+RAP compared to Con and GSI, but did not differ from each other ($p > 0.05$). Total nuclei also did not differ ($p > 0.05$) between Con

and GSI. Myotube number was significantly reduced ($p \leq 0.05$) in RAP and GSI+RAP compared to Con and GSI. RAP and GSI+RAP were not different ($P > 0.05$) in myotube number, nor were Con and GSI. Total myotube area was significantly increased ($p \leq 0.05$) in GSI compared to all groups (Figure 4.5.3A-D). Both RAP and GSI+RAP were reduced ($p \leq 0.05$) compared to Con, but were not different from each other ($p > 0.05$). The same was true of both area per myotube and myotube area per fused nuclei with GSI significantly increased ($p \leq 0.05$) above all other groups, RAP and GSI+RAP were reduced ($p \leq 0.05$) compared to Con, with no difference between RAP and GSI+RAP ($p > 0.05$).

4.3.3 GSI mediates protein synthesis independent of mTOR

Phosphorylated (p) mTOR at Ser2448 was significantly elevated in ($p \leq 0.05$) in GSI compared to all other groups (Con, RAP, GSI+RAP) (Figure 4.5.4A). RAP and GSI+RAP displayed reduced ($p \leq 0.05$) pmTORSer2448 compared to Con, but did not differ from each other ($p > 0.05$). pEF2Thr56 was increased ($p \leq 0.05$) in RAP and GSI+RAP relative to Con and GSI groups (Figure 4.5.4B). No differences occurred ($p > 0.05$) in pEF2Thr56 between RAP and GSI+RAP or Con and GSI. RAP and GSI+RAP had reduced expression ($p \leq 0.05$) of pp70S6KThr389 compared to Con and GSI (Figure 4.5.4C). Similar to eEF2, there were no differences ($p > 0.05$) in pp70S6KThr389 between RAP and GSI+RAP or Con and GSI. Interestingly, there was no difference ($p > 0.05$) in p4EBP1Thr37/46 expression between RAP or GSI+RAP compared to Con (Figure 4.5.4D). The only difference in p4EBP1Thr37/46 expression was between GSI and RAP ($p \leq 0.05$). Protein synthesis was elevated ($p \leq 0.05$) in GSI compared to all other groups (Figure 4.5.5). RAP exhibited reduced protein synthesis ($p \leq 0.05$)

compared to Con. Interestingly, protein synthesis of RAP treated cells was also lower than GSI+RAP treated cells ($p \leq 0.05$). Intriguingly, GSI+RAP treated cells did not differ from Con ($p > 0.05$).

4.3.4 API-1 ablates GSI-mediated elevations in myotube formation

In concert with previous experiments, GSI treatment increased all measured markers of myotube formation and fusion compared to all other groups (Con, API-1, GSI+API-1). Fused nuclei, nuclei per myotube, and fusion index were all elevated ($p \leq 0.05$) in GSI treated cells compared to all other groups (Figure 4.5.6A-F). API-1 and GSI+API-1 showed lower fused nuclei, nuclei per myotube, and fusion index compared to Con ($p \leq 0.05$), but did not differ from each other ($p > 0.05$). There was also a slight reduction in non-fused nuclei in GSI compared to Con ($p \leq 0.05$), however no other significant differences ($p > 0.05$) occurred between the other 3 groups. The lack of difference in non-fused nuclei between groups is likely due to the significant reduction seen in total nuclei with API-1 and GSI+API-1 treatment. Total nuclei per field was higher in Con and GSI compared to API-1 and GSI+API-1 ($p \leq 0.05$). Total nuclei did not differ ($p > 0.05$) between Con and GSI or between API-1 and GSI+API-1. Myotube number was significantly reduced ($p \leq 0.05$) in API-1 and GSI+API-1 compared to Con and GSI. API-1 and GSI+API-1 were not different ($P > 0.05$) in myotube number, nor were Con and GSI. Total myotube area was significantly increased ($p \leq 0.05$) in GSI-treated cells compared to all groups (Figure 4.5.7A-D). Both API-1 and GSI+API-1 were reduced ($p \leq 0.05$) compared to Con, but were not different from each other ($p > 0.05$) in total myotube area. The same was true of both area per myotube and myotube area per fused nuclei with GSI significantly increased ($p \leq 0.05$) above all other groups, API-1 and

GSI+API-1 reduced ($p \leq 0.05$) compared to Con, with no difference between API-1 and GSI+API-1 ($p > 0.05$).

4.3.5 GSI mediated increases in mTOR is halted by API-1

GSI-treated cells had significantly increased ($p \leq 0.05$) phosphorylation of AKT on Thr308 and Ser473 compared to all other groups (Con, API-1, GSI+API-1) (Figure 4.5.8A&B). Interestingly, API-1 or GSI+API-1 treatment did not reduce pAKTThr308 compared to Con or GSI ($p > 0.05$). API-1 and GSI+API-1 were not different ($p > 0.05$) from each other in pAKTThr308. Both API-1 and GSI+API-1 reduced ($p \leq 0.05$) pAKTSer473 compared to Con but were not different from each other ($p > 0.05$). GSI-treatment significantly elevated ($p \leq 0.05$) pmTORSer2448 compared to Con, API-1, and GSI+API-1 (Figure 4.5.9A). Intriguingly, API-1 and GSI+API-1 did not significantly lower ($p > 0.05$) pmTORSer2448 compared to Con, nor were they different from each other. Phosphorylation of eEF2 on Thr56 did not differ ($p > 0.05$) between Con and GSI (Figure 4.5.9B). API-1 treatment did lead to an increase ($p \leq 0.05$) in peEF2Thr56 compared to both Con and GSI. API-1 did not differ from GSI+API-1 in peEF2Thr56. GSI treatment reduced peEF2 compared to GSI+API-1 ($p \leq 0.05$), while a reduction in Con (compared to GSI+API-1) was trending ($p = 0.053$). Similar to previous works from our lab, pp70S6KThr389 was not increased ($p > 0.05$) in GSI compared to Con, nor was GSI different ($p > 0.05$) than API-1 (Figure 4.5.9C). Interestingly, pp70S6KThr389 was reduced ($p \leq 0.05$) in GSI+API-1 compared to both Con and GSI, but was not different ($p > 0.05$) from API-1. There were also no significant differences between any of the groups (Con, GSI, API-1, or GSI+API-1) in p4EBP1Thr37/46, however GSI was trending upward compared to Con ($p = 0.09$) (Figure 4.5.9D). Protein synthesis was

increased ($p \leq 0.05$) in GSI compared to all other groups (Figure 4.5.10). API-1 and GSI+API-1 treatment was not sufficient to reduce protein synthesis compared to Con ($p > 0.05$). API-1 and GSI+API-1 were also not significantly different from each other ($p > 0.05$).

4.3.6 GSI elevates protein synthesis independent of AKT and mTOR

Interestingly, there is an apparent rescue in phosphorylation of GSK3 β on Ser9 with GSI. GSI treated cells demonstrated elevations in pGSK3 β Ser9 compared to Con, API-1 and GSI+API-1 ($p \leq 0.05$) (Figure 4.5.11A). API-1 significantly reduced pGSK3 β Ser9 compared to Con ($p \leq 0.05$). An intriguing finding was that pGSK3 β Ser9 was elevated in GSI+API-1 compared to API-1 ($p \leq 0.05$), but was not different compared to Con ($p > 0.05$). Active β -catenin (ABC) followed a similar trend to pGSK3 β Ser9. GSI treatment increased ABC expression compared to all other groups ($p \leq 0.05$) (Figure 4.5.11B). API-1 treatment reduced ABC expression compared to both Con and GSI+API-1 ($p \leq 0.05$). GSI+API-1 was also reduced compared to Con ($p \leq 0.05$). The rescue of pGSK3 β ser9 with GSI in the presence of API-1 enticed us to observe protein synthesis under treatment of GSI, RAP, and API-1 together. As expected, GSI treatment increased ($p \leq 0.05$) protein synthesis compared to all other groups (Con, RAP+API-1, GSI+RAP+API-1) (Figure 4.5.12). RAP+API-1 significantly reduced protein synthesis compared to Con ($p \leq 0.05$). However, protein synthesis in RAP+API-1 was also reduced compared to GSI+RAP+API-1 ($p \leq 0.05$). GSI+RAP+API-1 was not different from Con ($p > 0.05$).

4.4 Discussion and Conclusion

Our lab recently demonstrated that notch inhibition via GSI treatment elevates protein synthesis in C2C12 muscle cells possibly through PTEN/AKT/mTOR. Despite extensive research on Notch signaling within skeletal muscle, we have been the first to investigate its impact on muscle growth via MPS. Though our findings indicated that GSI treatment elevated MPS, it was unclear whether or not the elevation in MPS was dependent upon mTOR, or if AKT was the mediator. The novel finding of the present study demonstrates that GSI mediated elevations in MPS are not only independent of mTOR, but that GSI treatment may also elevate MPS independent of AKT possibly through regulation of GSK3 β .

Notch which is steadily revealing itself as a molecular brake on muscle growth is a cell to cell communication pathway that is activated upon binding of a Notch transmembrane receptor (Notch1-4) to a transmembrane ligand for Notch (Delta-like protein (DLL) 1, DLL 3, DLL4, Jagged1, and Jagged2). The receptor ligand interaction stimulates a mechanical pull inducing a series of cleavages driven by metalloproteases and γ -secretases. The cleavages lead to the release of Notch intracellular domain (NICD) which can then translocate to the nucleus and induce expression of target genes including Hes1, hairy/enhancer-of-split related with YRPW motif protein 1 (Hey1), and avian myelocytomatosis viral oncogene homolog (Myc) [10; 22; 175; 176].

Use of γ -secretase inhibitors (GSIs) is a widely used method to chemically inhibit Notch signaling. Our group and others have demonstrated that use of GSI is sufficient to not only reduce Notch signaling but also to increase myotube formation and muscle growth (Chapter 3) [48; 177]. One goal of the present study was to determine if the GSI-

mediated elevations in myotube formation and growth was dependent on mTOR. mTOR is a pivotal regulator of the latter stages of myogenesis, particularly the onset of differentiation and maturation of forming myotubes [30-32]. It was intriguing to us that Notch is a known inhibitor of myotube formation, yet no one had investigated whether Notch acts through mTOR to elevate myogenesis. Here we show that GSI treatment significantly elevates a myriad of fusion and hypertrophy indices (including fusion index, area/myotube, and myotube area/fused nuclei) in C2C12 myotubes and that all of these elevations are completely ablated by the introduction of rapamycin, a mTOR inhibitor (Figures 4.5.2 & 4.5.3). This is in full support of the notion that mTOR is required for muscle cell differentiation and supports the notion that Notch acts through mTOR in its regulation of myogenesis. Previous literature had demonstrated that Notch has an inhibitory effect on myotube formation though the exact mechanism has remained elusive as several Notch effectors (Hes1/MyoD, Hey, MyoR (Musculin) have shown to blunt myogenesis [35; 36]. It is plausible that the key mediator of Notch's effects on myogenesis is mTOR.

Given the negating effect that rapamycin had on GSI-mediated elevations in C2C12 hypertrophy, we speculated that rapamycin would also abrogate GSI-mediated elevations in protein synthesis. An intriguing discovery was that GSI+RAP treatment together rescued the inhibition in protein synthesis seen with RAP treatment (Figure 4.5.4E), bringing protein synthesis back to basal control levels. This finding demonstrated that GSI may mediate protein synthesis through AKT rather than mTOR. Our previous findings did indicate that GSI treatment modulates PTEN/AKT/mTOR signaling in both C2C12 myoblasts and myotubes, highlighting a possibility that AKT is

the true mediator of Notch. Furthermore, AKT is known to elevate protein synthesis independent of mTOR through regulation of GSK3 β [172; 178]. It is plausible that mTOR phosphorylation is just a product of Notch acting on PTEN/AKT, and though mTOR is necessary for cellular differentiation and fusion, inhibiting Notch with a GSI may be an interesting approach alongside rapamycin treatment.

We then sought out to verify that Notch acts through AKT in its mediation of myotube formation and MPS. Co-treatment experiments with API-1 and GSI showed similar results to the RAP and GSI experiments. Again, GSI treatment augmented myotube formation, fusion index, nuclei/myotube (Figures 4.5.5 & 4.5.6), myotube area, area per myotube, and myotube area per fused nuclei all of which we have seen in previous experiments (Chapter 3; Figures 4.5.2 & 4.5.3). All myotube fusion and hypertrophy enhancements were diminished in the presence of API-1. In fact API-1 treatment had the same impact as RAP, with the exception of cellular turnover (as indicated by total nuclei/field). The reduced nuclei/field with API-1 is an expected outcome as AKT is a known pro-survival signaling pathway and API-1 has shown to induce apoptosis [179-181]. Despite their being no difference in non-fused nuclei between groups, fusion index and nuclei/myotube were still reduced with API-1 and GSI+API-1. Our findings are in concert with previous literature showing that AKT is essential for the initiation of myoblast differentiation [182]. These results further elude to AKT as the focal point of GSI-mediated elevations in myotube formation and MPS.

AKT has been identified not only has a key modulator of mTOR dependent-protein synthesis, but also is able to elevate protein synthesis independent of mTOR through its phosphorylation (Ser9) and inactivation of GSK3 β [172; 178]. Under active

conditions, GSK3 β inhibits the translation initiation factor eIF2B, in particular the catalytic subunit eIF2B ϵ (via phosphorylation) [174; 178]. When phosphorylated by AKT on Ser9, GSK3 β activity is reduced and its inhibitory phosphorylation on eIF2B ϵ subsides allowing for an increase in eIF2B ϵ functionality and subsequent translation initiation [183]. After the present findings that GSI was able to increase protein synthesis independent of mTOR, the working hypothesis was that GSI treatment was acting primarily via AKT and thus increasing GSK3 β Ser9 resulting in an increase in protein synthesis.

To inhibit AKT we used API-1, a novel small molecule inhibitor that has been gaining research attention in recent years as a possible therapeutic in cancerous states. While several publications have reported a reduction in pAKTSer473, to our knowledge no one has yet to report whether both phosphorylation sites (Thr308 and Ser473) are reduced with API-1 treatment. In concert with others, pAKTSer473 was significantly reduced in the presence of API-1 (Figure 4.5.7) [184-187]. Interestingly, pAKTThr308 was not reduced by API-1 (Figure 4.5.7). This in part, could explain why we did not observe reductions in mTOR signaling or protein synthesis with API-1 treatment (Figure 4.5.8). Though others have reported that reductions in AKT can blunt protein synthesis, there are several other proteins that influence mTOR independent of AKT, which could explain why use of API-1 is not sufficient enough to reduce protein synthesis [44; 163; 188]. In contrast, API-1 treatment did reduce another downstream target of AKT, pGSK3 β Ser9 and subsequent ABC protein expression, demonstrating that use of API-1 does negatively influence AKT function (Figure 4.5.9).

However, given that the underlying premise of this study was to gain better insight into the mechanism by which GSI treatment elevates protein synthesis, and since API-1 alone was not sufficient to reduce protein synthesis, we decided to conduct an additional experiment set introducing API-1 and RAP together. As expected, co-treating C2C12 myotubes with API-1 and RAP significantly reduced protein synthesis (Figure 4.5.10). In light of what we had previously seen with GSI treatment and the rescue of protein synthesis in the presence of RAP, we had fully expected that GSI treatment (Notch inhibition) was acting through AKT. A novel discovery in the present study was that GSI treatment was able to rescue protein synthesis rate in the presence of both API-1 and RAP, suggesting that GSI mediates protein synthesis independent of both AKT and mTOR. The elevation in protein synthesis with GSI treatment in the presence of both RAP and API-1 may be dependent on GSK3 β . As mentioned above, pGSK3 β Ser9 was significantly reduced with API-1 treatment. Interestingly, pGSK3 β Ser9 was rescued with GSI treatment in the presence of API-1, suggesting that Notch may act on GSK3 β independent of AKT (Figure 4.5.9). In concert with this finding, ABC was also rescued with GSI treatment indicating that function of GSK3 β may be independently impaired by Notch. This is not the first time that GSK3 β and Notch cross-talk has been postulated. Several studies outside of skeletal muscle research (including smooth muscle cells and fibroblasts) have identified Notch as a target of GSK3 β , by which GSK3 β serves to phosphorylate Notch [189-191]. Interestingly, these studies have differed on whether GSK3 β serves to activate or inhibit Notch signaling. Whether or not Notch regulates GSK3 β is a less studied area. One study within skeletal muscle did discuss a regulatory role of Notch on GSK3 β . Brack *et al* discussed GSK3 β as a mediator between Notch and

Wnt during skeletal muscle regeneration with Notch inhibition elevating pGSK3 β Ser9 similar to our present findings [28]. However, they failed to discuss GSK3 β as a mediator of protein synthesis and did not address that Notch may impact MPS via GSK3 β . GSK3 β is a known regulator of MPS and overexpression of its downstream target eIF2 β has shown to significantly increase rates of MPS and induce muscle hypertrophy [178; 192]. Additionally, Notch signaling has been implicated in regulating muscle hypertrophy in both in vivo and in vitro models [23; 24; 48; 127], however Notch regulation over MPS was an ignored topic until our lab's recent investigations (Chapters 2 and 3). To our knowledge we are the first to address the research paradigm of Notch as a regulator of MPS and have shown for the first time that Notch (via GSI treatment) may modulate protein synthesis independently of mTOR and AKT.

A negative finding of this study was that we were unable to demonstrate protein-protein interactions between the Notch and mTOR pathways. Our prior findings that GSI-treatment elevated MPS via apparent modulation of the PTEN/AKT/mTOR signaling cascade led us to postulate that a protein-protein interaction would exist somewhere between the two pathways (Notch and mTOR). Literature outside of skeletal muscle led us to investigate protein-protein interactions between Hes1-PTEN, c-Myc-TSC2, and NICD-mTOR [45; 46; 154]. Though we did not uncover interactions between these sites, we still postulate that an interaction may exist. Normal C2C12 cellular conditions may not be optimal to determine interactions of Notch-related proteins. NICD has a half-life of only 3 hours, so it is entirely plausible that any interactions of Notch proteins would have been missed in the current study [193; 194]. A better approach to investigating Notch protein interactions would be to overexpress Notch signaling, either

through ligand-induced activation or genetic manipulation preventing Notch degradation. It is entirely possible that protein-protein interactions between Hes1-PTEN, c-Myc-TSC2, or NICD-mTOR would still not be identified in cases of overexpressed Notch signaling, especially if the mode of action is via GSK3 β . Literature outside of skeletal muscle has shown protein-protein interactions between GSK3 β and NICD directly via an interaction with the Notch1 coactivator MAML1 [190; 195; 196]. Interestingly, recent data has indicated a possible non-canonical role by which cytosolic Notch (via generation of a membrane tethered Notch1) may inhibit GSK3 β function. This opens up another plausible approach to test for protein-protein interactions and roles of Notch occurring in the cytosol, one of which may be with GSK3 β .

One puzzling finding from our lab's prior work was that 4EBP1 was the only downstream effector of mTOR that was altered in a protein synthesis positive fashion with Notch inhibition. This could be due to the fact that the mode of action is truly through GSK3 β . In fact, recent studies within cancer cell lines have implicated GSK3 β directly in the phosphorylation of 4EBP1 [197; 198]. Though in the instances just mentioned, GSK3 β had a positive influence on 4EBP1, it is plausible that GSK3 β has differing effects on 4EBP1 in skeletal muscle. We had also previously postulated that GSI treatment modulated the PTEN/AKT/mTOR cascade in its elevation of MPS. It is still plausible that this is the case, however, interestingly GSK3 β has been implicated in regulating PTEN stabilization [199; 200]. So it is also plausible that GSI treatment induces changes in GSK3 β which results in modulation of PTEN/AKT/mTOR.

This study further elucidated the mechanistic braking effect that Notch signaling has on MPS. We demonstrated that GSI treatment increases MPS in C2C12 myotubes

independently of AKT and mTOR, possibly through regulation of GSK3 β . GSI treatment may elevate MPS via several routes including PTEN/AKT/mTOR and GSK3 β . These findings warrant investigation on the roles of Notch in muscle wasting conditions, in particular instances in which tumor suppressing drugs (Rapamycin, API-1) are used, as targeting Notch may elevate MPS and help to sustain skeletal muscle mass.

4.5 Figures

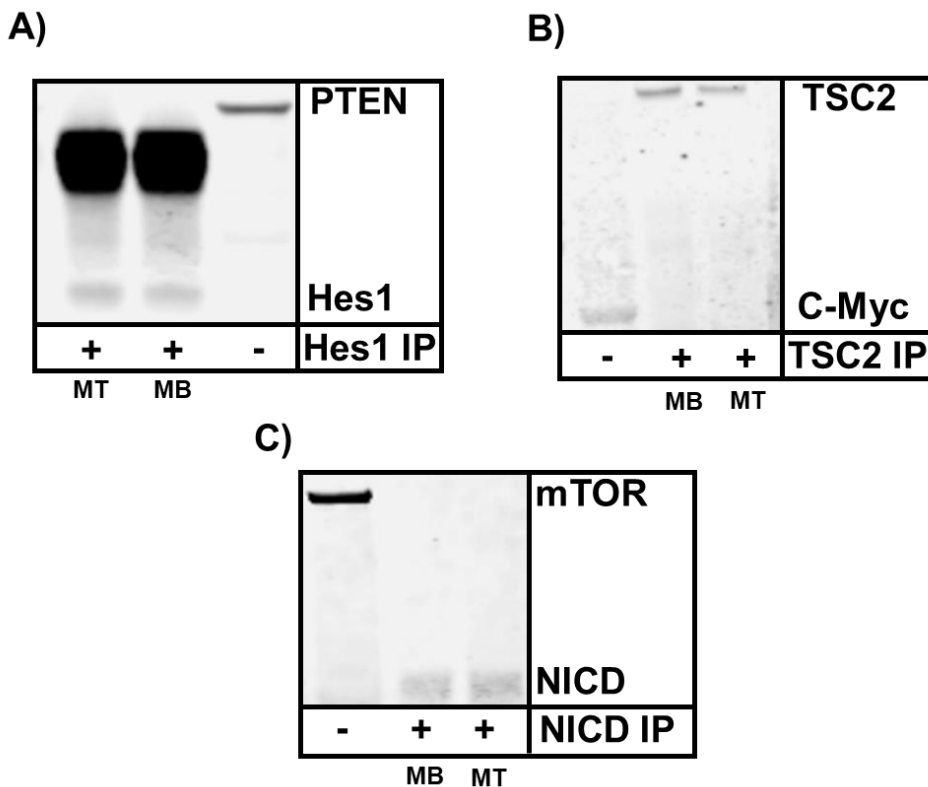


Figure 4.5.1. Immunoprecipitation in C2C12 Myoblasts and Myotubes. A) Phosphatase and tensin homolog (PTEN)- hairy/enhancer of split 1 (Hes1); B) Tuberous sclerosis complex 2 (TSC2)- c-avian myelocytomatosis viral oncogene homolog (Myc); C) mechanistic target of rapamycin (mTOR)-notch intracellular domain (NICD) representative western blots for protein-protein interactions. 48-hour myoblasts (MBs) and 96-hour myotubes (MTs) were collected for co-immunoprecipitation analysis. No protein-protein interactions were found between PTEN-Hes1, TSC2-c-Myc, or mTOR-NICD (n = 6 experiments).

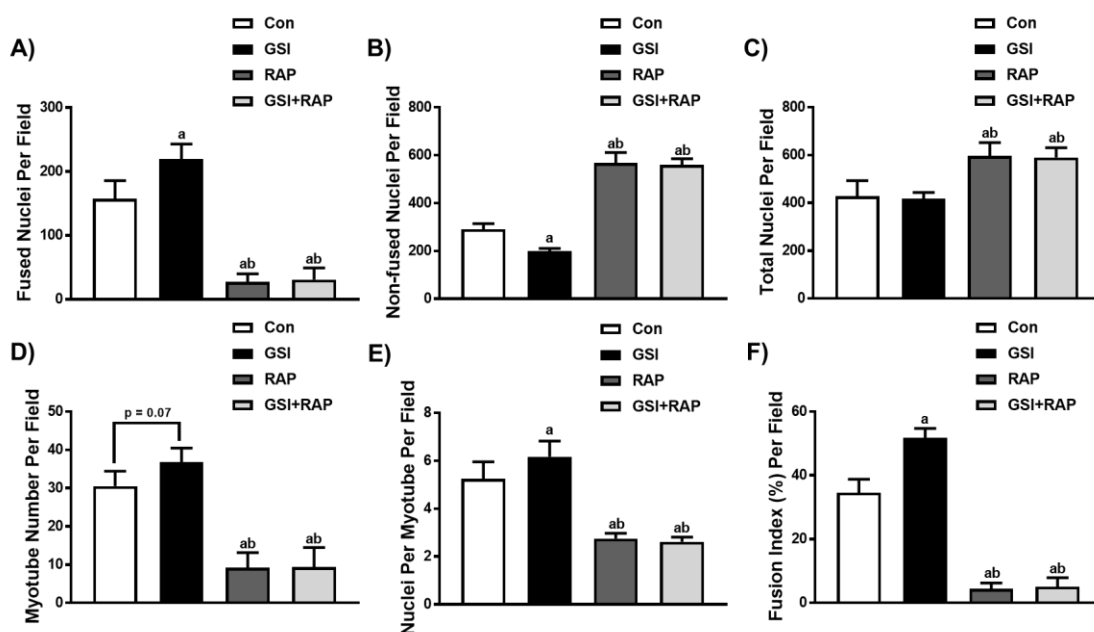


Figure 4.5.2. Indices of Fusion in C2C12 Myotubes with GSI and RAP. A) Fused nuclei per field; B) Non-fused nuclei per field; C) Total nuclei per field; D) Myotube number per field; E) Nuclei per myotube per field; F) Fusion index per field in 96-hour cultured myotubes. At the onset of differentiation C2C12 cells were treated every 12 hours with either control (Con), 4 μ M γ -secretase inhibitor (GSI), 100nM rapamycin (RAP), or GSI + RAP co-treatment. Data were analyzed using a one-way ANOVA followed by Tukey's multiple comparison test. a: significantly ($p \leq 0.05$) different than Con; b: significantly different than GSI ($n = 2$ experiments). Data are mean \pm SD.

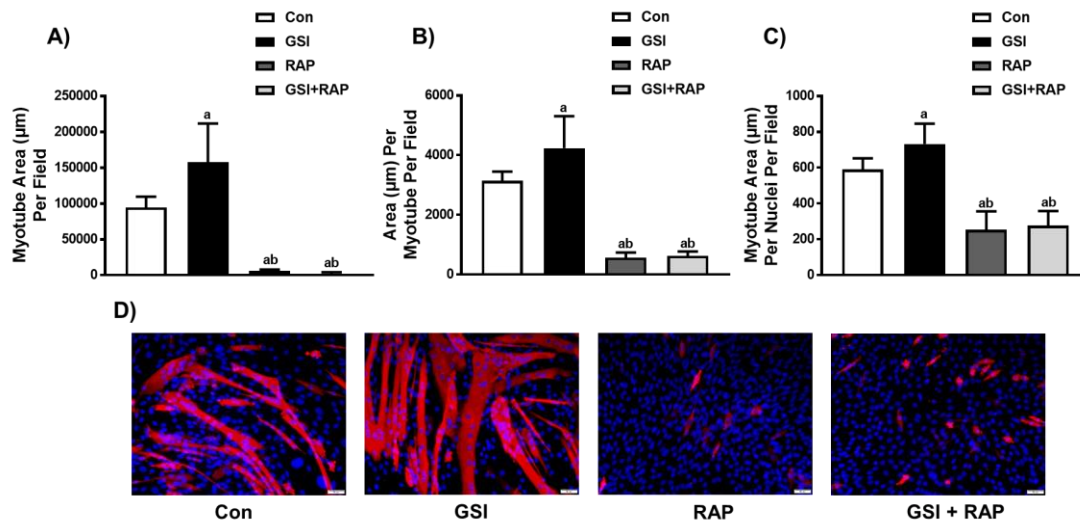


Figure 4.5.3. Indices of Hypertrophy in C2C12 Myotubes with GSI and RAP. A) Myotube area (μm) per field; B) Area (μm) per myotube per field; C) Myotube area (μm) per nuclei per field; D) Representative images of 96-hour cultured myotubes. At the onset of differentiation C2C12 cells were treated every 12 hours with either control (Con), $4\mu\text{M}$ γ -secretase inhibitor (GSI), 100nM rapamycin (RAP), or GSI + RAP co-treatment. Representative images are taken at 20x. Data were analyzed using a one-way ANOVA followed by Tukey's multiple comparison test. a: significantly ($p \leq 0.05$) different than Con; b: significantly different than GSI ($n = 2$ experiments). Data are mean \pm SD.

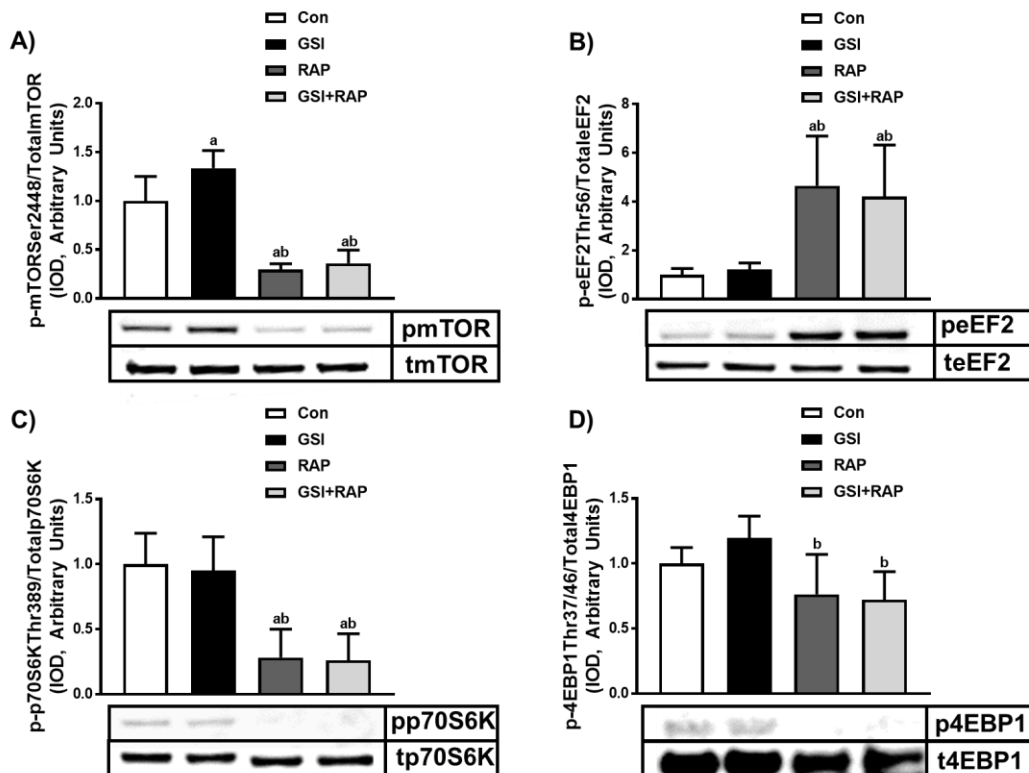


Figure 4.5.4. mTOR Signaling in Cultured C2C12 Myotubes with GSI and RAP. A) Phospho (p)- mechanistic target of rapamycin (mTOR) Ser2448/Total mTOR; B) p- eukaryotic elongation factor 2 (eEF2) Thr56/Total eEF2; C) p-70 kDa ribosomal protein S6 kinase (p70S6K) Thr389; D) p- eukaryotic initiation factor 4E binding protein (4EBP1) Thr37/46/Total 4EBP1 expression (Integrated optical density, IOD) in 96-hour myotubes. 72 hours post-differentiation, C2C12 cells were treated every 12 hours with either control (Con), 4 μ M γ -secretase inhibitor (GSI), 100nM rapamycin (RAP), or GSI + RAP co-treatment until 96 hours post-differentiation. 30 minutes prior to collection all cells were treated with 1 μ M puromycin. Data were analyzed using a one-way ANOVA followed by Tukey's multiple comparison test. a: significantly ($p \leq 0.05$) different than Con; b: significantly different than GSI ($n = 2$ experiments). Data are mean \pm SD.

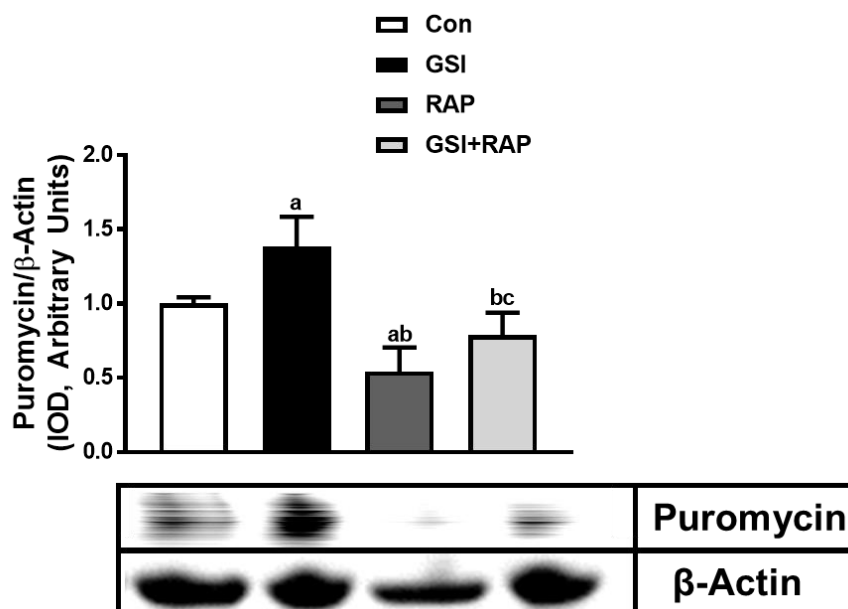


Figure 4.5.5. Muscle Protein Synthesis Rate in Cultured C2C12 Myotubes with GSI and RAP. Puromycin/β-Actin expression (Integrated optical density, IOD) in 96-hour myotubes. 72 hours post-differentiation, C2C12 cells were treated every 12 hours with either control (Con), 4μM γ-secretase inhibitor (GSI), 100nM rapamycin (RAP), or GSI + RAP co-treatment until 96 hours post-differentiation. 30 minutes prior to collection all cells were treated with 1μM puromycin. Data were analyzed using a one-way ANOVA followed by Tukey's multiple comparison test. a: significantly ($p \leq 0.05$) different than Con; b: significantly different than GSI. c: significantly different than RAP (n = 2 experiments). Data are mean \pm SD.

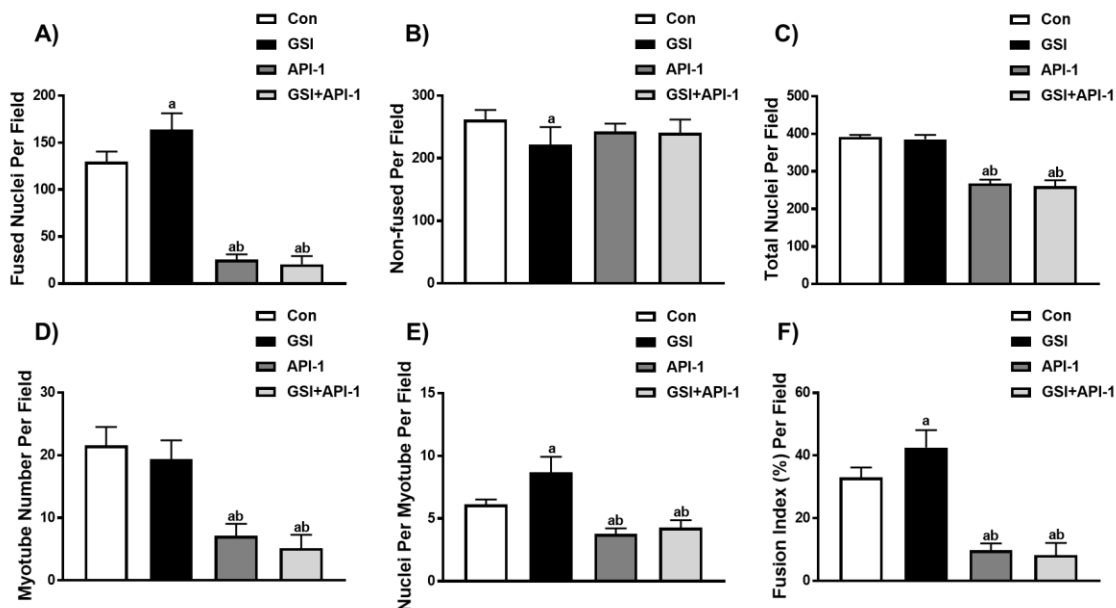


Figure 4.5.6. Indices of Fusion in C2C12 Myotubes with GSI and API-1. A) Fused nuclei per field; B) Non-fused nuclei per field; C) Total nuclei per field; D) Myotube number per field; E) Nuclei per myotube per field; F) Fusion index per field in 96-hour cultured myotubes. At the onset of differentiation C2C12 cells were treated every 12 hours with either control (Con), 4 μ M γ -secretase inhibitor (GSI), 10 μ M 4-Amino-5,8-dihydro-5-oxo-8- β -D-ribofuranosyl-pyrido[2,3-*d*]pyrimidine-6-carboxamide (API-1), or GSI + API-1 co-treatment. Data were analyzed using a one-way ANOVA followed by Tukey's multiple comparison test. a: significantly ($p \leq 0.05$) different than Con; b: significantly different than GSI ($n = 2$ experiments). Data are mean \pm SD.

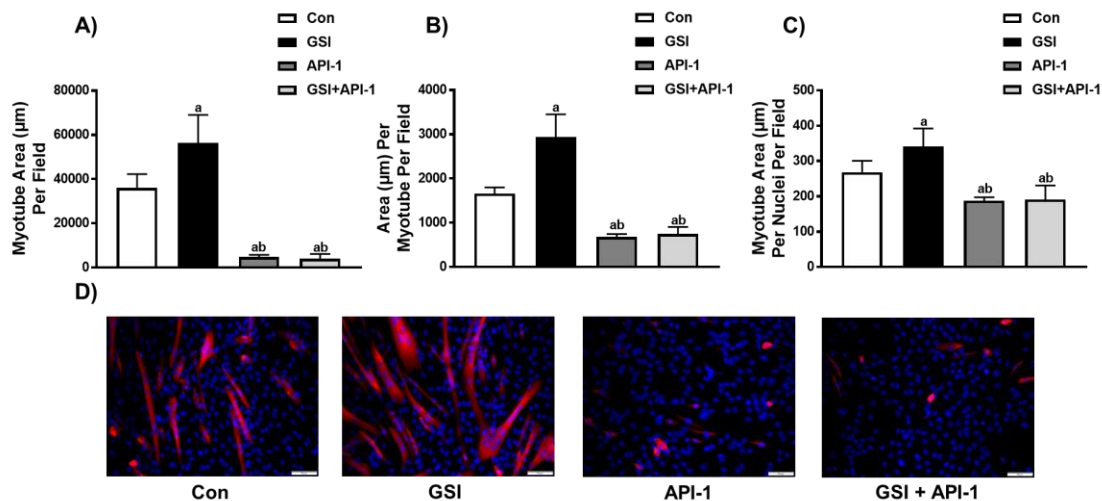


Figure 4.5.7. Indices of Hypertrophy in C2C12 Myotubes with GSI and API-1. A) Myotube area (μm) per field; B) Area (μm) per myotube per field; C) Myotube area (μm) per nuclei per field; D) Representative images of 96-hour cultured myotubes. At the onset of differentiation C2C12 cells were treated every 12 hours with either control (Con), 4μM γ-secretase inhibitor (GSI), 10μM 4-Amino-5,8-dihydro-5-oxo-8-β-D-ribofuranosyl-pyrido[2,3-*d*]pyrimidine-6-carboxamide (API-1), or GSI + API-1 co-treatment. Representative images are taken at 20x. Data were analyzed using a one-way ANOVA followed by Tukey's multiple comparison test. a: significantly ($p \leq 0.05$) different than Con; b: significantly different than GSI ($n = 2$ experiments). Data are mean \pm SD.

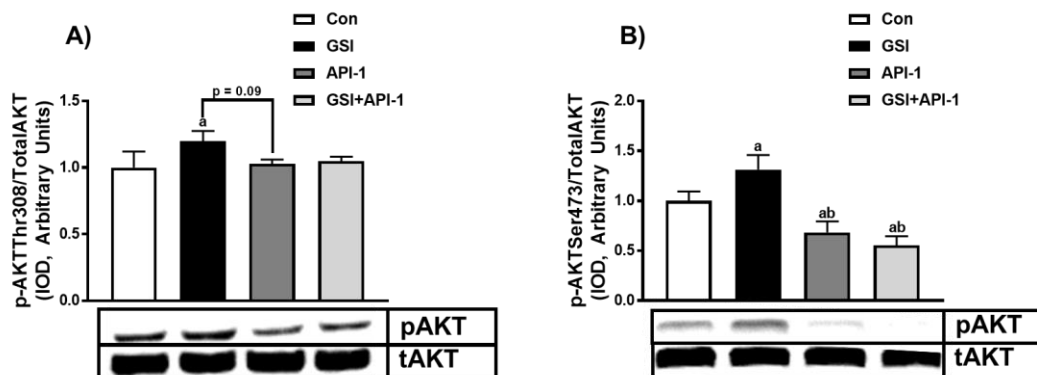


Figure 4.5.8. AKT in Cultured C2C12 Myotubes. A) Phospho (p)-protein kinase B (AKT) Thr308/Total AKT; B) p-AKT Ser473/Total AKT expression (Integrated optical density, IOD) in 96-hour myotubes. 72 hours post-differentiation, C2C12 cells were treated every 12 hours with either control (Con), 4 μ M γ -secretase inhibitor (GSI), 10 μ M 4-Amino-5,8-dihydro-5-oxo-8- β -D-ribofuranosyl-pyrido[2,3-*d*]pyrimidine-6-carboxamide (API-1), or GSI + API-1 co-treatment until 96 hours post-differentiation. 30 minutes prior to collection all cells were treated with 1 μ M puromycin. Data were analyzed using a one-way ANOVA followed by Tukey's multiple comparison test. a: significantly ($p \leq 0.05$) different than Con; b: significantly different than GSI ($n = 2$ experiments). Data are mean \pm SD.

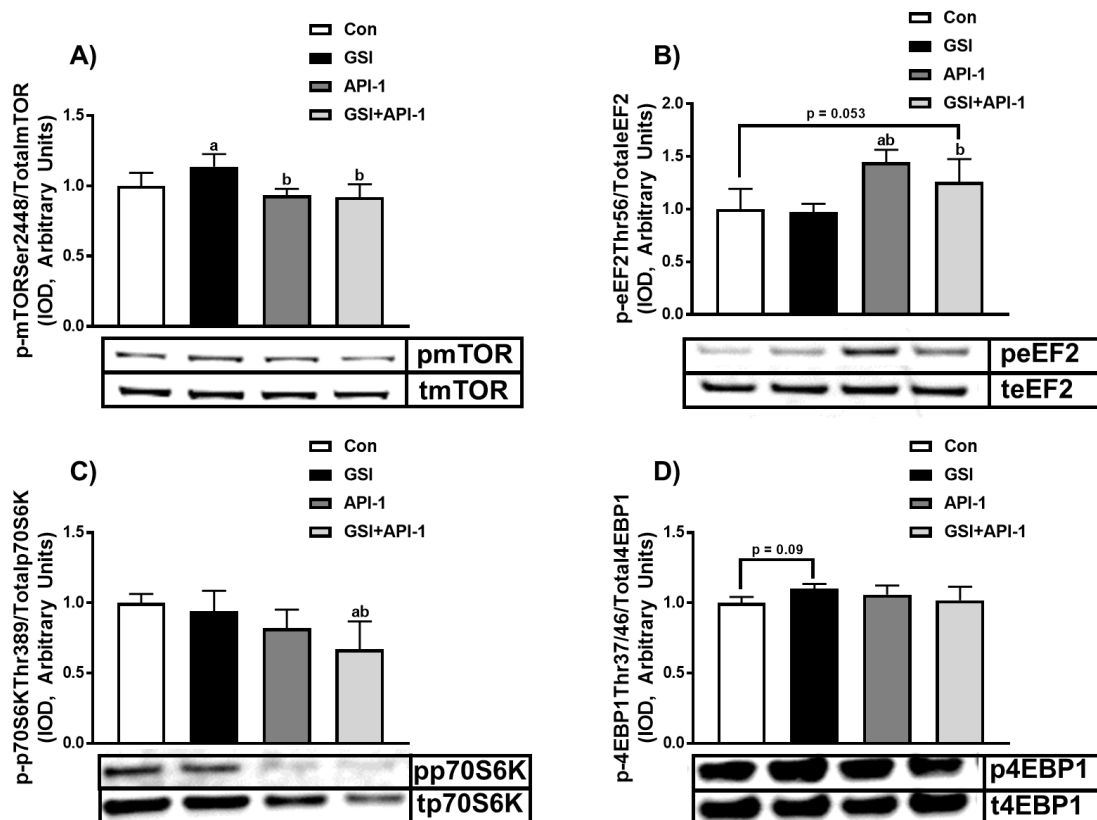


Figure 4.5.9. mTOR Signaling in Cultured C2C12 Myotubes with GSI and API-1. A) Phospho (p)- mechanistic target of rapamycin (mTOR) Ser2448/Total mTOR; B) p-eukaryotic elongation factor 2 (eEF2) Thr56/Total eEF2; C) p-70 kDa ribosomal protein S6 kinase (p70S6K) Thr389; D) p-eukaryotic initiation factor 4E binding protein (4EBP1) Thr37/46/Total 4EBP1 expression (Integrated optical density, IOD) in 96-hour myotubes. 72 hours post-differentiation, C2C12 cells were treated every 12 hours with either control (Con), 4 μ M γ -secretase inhibitor (GSI), 10 μ M 4-Amino-5,8-dihydro-5-oxo-8- β -D-ribofuranosyl-pyrido[2,3-*d*]pyrimidine-6-carboxamide (API-1), or GSI + API-1 co-treatment until 96 hours post-differentiation. 30 minutes prior to collection all cells were treated with 1 μ M puromycin. Data were analyzed using a one-way ANOVA followed by Tukey's multiple comparison test. a: significantly ($p \leq 0.05$) different than Con; b: significantly different than GSI ($n = 2$ experiments). Data are mean \pm SD.

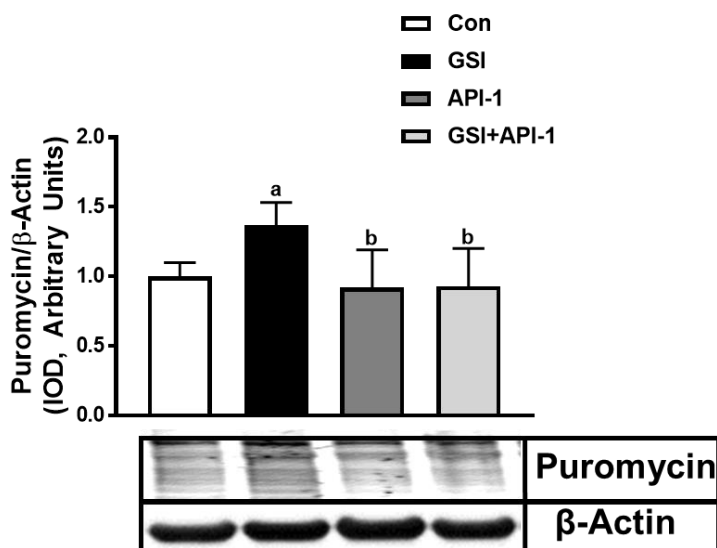


Figure 4.5.10. Muscle Protein Synthesis Rate in Cultured C2C12 Myotubes with GSI and API-1. Puromycin/β-Actin expression (Integrated optical density, IOD) in 96-hour myotubes. 72 hours post-differentiation, C2C12 cells were treated every 12 hours with either control (Con), 4μM γ-secretase inhibitor (GSI), 10μM 4-Amino-5,8-dihydro-5-oxo-8-β-D-ribofuranosyl-pyrido[2,3-*d*]pyrimidine-6-carboxamide (API-1), or GSI + API-1 co-treatment until 96 hours post-differentiation. 30 minutes prior to collection all cells were treated with 1μM puromycin. Data were analyzed using a one-way ANOVA followed by Tukey's multiple comparison test. a: significantly ($p \leq 0.05$) different than Con; b: significantly different than GSI ($n = 2$ experiments). Data are mean \pm SD.

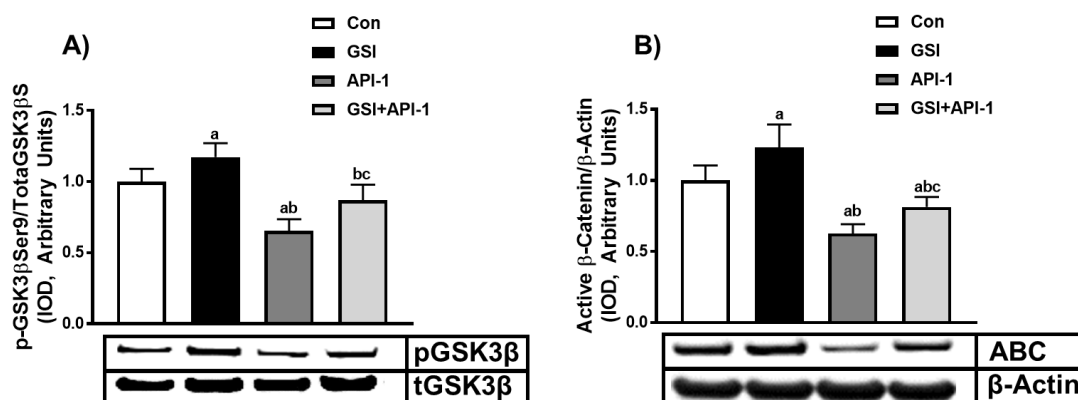


Figure 4.5.11. GSK3 β and ABC in Cultured C2C12 Myotubes with GSI and API-1.

A) Phospho (p)-glycogen synthase kinase 3 beta (GSK3 β)/total GSK3 β ; B) Active β -catenin (ABC)/ β -Actin expression (Integrated optical density, IOD) in 96-hour myotubes. 72 hours post-differentiation, C2C12 cells were treated every 12 hours with either control (Con), 4 μ M γ -secretase inhibitor (GSI), 10 μ M 4-Amino-5,8-dihydro-5-oxo-8- β -D-ribofuranosyl-pyrido[2,3-*d*]pyrimidine-6-carboxamide (API-1), or GSI + API-1 co-treatment until 96 hours post-differentiation. 30 minutes prior to collection all cells were treated with 1 μ M puromycin. Data were analyzed using a one-way ANOVA followed by Tukey's multiple comparison test. a: significantly ($p \leq 0.05$) different than Con; b: significantly different than GSI; c: significantly different than API-1 ($n = 2$ experiments). Data are mean \pm SD.

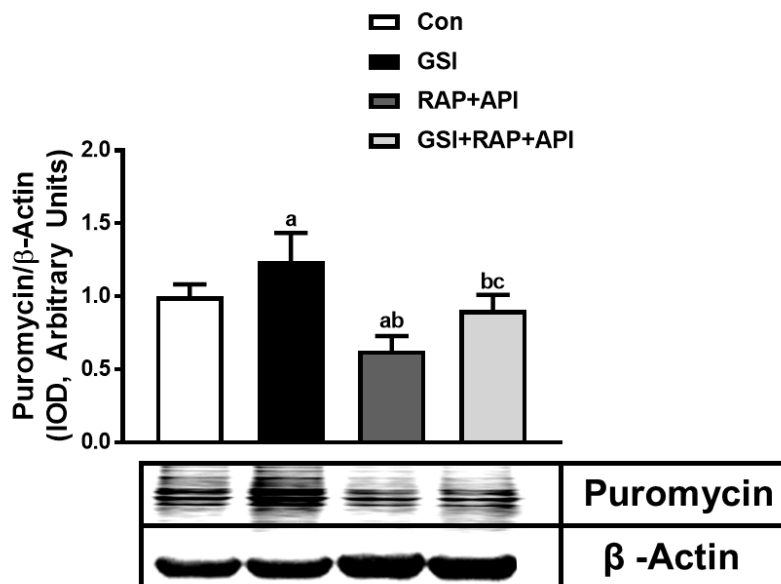


Figure 4.5.12. Muscle Protein Synthesis Rate in Cultured C2C12 Myotubes with GSI, RAP, and API-1. Puromycin/ β -Actin expression (Integrated optical density, IOD) in 96-hour myotubes. 72 hours post-differentiation, C2C12 cells were treated every 12 hours with either control (Con), 4 μ M γ -secretase inhibitor (GSI), 100nM rapamycin (RAP) and 10 μ M 4-Amino-5,8-dihydro-5-oxo-8- β -D-ribofuranosyl-pyrido[2,3-*d*]pyrimidine-6-carboxamide (API-1) or GSI + RAP + API-1 until 96 hours post-differentiation. 30 minutes prior to collection all cells were treated with 1 μ M puromycin. Data were analyzed using a one-way ANOVA followed by Tukey's multiple comparison test. a: significantly ($p \leq 0.05$) different than Con; b: significantly different than GSI; c: significantly different than RAP + API-1 ($n = 2$ experiments). Data are mean \pm SD.

4.6 Tables

Table 4.6.1. *Antibodies used for Western Blot Analysis.*

| <u>Antibody</u> | <u>Catalog #, Company</u> | <u>Dilution</u> |
|------------------------|----------------------------------|------------------------|
| p-AKT Thr308 | (#13038, CS) | 1:500 |
| p-AKT Ser473 | (#4060, CS) | 1:500 |
| Total AKT | (#2920, CS) | 1:1000 |
| p-mTOR Ser2448 | (#5536, CS) | 1:500 |
| Total mTOR | (#4517, CS) | 1:1000 |
| p-4EBP1 Thr37/46 | (#2855, CS) | 1:500 |
| Total 4EBP1 | (#9644, CS) | 1:1000 |
| p-eEF2 Thr56 | (#2331, CS) | 1:500 |
| Total eEF2 | (#2332, CS) | 1:500 |
| p-p70S6K Thr389 | (#9234, CS) | 1:500 |
| Total p70S6K | (#2708, CS) | 1:1000 |
| p-GSK3 β Ser9 | (#8566, CS) | 1:500 |
| Total GSK3 β | (#5676, CS) | 1:1000 |
| ABC | (#8814, CS) | 1:1000 |
| c-Myc | (#13987, CS) | 1:500 |
| PTEN | (#9188, CS) | 1:1000 |
| Total TSC2 | (#4308, CS) | 1:1000 |
| Cleaved Notch | (#4147, CS) | 1:500 |
| PTEN | (#9556, CS) | 1:1000 |
| Hes1 | (#11988, CS) | 1:500 |
| Puromycin | (#MABE343EMD Millipore) | 1:5000 |
| Beta Actin | (#A2228, Sigma Aldrich) | 1:10000 |

p: phosphorylated; AKT: protein kinase B; mTOR: mechanistic target of rapamycin; 4EBP1: eukaryotic initiation factor 4E binding protein; eEF2: eukaryotic elongation factor 2; p70S6K: 70 kDa ribosomal protein S6 kinase; GSK: Glycogen Synthase Kinase; ABC: Active β -catenin; Myc: avian myelocytomatosis viral oncogene homolog; PTEN: phosphatase and tensin homolog; TSC: tuberous sclerosis complex; Hes1: hairy/enhancer of split 1; CS: Cell signaling

Table 4.6.2. *Antibodies used for Immunoprecipitation.*

| <u>Antibody</u> | <u>Catalog #, Company</u> | <u>Dilution</u> |
|------------------------|----------------------------------|------------------------|
| Total mTOR | (#4517, CS) | 1:100 |
| c-Myc | (#13987, CS) | 1:50 |
| PTEN | (#9188, CS) | 1:50 |
| Total TSC2 | (#4308, CS) | 1:50 |
| Cleaved Notch | (#4147, CS) | 1:100 |
| PTEN | (#9556, CS) | 1:50 |
| Hes1 | (#11988, CS) | 1:100 |

mTOR: mechanistic target of rapamycin; Myc: avian myelocytomatosis viral oncogene homolog; PTEN: phosphatase and tensin homolog; TSC: tuberous sclerosis complex; Hes1: hairy/enhancer of split 1; CS: Cell signaling

CHAPTER 5: DISSERTATION DISCUSSION

Aging can be accompanied by aggressive loss of muscle mass (sarcopenia), a prevalent issue in more than 50% of individuals 80 years and older. Sarcopenia is thought to be a driving factor of the reduced ability of the elderly to accomplish basic daily activities [1; 2]. Moreover, sarcopenia preferentially affects fast-twitch fibers leading to lower muscular strength and power resulting in slower movement patterns, increasing frailty of aging individuals and increasing in the risk of injury, primarily by falling [3]. Several mechanisms within aged skeletal muscle are thought to drive the development of sarcopenia, including a delayed myogenic response when exposed to injury and blunted muscle protein synthesis (MPS) [10; 15-19]. The process of myogenesis (skeletal muscle repair) comprises the activation, proliferation, differentiation, and fusion of adult skeletal muscle stem cells (satellite cells (SCs)) [10]. Aging is associated with deleterious modifications to the intrinsic properties of SCs and the signaling pathways that regulate myogenesis, including Notch and mechanistic target of rapamycin (mTOR) signaling [10; 20; 21]. Notch signaling is pivotal to the regulation of the early stages of myogenesis, primarily through its ability to dictate SC fate [10; 26; 27]. mTOR has been identified as a critical regulator of the differentiation and maturation of myofibers [30-32]. While it was previously unknown whether Notch and mTOR communicated during myogenesis, the Arthur lab had recently demonstrated that Notch inhibition elevated phosphorylated mTOR in C2C12 myoblasts and myotubes suggesting that Notch may regulate mTOR. The Arthur lab has also shown that MPS rates increased in C2C12 cells following Notch inhibition. Taken together; recent

observations of Notch as a negative regulator of skeletal muscle mass [23; 24; 48; 133], the dysfunctional Notch signaling witnessed in aged skeletal muscle [26; 74], and the blunted myogenic and MPS processes in aged populations [10; 26; 38-40], suggest that Notch signaling plays a critical role towards the development of sarcopenia. Thus, the overall hypothesis of this dissertation was that Notch serves as a molecular brake on regeneration, MPS, and growth of skeletal muscle. Specifically, we postulated that Notch inhibition would elevate MPS rates in C2C12 cells through regulation of mTOR. Further, based on preliminary data from our own lab (Figures 1.3 & 1.4) and published findings from others [19; 26; 28], we also speculated that reducing Notch *in vivo* would induce a dysfunctional myogenic response thus compromising the regeneration capacity of young mice.

This dissertation research led to the following key findings: 1) Notch1 knockdown in conjunction with exercise (downhill running (DHR)) elevated the myogenic response and remodeling of skeletal muscle (Chapter 2). 2) Notch1 knockdown elevated phosphorylated mTOR and MPS rates *in vivo*, albeit through an unknown mechanism (Chapter 2). The elevation of MPS rate was confirmed *in vitro* using C2C12 myoblasts and myotubes (Chapter 3). 3) The elevations in MPS were accompanied by modulation of the PTEN/AKT/mTOR pathway, leading us to believe that Notch acts through mTOR to regulate muscle growth and regeneration. 4) We then determined that Notch (via GSI treatment) inhibition elevated MPS in the presence of rapamycin (an mTOR inhibitor) indicating that Notch may regulate MPS independent of mTOR, possibly via AKT (Chapter 4). 5) Further experimental exploration indicated that GSI treatment can elevate MPS in the presence of both rapamycin and API-1 (an AKT

inhibitor) (Chapter 4). We then demonstrated that GSI-treatment elevates pGSK3 β ser9 independently of AKT (Chapter 4), providing an additional plausible modality in which Notch regulates MPS.

The first key finding that Notch1 knockdown elevated the myogenic response and remodeling in skeletal muscle (Chapter 2: Increased MyoD and Myogenin at 24hrs; increased eMHC at 96 hrs) is an intriguing, yet controversial finding since it opposes several currently published findings and our own hypothesis. Our hypothesis was that Notch1 knockdown would lead to a dysfunctional and impaired myogenic response. This was due to prior research indicating that inhibition of Notch signaling impaired skeletal muscle regeneration in young mice while activation of Notch signaling rejuvenated skeletal muscle repair in aged muscle [26; 28]. Furthermore, our labs own unpublished data suggested that Notch inhibition (via GSI treatment) impaired regeneration of aged skeletal muscle. However, in recent years Notch has resurfaced as a negative regulator of regeneration with in vivo studies showing increased regenerative capacity attributed to lowered Notch signaling [23; 132; 133], further adding to the controversy. However, none of these studies examined regeneration or Notch signaling following physiological stimuli. We attribute the differences to two major differences: the mode of Notch manipulation and the stimulus (injury/damage) model used to study the regeneration response.

The original studies that investigated the impact of Notch on skeletal muscle regeneration utilized focal, artificial models to induce muscle injury. These models certainly induce a robust regenerative response; however, they lack practicality, are physiologically irrelevant, and ignore the secretory impact of skeletal muscle contraction.

Skeletal muscle has widely been viewed as a locomotive organ system, however, in recent years skeletal muscle which accounts for nearly 50% of total body mass in young individuals [6], has established itself as a pivotal secretory organ. Additionally, the secretory functions of skeletal muscle appear to be largely exercise dependent [87-89]. To gain a complete understanding of regeneration mechanics, physiological relevant models need to be employed. This is in large part due to the fact that myokines (IL-15, LIF, BDNF, Irisin) secreted by exercising muscle have the ability to influence SC dynamics by promoting activation, proliferation, and differentiation [90-107]. Notch down regulation is required for SC activation and inhibition of Notch leads to premature differentiation and dysfunctional regeneration in the absence of exercise [26; 28; 134]. However, reductions of Notch signaling in the presence of pro-myogenic myokines secreted with exercise may summate to induce a heightened regeneration response as we observed in our present study.

The other main factor contributing to the conflicting outcomes of muscle regeneration is the mode of Notch manipulation. A common technique used to inhibit Notch signaling is to use GSIs, which prevent the terminal cleavage of the Notch receptor and inhibit the release of NICD. When used *in vitro*, GSIs can have confounding results as we see in chapter 3 with the treatment of proliferating and differentiating C2C12 cells. When myoblasts are treated with GSIs proliferation is reduced (a dysfunctional myogenic symptom), likely do to the cells prematurely different as indicated by others [122; 131]. However, when treated with GSIs during differentiation, myogenesis is enhanced leading to larger myotubes and increased MHC protein expression (Chapter 3). Our results are likely due to the fact that Notch has distinct roles based on the context of the cell as

described by others [22; 53]. Moreover, GSI treatment is not specific to a certain Notch receptor, and thus inhibits activity of all Notch receptors (1-4), three of which (Notch1-3) are expressed in SCs [27; 108; 109]. Others have recently demonstrated that Notch1, Notch2, and Notch3, have different roles in SC regulation [28; 110-112]. Furthermore, these receptors appear to play an essential myogenic coordinating role [112]. GSI treatment likely disrupts this necessary coordination of Notch receptor function and is responsible for the impaired regenerative response seen by others [28] and our own unpublished data. Solely knocking down the Notch1 receptor is sufficient to elevate the regeneration response without derailing proper SC dynamics, at least in the presence of exercise. Given the different nature of the models used to stimulate regeneration and the different techniques used to reduce Notch signaling we feel that further investigations are warranted. In particular, it would be interesting if the prior studies conducted using artificial means of stimulating regeneration used an exercise model to see if Notch inhibition had a different impact from the prior findings (i.e. an elevation in regeneration). Moreover, it would be interesting to see if use of GSIs with exercise yielded the same results as our present study. It appears we are only scratching the surface of Notch signaling's impact on skeletal muscle regeneration. We also need to further investigate if our present findings carry over into an aged rodent model. Aged muscle regeneration may be impaired using the same exercise model and Notch1 knockdown given the myriad of physiological differences between young and old populations.

Sarcopenia is the result of several physiological changes that occur with age, not limited solely to an impaired regeneration response. In fact, several of the age-related

physiological changes likely contribute to the impaired regeneration seen in aged muscle. For example, elevated levels of pro-inflammatory cytokines including TNF α and IL-6 seen in older individuals are associated with reductions in muscle mass and strength and can also induce anabolic resistance [58]. These same cytokines have also been implicated in impairing SC function resulting in dysfunctional regeneration [10]. Additionally, there are decreased sex hormones in aged individuals. In particular, testosterone is known to have a positive myogenic effect and the decline seen in aged muscle likely contributes to the dysfunctional regeneration. Because of the physiological age differences, it is entirely possible that Notch1 knockdown would not elevate regeneration and may actually impair regeneration as others have previously described [26; 28]. This research has yet to be done and requires further investigation. If Notch1 knockdown did not elevate regeneration with an acute bout of exercise in aged muscle it could be attributed to the lifestyle of the subject (a sedentary human or a sedentary rodent throughout life). One factor contributing to the impaired regenerative response in aged muscle is the decline in SC number [10]. Interestingly, exercise increases SC number in aged muscle [10]. In light of this it would also be interesting to investigate whether activity throughout the lifespan in conjunction with Notch1 knockdown would increase the regeneration response in aged muscle.

Notch1 knockdown (Chapter 2) increased MPS rate *in vivo*. We then further demonstrated that Notch signaling has a role in regulating MPS *in vitro* (Chapter 3). Several prior *in vitro* and *in vivo* studies have indicated a role for Notch in regulating muscle hypertrophy [23; 24; 48; 127; 132]. Yet none of these studies examined anabolic signaling or MPS rates or even considered that Notch may play a role in hypertrophy via

modulation of MPS. Prior studies examining Notch signaling have focused solely on its role in regulation over SC fate and regeneration (cellular fusion), but did not investigate other muscle processes including MPS. There are two modes of hypertrophy: 1) increasing cellular fusion (myonuclear accretion via enhancement of regeneration) 2) increasing protein synthesis (expansion of myonuclear domain). Other proteins are known to have roles in both fusion and protein synthesis (IGF-1, Myostatin, mTOR) [10; 32; 34; 44; 163]. Further, in cancer cell line models, Notch signaling works as a regulator of anabolic signaling pathways [42; 154; 160; 161]. To our knowledge we are the first to investigate Notch modulation over mTOR signaling and ultimately MPS in skeletal muscle.

In chapter 3 we demonstrated that GSI treatment modulated the PTEN/AKT/mTOR signaling pathway thereby elevating MPS in C2C12 myoblasts and myotubes. The increases in MPS rate were accompanied by myotube hypertrophy via both an increase in myonuclear accretion and expansion of myonuclear domain. To our knowledge we are the first to indicate that Notch signaling may regulate both means of hypertrophy. Others have recently reported hypertrophy of muscle cells with GSI, however this hypertrophy was determined to be independent of Notch1 [136]. Given the context-based roles of Notch signaling, it is possible that Notch1 knockdown in myoblasts would lead to premature differentiation of muscle cells and an impaired hypertrophic response as others have found in Delta1 (one of the Notch ligands) mutants [134]. We recognize that it is plausible that Notch1 knockdown alone may not induce a hypertrophic response. Notch receptors may also coordinate to mediate hypertrophy just as they have been implicated in mediating regeneration. It would be interesting to see if

Notch1 knockdown in C2C12 cells would increase MPS rate and induce a hypertrophic response like we see with GSI treatment. Though these studies have not yet been conducted, we believe the elevations seen in MPS rates with Notch1 knockdown *in vivo* (Chapter 2) would likely carry over to cultured cells.

In chapter 4 we demonstrated that GSI treatment was able to elevate MPS independent of mTOR (via co-treatment of GSI+RAP). The experiments conducted in chapter 4 were performed in light of the chapter 3 finding that 4EBP1 was the only downstream target of mTOR was positively changed with GSI treatment. If GSI treatment was elevating MPS rate via mTOR, positive changes in the phosphorylation of p70S6K and eEF2 would be expected, neither of which were observed. With the changes seen in PTEN and AKT in chapter 3, and the minimal change seen in p70S6K and eEF2 we began to suspect that Notch inhibition (via GSI treatment) was acting through AKT. Furthermore, we began to speculate that GSI treatment could enforce its modulation over MPS independent of mTOR. We confirmed this notion demonstrating that GSI could elevate MPS independent of mTOR. However, we did determine that elevation of myotube formation and hypertrophy with GSI treatment was dependent on mTOR as all indices of myotube fusion and hypertrophy were ablated with GSI+RAP treatment. Interestingly, others have recently reported that GSI was able to rescue myotube hypertrophy in the presence of rapamycin, though this study did not measure MPS rate [136]. These conflicting results could be attributed to a difference in timing of treatment as our experiments for myotube fusion/area began treatment of Con, GSI, RAP, and GSI+RAP at the onset of differentiation and mTOR is necessary for myogenic differentiation [32; 34]. GSI's ability to elevate MPS in the presence of RAP may be

sufficient to rescue hypertrophy of formed myotubes, but these studies need to be completed. Taken together, GSIs elevations in PTEN/AKT (Chapter 3), and GSIs ability to increase MPS in the presence of RAP (Chapter 4), suggest Notch signaling acts through AKT in its regulation over MPS. Further, AKT is known to elevate protein synthesis independent of mTOR, via regulation of GSK3 β [172; 178]. We then sought out to clarify that GSI was elevating MPS rate via AKT by using a novel small molecule AKT inhibitor, API-1.

This experiment set led us to the finding that GSI treatment is able to regulate MPS rate independent of both mTOR and AKT. Our first experiment sets using API-1 and GSI had both promising and lackluster results. The fusion experiments that we conducted strengthened and supported our hypothesis that Notch acts through AKT as all myotube fusion and hypertrophy indices were ablated with GSI+API-1 treatment (similar to what was seen with GSI+RAP). These findings are in agreement with others demonstrating that AKT (just as mTOR) is necessary for myogenic differentiation [182]. API-1 treatment was not sufficient to reduce MPS rate. Though AKT reductions have been implicated in reducing MPS and hypertrophy, mTOR has several upstream inputs that can likely explain the maintenance of MPS rate with API-1 treatment [44; 163; 188]. In addition, API-1 did not reduce pmTORSer2448 which further supports the maintenance of MPS rate. To verify that API-1 treatment was effective in reducing AKT function, we measured pGSK3 β Ser9 which was reduced. In these same experiments we demonstrated that GSI treatment increased pGSK3 β Ser9 in the presence of API-1, suggesting that Notch may act on GSK3 β (and MPS) independent of AKT. We then conducted an experiment set with the sole intention of determining if MPS could be

elevated with GSI independent of mTOR and AKT. Triple treatment of GSI+RAP+API-1 revealed that GSI was able to regulate MPS rate independent of mTOR and AKT. This finding has focused our working hypothesis that Notch may regulate MPS rate via multiple routes including PTEN/AKT and GSK3 β .

Though we believe it is plausible that GSI acts through PTEN/AKT, our own research and the work of others is steadily building the case that the true mode of action is via GSK3 β . For example, others have previously identified GSK3 β as a target of Notch. Although, these studies focused solely on myogenesis and ignored anabolic signaling/MPS rate despite GSK3 β 's involvement in regulating MPS [28; 178; 201]. As mentioned previously we only witnessed positive changes in 4EBP1 with GSI treatment in our earlier studies (chapter 3). Interestingly, others have identified GSK3 β as a regulator of 4EBP1 albeit the research is outside of skeletal muscle [197; 198]. To further support that the mode of action is via GSK3 β , our protein-protein interaction measures did not reveal any binding between Hers1-PTEN, NICD-mTOR, or c-Myc-TSC2. It is possible that an interaction between these proteins does exist, but was not identified in the current dissertation. As discussed in chapter 4 overexpressing or ligand activating Notch would be a better model to test for Notch based protein interactions. A protein interaction may exist between Notch and GSK3 β , however that was not assessed in this dissertation. In fact others have demonstrated that NICD and GSK3 β directly interact with one another [190; 195; 196]. Although these studies elude to GSK3 β as a regulator of Notch, it is entirely plausible that NICD may directly regulate GSK3 β . This notion of NICD regulating GSK3 β has been speculated within muscle, although direct interaction has not been determined [28; 201]. The downstream target of GSK3 β , eIF2B ϵ is a pivotal

regulator of cap dependent translation and overexpression of eIF2B ϵ is sufficient to increase MPS rate and hypertrophy [178; 192]. It would be interesting to examine if eIF2B ϵ is elevated with GSIs or Notch1 knockdown, which would shed more light on the MPS rate mechanistic action of Notch. It would also be interesting to treat muscle cells with a GSI and a GSK3 β mutant (e.g. altering the serine residue) to sustain its activity. This would determine if Notch can also act independent of GSK3 β to regulate MPS.

In summary, we demonstrated that Notch serves as a molecular brake on myogenesis, MPS, and muscle growth. Notch1 knockdown in conjunction with exercise caused a heightened MRF response leading to an elevation in newly forming fibers 4 days later. This differs from much of the previous literature in which reduced Notch (using artificial insult) impairs the regenerative response (Figure 5.1). Moreover, Notch1 knockdown elevated MPS rate in young muscle. The use of a GSI in cultured C2C12 muscle cells led to elevations in cellular fusion, myotube formation, myotube hypertrophy, and MPS rate. Several follow-up experiments demonstrated that Notch may act through PTEN/AKT/mTOR in its regulation of MPS, but is also able to elevate MPS rate independently of AKT and mTOR via GSK3 β (Figure 5.2). These studies support the notion that targeting (inhibiting) Notch may provide relief to sarcopenia or other muscle wasting conditions via its action on increasing myonuclear accretion and myonuclear domain. However, more studies need to be conducted to verify this as the present experiments were not performed on aged or diseased muscle. Furthermore, additional follow-up studies need to be performed to further elucidate the mechanism by which Notch acts on MPS. In particular, if GSI treatment is sufficient to sustain MPS rate and muscle mass in the presence of AKT or mTOR inhibitors used in treating cancer,

or in longevity studies, then our present findings may have uncovered a huge step in maintaining functionality and quality of life in not only the ageing population, but all muscle wasting conditions.

Figures:

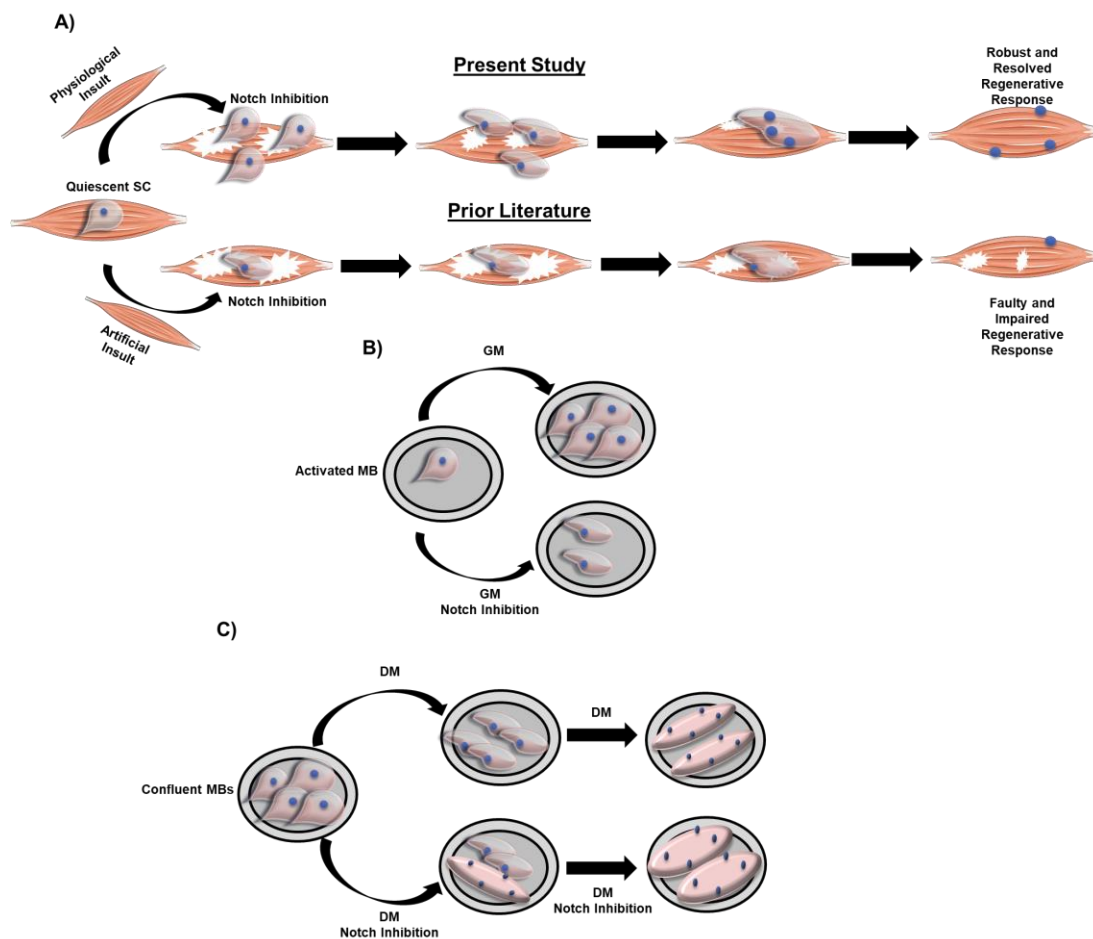


Figure 5.1. Influence of Notch Over Myogenesis. A) Previous *in vivo* literature has indicated that inhibition of Notch signaling along with artificial modes of insult leads to a faulty myogenic response impairing resolution of injury. In the present study we reveal that Notch inhibition along with physiological insult elevates the regenerative response. B) Our *in vitro* work in C2C12 cells demonstrates that Notch inhibition blunts myoblast proliferation, likely due to premature cellular differentiation. C) In contrast, if Notch inhibition is employed during later stages of myogenesis it enhances myotube formation and induces hypertrophy. SC: satellite cell; MB: myoblast; GM: growth media; DM: differentiation media.

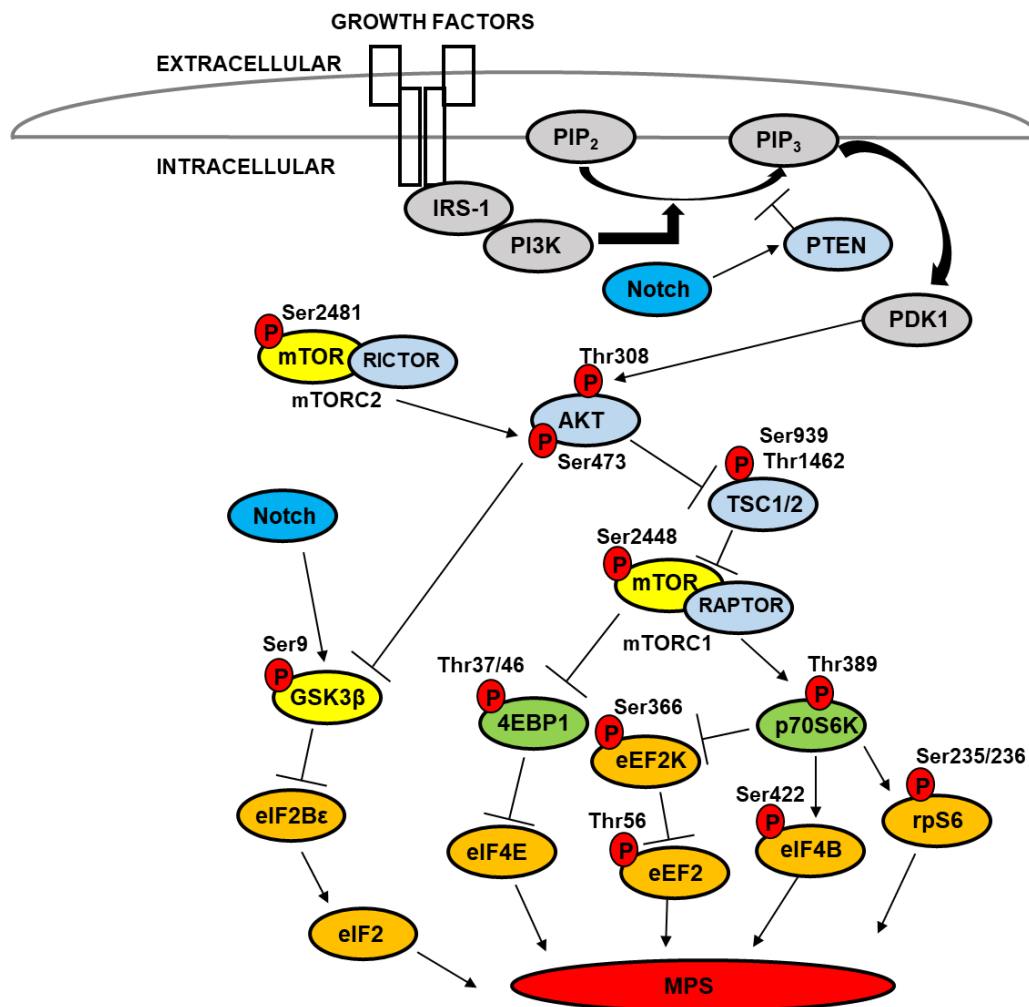


Figure 5.2. Regulation of Muscle Protein Synthesis. Overview of the two identified roles for Notch in the regulation of muscle protein synthesis (MPS). Chapter 3 revealed that Notch inhibition reduced phosphatase and tensin homolog (PTEN) protein expression. PTEN prevents the conversion of Phosphatidylinositol (4,5) –bisphosphate (PIP₂) to Phosphatidylinositol (3,4,5)-trisphosphate (PIP₃), thereby preventing subsequent phosphorylation of protein kinase B (AKT) on Threonine 308 by Phosphoinositide-dependent kinase-1 (PDK1). The reduction in PTEN with Notch inhibition lead to subsequent increases in phosphorylation of AKT, tuberous sclerosis complex (TSC1/2), and mechanistic target of rapamycin (mTOR) thereby increasing MPS. Chapter 4 revealed that Notch inhibition was able to influence MPS independent of AKT and mTOR, likely through glycogen synthase kinase 3 (GSK3β).

REFERENCES

- [1] Morley, J. E., Baumgartner, R. N., Roubenoff, R., Mayer, J., & Nair, K. S. (2001). Sarcopenia. *J Lab Clin Med*, 137(4), 231-243. doi:10.1067/mlc.2001.113504
- [2] Lexell, J. (1995). Human aging, muscle mass, and fiber type composition. *J Gerontol A Biol Sci Med Sci*, 50 Spec No, 11-16.
- [3] Landi, F., Liperoti, R., Russo, A., Giovannini, S., Tosato, M., Capoluongo, E., . . . Onder, G. (2012). Sarcopenia as a risk factor for falls in elderly individuals: results from the iSIRENTE study. *Clin Nutr*, 31(5), 652-658. doi:10.1016/j.clnu.2012.02.007
- [4] Fielding, R. A., Vellas, B., Evans, W. J., Bhasin, S., Morley, J. E., Newman, A. B., . . . Zamboni, M. (2011). Sarcopenia: an undiagnosed condition in older adults. Current consensus definition: prevalence, etiology, and consequences. International working group on sarcopenia. *J Am Med Dir Assoc*, 12(4), 249-256. doi:10.1016/j.jamda.2011.01.003
- [5] Wang, C., & Bai, L. (2012). Sarcopenia in the elderly: basic and clinical issues. *Geriatr Gerontol Int*, 12(3), 388-396. doi:10.1111/j.1447-0594.2012.00851.x
- [6] Short, K. R., Vittone, J. L., Bigelow, M. L., Proctor, D. N., & Nair, K. S. (2004). Age and aerobic exercise training effects on whole body and muscle protein metabolism. *Am J Physiol Endocrinol Metab*, 286(1), E92-101. doi:10.1152/ajpendo.00366.2003
- [7] Pedersen, B. K., & Febbraio, M. A. (2012). Muscles, exercise and obesity: skeletal muscle as a secretory organ. *Nat Rev Endocrinol*, 8(8), 457-465. doi:10.1038/nrendo.2012.49
- [8] Rolfe, D. F., & Brown, G. C. (1997). Cellular energy utilization and molecular origin of standard metabolic rate in mammals. *Physiol Rev*, 77(3), 731-758.
- [9] Walston, J. D. (2012). Sarcopenia in older adults. *Curr Opin Rheumatol*, 24(6), 623-627. doi:10.1097/BOR.0b013e328358d59b
- [10] Arthur, S. T., & Cooley, I. D. (2012). The effect of physiological stimuli on sarcopenia; impact of Notch and Wnt signaling on impaired aged skeletal muscle repair. *Int J Biol Sci*, 8(5), 731-760. doi:10.7150/ijbs.4262
- [11] Pentikainen, H., Ngandu, T., Liu, Y., Savonen, K., Komulainen, P., Hallikainen, M., . . . Soinen, H. (2017). Cardiorespiratory fitness and brain volumes in men and women in the FINGER study. *Age Ageing*. doi:10.1093/ageing/afw191

- [12]Vidoni, E. D., Honea, R. A., Billinger, S. A., Swerdlow, R. H., & Burns, J. M. (2012). Cardiorespiratory fitness is associated with atrophy in Alzheimer's and aging over 2 years. *Neurobiol Aging*, *33*(8), 1624-1632. doi:10.1016/j.neurobiolaging.2011.03.016
- [13]Kim, T. N., & Choi, K. M. (2015). The implications of sarcopenia and sarcopenic obesity on cardiometabolic disease. *J Cell Biochem*, *116*(7), 1171-1178. doi:10.1002/jcb.25077
- [14]Chau, D., Cho, L. M., Jani, P., & St Jeor, S. T. (2008). Individualizing recommendations for weight management in the elderly. *Curr Opin Clin Nutr Metab Care*, *11*(1), 27-31. doi:10.1097/MCO.0b013e3282f31744
- [15]Churchward-Venne, T. A., Breen, L., & Phillips, S. M. (2014). Alterations in human muscle protein metabolism with aging: Protein and exercise as countermeasures to offset sarcopenia. *Biofactors*, *40*(2), 199-205. doi:10.1002/biof.1138
- [16]Michalakis, K., Goulis, D. G., Vazaiou, A., Mintzioti, G., Polymeris, A., & Abrahamian-Michalakis, A. (2013). Obesity in the ageing man. *Metabolism*, *62*(10), 1341-1349. doi:10.1016/j.metabol.2013.05.019
- [17]Mosole, S., Carraro, U., Kern, H., Loeffler, S., Fruhmann, H., Vogelauer, M., . . . Zampieri, S. (2014). Long-term high-level exercise promotes muscle reinnervation with age. *J Neuropathol Exp Neurol*, *73*(4), 284-294. doi:10.1097/NEN.0000000000000032
- [18]Chabi, B., Ljubcic, V., Menzies, K. J., Huang, J. H., Saleem, A., & Hood, D. A. (2008). Mitochondrial function and apoptotic susceptibility in aging skeletal muscle. *Aging Cell*, *7*(1), 2-12. doi:10.1111/j.1474-9726.2007.00347.x
- [19]Carlson, M. E., Suetta, C., Conboy, M. J., Aagaard, P., Mackey, A., Kjaer, M., & Conboy, I. (2009). Molecular aging and rejuvenation of human muscle stem cells. *EMBO Mol Med*, *1*(8-9), 381-391. doi:10.1002/emmm.200900045
- [20]Flati, V., Caliaro, F., Specia, S., Corsetti, G., Cardile, A., Nisoli, E., . . . G, D. A. (2010). Essential amino acids improve insulin activation of AKT/MTOR signaling in soleus muscle of aged rats. *Int J Immunopathol Pharmacol*, *23*(1), 81-89.
- [21]Paturi, S., Gutta, A. K., Katta, A., Kakarla, S. K., Arvapalli, R. K., Gadde, M. K., . . . Blough, E. (2010). Effects of aging and gender on muscle mass and regulation of Akt-mTOR-p70s6k related signaling in the F344BN rat model. *Mech Ageing Dev*, *131*(3), 202-209. doi:10.1016/j.mad.2010.01.008
- [22]Mourikis, P., & Tajbakhsh, S. (2014). Distinct contextual roles for Notch signalling in skeletal muscle stem cells. *BMC Dev Biol*, *14*, 2. doi:10.1186/1471-213X-14-2

- [23]Al Jaam, B., Heu, K., Pennarubia, F., Segelle, A., Magnol, L., Germot, A., . . . Maftah, A. (2016). Reduced Notch signalling leads to postnatal skeletal muscle hypertrophy in *Pofut1*^{cax/cax} mice. *Open Biol*, 6(9). doi:10.1098/rsob.160211
- [24]Pelisse, M., Der Vartanian, A., Germot, A., & Maftah, A. (2018). Protein O-Glucosyltransferase 1 Expression Influences Formation of Differentiated Myotubes in C2C12 Cell Line. *DNA Cell Biol*, 37(4), 359-372. doi:10.1089/dna.2017.4052
- [25]Shan, T., Xu, Z., Wu, W., Liu, J., & Wang, Y. (2016). Roles of Notch1 Signaling in Regulating Satellite Cell Fates Choices and Postnatal Skeletal Myogenesis. *J Cell Physiol*. doi:10.1002/jcp.25730
- [26]Conboy, I. M., Conboy, M. J., Smythe, G. M., & Rando, T. A. (2003). Notch-mediated restoration of regenerative potential to aged muscle. *Science*, 302(5650), 1575-1577. doi:10.1126/science.1087573
- [27]Conboy, I. M., & Rando, T. A. (2002). The regulation of Notch signaling controls satellite cell activation and cell fate determination in postnatal myogenesis. *Dev Cell*, 3(3), 397-409.
- [28]Brack, A. S., Conboy, I. M., Conboy, M. J., Shen, J., & Rando, T. A. (2008). A temporal switch from notch to Wnt signaling in muscle stem cells is necessary for normal adult myogenesis. *Cell Stem Cell*, 2(1), 50-59. doi:10.1016/j.stem.2007.10.006
- [29]Wen, Y., Bi, P., Liu, W., Asakura, A., Keller, C., & Kuang, S. (2012). Constitutive Notch activation upregulates Pax7 and promotes the self-renewal of skeletal muscle satellite cells. *Mol Cell Biol*, 32(12), 2300-2311. doi:10.1128/MCB.06753-11
- [30]Park, I. H., & Chen, J. (2005). Mammalian target of rapamycin (mTOR) signaling is required for a late-stage fusion process during skeletal myotube maturation. *J Biol Chem*, 280(36), 32009-32017. doi:10.1074/jbc.M506120200
- [31]Jansen, K. M., & Pavlath, G. K. (2008). Molecular control of mammalian myoblast fusion. *Methods Mol Biol*, 475, 115-133. doi:10.1007/978-1-59745-250-2_7
- [32]Ge, Y., & Chen, J. (2012). Mammalian target of rapamycin (mTOR) signaling network in skeletal myogenesis. *J Biol Chem*, 287(52), 43928-43935. doi:10.1074/jbc.R112.406942
- [33]Sun, Y., Ge, Y., Drnevich, J., Zhao, Y., Band, M., & Chen, J. (2010). Mammalian target of rapamycin regulates miRNA-1 and follistatin in skeletal myogenesis. *J Cell Biol*, 189(7), 1157-1169. doi:10.1083/jcb.200912093
- [34]Ge, Y., Wu, A. L., Warnes, C., Liu, J., Zhang, C., Kawasome, H., . . . Chen, J. (2009). mTOR regulates skeletal muscle regeneration in vivo through kinase-

dependent and kinase-independent mechanisms. *Am J Physiol Cell Physiol*, 297(6), C1434-1444. doi:10.1152/ajpcell.00248.2009

- [35] Buas, M. F., Kabak, S., & Kadesch, T. (2009). Inhibition of myogenesis by Notch: evidence for multiple pathways. *J Cell Physiol*, 218(1), 84-93. doi:10.1002/jcp.21571
- [36] Sun, J., Kamei, C. N., Layne, M. D., Jain, M. K., Liao, J. K., Lee, M. E., & Chin, M. T. (2001). Regulation of myogenic terminal differentiation by the hairy-related transcription factor CHF2. *J Biol Chem*, 276(21), 18591-18596. doi:10.1074/jbc.M101163200
- [37] Zhang, P., Liang, X., Shan, T., Jiang, Q., Deng, C., Zheng, R., & Kuang, S. (2015). mTOR is necessary for proper satellite cell activity and skeletal muscle regeneration. *Biochem Biophys Res Commun*, 463(1-2), 102-108. doi:10.1016/j.bbrc.2015.05.032
- [38] Tsivitse, S. (2010). Notch and Wnt signaling, physiological stimuli and postnatal myogenesis. *Int J Biol Sci*, 6(3), 268-281.
- [39] Blough, E. R., & Linderman, J. K. (2000). Lack of skeletal muscle hypertrophy in very aged male Fischer 344 x Brown Norway rats. *J Appl Physiol (1985)*, 88(4), 1265-1270.
- [40] Kosek, D. J., Kim, J. S., Petrella, J. K., Cross, J. M., & Bamman, M. M. (2006). Efficacy of 3 days/wk resistance training on myofiber hypertrophy and myogenic mechanisms in young vs. older adults. *J Appl Physiol (1985)*, 101(2), 531-544. doi:10.1152/jappphysiol.01474.2005
- [41] Fry, C. S., Drummond, M. J., Glynn, E. L., Dickinson, J. M., Gundermann, D. M., Timmerman, K. L., . . . Rasmussen, B. B. (2011). Aging impairs contraction-induced human skeletal muscle mTORC1 signaling and protein synthesis. *Skelet Muscle*, 1(1), 11. doi:10.1186/2044-5040-1-11
- [42] Chan, S. M., Weng, A. P., Tibshirani, R., Aster, J. C., & Utz, P. J. (2007). Notch signals positively regulate activity of the mTOR pathway in T-cell acute lymphoblastic leukemia. *Blood*, 110(1), 278-286. doi:10.1182/blood-2006-08-039883
- [43] Tohda, S. (2014). NOTCH signaling roles in acute myeloid leukemia cell growth and interaction with other stemness-related signals. *Anticancer Res*, 34(11), 6259-6264.
- [44] Shimobayashi, M., & Hall, M. N. (2014). Making new contacts: the mTOR network in metabolism and signalling crosstalk. *Nat Rev Mol Cell Biol*, 15(3), 155-162. doi:10.1038/nrm3757

- [45]Ravitz, M. J., Chen, L., Lynch, M., & Schmidt, E. V. (2007). c-myc Repression of TSC2 contributes to control of translation initiation and Myc-induced transformation. *Cancer Res*, 67(23), 11209-11217. doi:10.1158/0008-5472.CAN-06-4351
- [46]Perumalsamy, L. R., Nagala, M., Banerjee, P., & Sarin, A. (2009). A hierarchical cascade activated by non-canonical Notch signaling and the mTOR-Rictor complex regulates neglect-induced death in mammalian cells. *Cell Death Differ*, 16(6), 879-889. doi:10.1038/cdd.2009.20
- [47]Ge, W., & Ren, J. (2012). mTOR-STAT3-notch signalling contributes to ALDH2-induced protection against cardiac contractile dysfunction and autophagy under alcoholism. *J Cell Mol Med*, 16(3), 616-626. doi:10.1111/j.1582-4934.2011.01347.x
- [48]Mu, X., Agarwal, R., March, D., Rothenberg, A., Voigt, C., Tebbets, J., . . . Weiss, K. (2016). Notch Signaling Mediates Skeletal Muscle Atrophy in Cancer Cachexia Caused by Osteosarcoma. *Sarcoma*, 2016, 3758162. doi:10.1155/2016/3758162
- [49]Amin, H., Vachris, J., Hamilton, A., Steuerwald, N., Howden, R., & Arthur, S. T. (2014). GSK3beta inhibition and LEF1 upregulation in skeletal muscle following a bout of downhill running. *J Physiol Sci*, 64(1), 1-11. doi:10.1007/s12576-013-0284-5
- [50]Qin, L., Xu, J., Wu, Z., Zhang, Z., Li, J., Wang, C., & Long, Q. (2013). Notch1-mediated signaling regulates proliferation of porcine satellite cells (PSCs). *Cell Signal*, 25(2), 561-569. doi:10.1016/j.cellsig.2012.11.003
- [51]Zhang, R., Wang, L., He, L., Yang, B., Yao, C., Du, P., . . . Hua, Z. C. (2014). Fas-Associated Protein with Death Domain Regulates Notch Signaling during Muscle Regeneration. *Cells Tissues Organs*, 200(3-4), 253-264. doi:10.1159/000437258
- [52]Bjornson, C. R., Cheung, T. H., Liu, L., Tripathi, P. V., Steeper, K. M., & Rando, T. A. (2012). Notch signaling is necessary to maintain quiescence in adult muscle stem cells. *Stem Cells*, 30(2), 232-242. doi:10.1002/stem.773
- [53]Mourikis, P., Sambasivan, R., Castel, D., Rocheteau, P., Bizzarro, V., & Tajbakhsh, S. (2012). A critical requirement for notch signaling in maintenance of the quiescent skeletal muscle stem cell state. *Stem Cells*, 30(2), 243-252. doi:10.1002/stem.775
- [54]Bi, P., Yue, F., Sato, Y., Wirbisky, S., Liu, W., Shan, T., . . . Kuang, S. (2016). Stage-specific effects of Notch activation during skeletal myogenesis. *Elife*, 5. doi:10.7554/eLife.17355

- [55]Berger, M. J., & Doherty, T. J. (2010). Sarcopenia: prevalence, mechanisms, and functional consequences. *Interdiscip Top Gerontol*, 37, 94-114. doi:10.1159/000319997
- [56]Fabbri, E., Chiles Shaffer, N., Gonzalez-Freire, M., Shardell, M. D., Zoli, M., Studenski, S. A., & Ferrucci, L. (2017). Early body composition, but not body mass, is associated with future accelerated decline in muscle quality. *J Cachexia Sarcopenia Muscle*, 8(3), 490-499. doi:10.1002/jcsm.12183
- [57]Newman, A. B., Kupelian, V., Visser, M., Simonsick, E. M., Goodpaster, B. H., Kritchevsky, S. B., . . . Harris, T. B. (2006). Strength, but not muscle mass, is associated with mortality in the health, aging and body composition study cohort. *J Gerontol A Biol Sci Med Sci*, 61(1), 72-77.
- [58]Tournadre, A., Vial, G., Capel, F., Soubrier, M., & Boirie, Y. (2018). Sarcopenia. *Joint Bone Spine*. doi:10.1016/j.jbspin.2018.08.001
- [59]Mashinchian, O., Pisconti, A., Le Moal, E., & Bentzinger, C. F. (2018). The Muscle Stem Cell Niche in Health and Disease. *Curr Top Dev Biol*, 126, 23-65. doi:10.1016/bs.ctdb.2017.08.003
- [60]Dardevet, D., Sornet, C., Balage, M., & Grizard, J. (2000). Stimulation of in vitro rat muscle protein synthesis by leucine decreases with age. *J Nutr*, 130(11), 2630-2635. doi:10.1093/jn/130.11.2630
- [61]Guillet, C., Delcourt, I., Rance, M., Giraudet, C., Walrand, S., Bedu, M., . . . Boirie, Y. (2009). Changes in basal and insulin and amino acid response of whole body and skeletal muscle proteins in obese men. *J Clin Endocrinol Metab*, 94(8), 3044-3050. doi:10.1210/jc.2008-2216
- [62]Guillet, C., Prod'homme, M., Balage, M., Gachon, P., Giraudet, C., Morin, L., . . . Boirie, Y. (2004). Impaired anabolic response of muscle protein synthesis is associated with S6K1 dysregulation in elderly humans. *FASEB J*, 18(13), 1586-1587. doi:10.1096/fj.03-1341fje
- [63]Mangner, N., Linke, A., Oberbach, A., Kullnick, Y., Gielen, S., Sandri, M., . . . Adams, V. (2013). Exercise training prevents TNF-alpha induced loss of force in the diaphragm of mice. *PLoS One*, 8(1), e52274. doi:10.1371/journal.pone.0052274
- [64]Mitchell, W. K., Williams, J., Atherton, P., Larvin, M., Lund, J., & Narici, M. (2012). Sarcopenia, dynapenia, and the impact of advancing age on human skeletal muscle size and strength; a quantitative review. *Front Physiol*, 3, 260. doi:10.3389/fphys.2012.00260
- [65]Schaap, L. A., Pluijm, S. M., Deeg, D. J., & Visser, M. (2006). Inflammatory markers and loss of muscle mass (sarcopenia) and strength. *Am J Med*, 119(6), 526 e529-517. doi:10.1016/j.amjmed.2005.10.049

- [66]Tardif, N., Salles, J., Guillet, C., Tordjman, J., Reggio, S., Landrier, J. F., . . . Walrand, S. (2014). Muscle ectopic fat deposition contributes to anabolic resistance in obese sarcopenic old rats through eIF2alpha activation. *Aging Cell*, 13(6), 1001-1011. doi:10.1111/accel.12263
- [67]Tournadre, A., Pereira, B., Dutheil, F., Giraud, C., Courteix, D., Sapin, V., . . . Soubrier, M. (2017). Changes in body composition and metabolic profile during interleukin 6 inhibition in rheumatoid arthritis. *J Cachexia Sarcopenia Muscle*, 8(4), 639-646. doi:10.1002/jcsm.12189
- [68]Tsujinaka, T., Fujita, J., Ebisui, C., Yano, M., Kominami, E., Suzuki, K., . . . Monden, M. (1996). Interleukin 6 receptor antibody inhibits muscle atrophy and modulates proteolytic systems in interleukin 6 transgenic mice. *J Clin Invest*, 97(1), 244-249. doi:10.1172/JCI118398
- [69]Brack, A. S., Murphy-Seiler, F., Hanifi, J., Deka, J., Eyckerman, S., Keller, C., . . . Rando, T. A. (2009). BCL9 is an essential component of canonical Wnt signaling that mediates the differentiation of myogenic progenitors during muscle regeneration. *Dev Biol*, 335(1), 93-105. doi:10.1016/j.ydbio.2009.08.014
- [70]Marsh, D. R., Criswell, D. S., Carson, J. A., & Booth, F. W. (1997). Myogenic regulatory factors during regeneration of skeletal muscle in young, adult, and old rats. *J Appl Physiol (1985)*, 83(4), 1270-1275. doi:10.1152/jappl.1997.83.4.1270
- [71]Otto, A., Schmidt, C., Luke, G., Allen, S., Valasek, P., Muntoni, F., . . . Patel, K. (2008). Canonical Wnt signalling induces satellite-cell proliferation during adult skeletal muscle regeneration. *J Cell Sci*, 121(Pt 17), 2939-2950. doi:10.1242/jcs.026534
- [72]Tsivitse, S. K., Peters, M. G., Stoy, A. L., Mundy, J. A., & Bowen, R. S. (2009). The effect of downhill running on Notch signaling in regenerating skeletal muscle. *Eur J Appl Physiol*, 106(5), 759-767. doi:10.1007/s00421-009-1077-7
- [73]Akiho, M., Nakashima, H., Sakata, M., Yamasa, Y., Yamaguchi, A., & Sakuma, K. (2010). Expression profile of Notch-1 in mechanically overloaded plantaris muscle of mice. *Life Sci*, 86(1-2), 59-65. doi:10.1016/j.lfs.2009.11.011
- [74]Carey, K. A., Farnfield, M. M., Tarquinio, S. D., & Cameron-Smith, D. (2007). Impaired expression of Notch signaling genes in aged human skeletal muscle. *J Gerontol A Biol Sci Med Sci*, 62(1), 9-17.
- [75]D'Souza, D. M., Zhou, S., Rebalka, I. A., MacDonald, B., Moradi, J., Krause, M. P., . . . Hawke, T. J. (2016). Decreased Satellite Cell Number and Function in Humans and Mice With Type 1 Diabetes Is the Result of Altered Notch Signaling. *Diabetes*, 65(10), 3053-3061. doi:10.2337/db15-1577

- [76]Fujimaki, S., Wakabayashi, T., Asashima, M., Takemasa, T., & Kuwabara, T. (2016). Treadmill running induces satellite cell activation in diabetic mice. *Biochem Biophys Res*, 8, 6-13. doi:10.1016/j.bbrep.2016.07.004
- [77]MacKenzie, M. G., Hamilton, D. L., Pepin, M., Patton, A., & Baar, K. (2013). Inhibition of myostatin signaling through Notch activation following acute resistance exercise. *PLoS One*, 8(7), e68743. doi:10.1371/journal.pone.0068743
- [78]Palstra, A. P., Rovira, M., Rizo-Roca, D., Torrella, J. R., Spaink, H. P., & Planas, J. V. (2014). Swimming-induced exercise promotes hypertrophy and vascularization of fast skeletal muscle fibres and activation of myogenic and angiogenic transcriptional programs in adult zebrafish. *BMC Genomics*, 15, 1136. doi:10.1186/1471-2164-15-1136
- [79]Carlson, M. E., Hsu, M., & Conboy, I. M. (2008). Imbalance between pSmad3 and Notch induces CDK inhibitors in old muscle stem cells. *Nature*, 454(7203), 528-532. doi:10.1038/nature07034
- [80]Wu, C. L., & Kandarian, S. C. (2012). Protein overexpression in skeletal muscle using plasmid-based gene transfer to elucidate mechanisms controlling fiber size. *Methods Mol Biol*, 798, 231-243. doi:10.1007/978-1-61779-343-1_13
- [81]Boppart, M. D., Burkin, D. J., & Kaufman, S. J. (2006). Alpha7beta1-integrin regulates mechanotransduction and prevents skeletal muscle injury. *Am J Physiol Cell Physiol*, 290(6), C1660-1665. doi:10.1152/ajpcell.00317.2005
- [82]Goodman, C. A., Mabrey, D. M., Frey, J. W., Miu, M. H., Schmidt, E. K., Pierre, P., & Hornberger, T. A. (2011). Novel insights into the regulation of skeletal muscle protein synthesis as revealed by a new nonradioactive in vivo technique. *FASEB J*, 25(3), 1028-1039. doi:10.1096/fj.10-168799
- [83]Peck, B., Huot, J., Renzi, T., Arthur, S., Turner, M. J., & Marino, J. S. (2018). Mice lacking PKC-theta in skeletal muscle have reduced intramyocellular lipid accumulation and increased insulin responsiveness in skeletal muscle. *Am J Physiol Regul Integr Comp Physiol*, 314(3), R468-R477. doi:10.1152/ajpregu.00521.2016
- [84]McCarthy, J. J., Mula, J., Miyazaki, M., Erfani, R., Garrison, K., Farooqui, A. B., . . . Peterson, C. A. (2011). Effective fiber hypertrophy in satellite cell-depleted skeletal muscle. *Development*, 138(17), 3657-3666. doi:10.1242/dev.068858
- [85]Goodman, C. A., & Hornberger, T. A. (2013). Measuring protein synthesis with SUnSET: a valid alternative to traditional techniques? *Exerc Sport Sci Rev*, 41(2), 107-115. doi:10.1097/JES.0b013e3182798a95
- [86]Wang, Y. X., & Rudnicki, M. A. (2011). Satellite cells, the engines of muscle repair. *Nat Rev Mol Cell Biol*, 13(2), 127-133. doi:10.1038/nrm3265

- [87]Huh, J. Y. (2018). The role of exercise-induced myokines in regulating metabolism. *Arch Pharm Res*, 41(1), 14-29. doi:10.1007/s12272-017-0994-y
- [88]Sabaratnam, R., Pedersen, A. J. T., Kristensen, J. M., Handberg, A., Wojtaszewski, J. F. P., & Hojlund, K. (2018). Intact regulation of muscle expression and circulating levels of myokines in response to exercise in patients with type 2 diabetes. *Physiol Rep*, 6(12), e13723. doi:10.14814/phy2.13723
- [89]So, B., Kim, H. J., Kim, J., & Song, W. (2014). Exercise-induced myokines in health and metabolic diseases. *Integr Med Res*, 3(4), 172-179. doi:10.1016/j.imr.2014.09.007
- [90]Bostrom, P., Wu, J., Jedrychowski, M. P., Korde, A., Ye, L., Lo, J. C., . . . Spiegelman, B. M. (2012). A PGC1-alpha-dependent myokine that drives brown-fat-like development of white fat and thermogenesis. *Nature*, 481(7382), 463-468. doi:10.1038/nature10777
- [91]Broholm, C., Laye, M. J., Brandt, C., Vadulasetty, R., Pilegaard, H., Pedersen, B. K., & Scheele, C. (2011). LIF is a contraction-induced myokine stimulating human myocyte proliferation. *J Appl Physiol (1985)*, 111(1), 251-259. doi:10.1152/jappphysiol.01399.2010
- [92]Broholm, C., Mortensen, O. H., Nielsen, S., Akerstrom, T., Zankari, A., Dahl, B., & Pedersen, B. K. (2008). Exercise induces expression of leukaemia inhibitory factor in human skeletal muscle. *J Physiol*, 586(8), 2195-2201. doi:10.1113/jphysiol.2007.149781
- [93]Dupont-Versteegden, E. E., Houle, J. D., Dennis, R. A., Zhang, J., Knox, M., Wagoner, G., & Peterson, C. A. (2004). Exercise-induced gene expression in soleus muscle is dependent on time after spinal cord injury in rats. *Muscle Nerve*, 29(1), 73-81. doi:10.1002/mus.10511
- [94]Huh, J. Y., Panagiotou, G., Mougios, V., Brinkoetter, M., Vamvini, M. T., Schneider, B. E., & Mantzoros, C. S. (2012). FNDC5 and irisin in humans: I. Predictors of circulating concentrations in serum and plasma and II. mRNA expression and circulating concentrations in response to weight loss and exercise. *Metabolism*, 61(12), 1725-1738. doi:10.1016/j.metabol.2012.09.002
- [95]Kim, H. J., Park, J. Y., Oh, S. L., Kim, Y. A., So, B., Seong, J. K., & Song, W. (2013). Effect of treadmill exercise on interleukin-15 expression and glucose tolerance in zucker diabetic Fatty rats. *Diabetes Metab J*, 37(5), 358-364. doi:10.4093/dmj.2013.37.5.358
- [96]Matthews, V. B., Astrom, M. B., Chan, M. H., Bruce, C. R., Krabbe, K. S., Prelovsek, O., . . . Febbraio, M. A. (2009). Brain-derived neurotrophic factor is produced by skeletal muscle cells in response to contraction and enhances fat oxidation via activation of AMP-activated protein kinase. *Diabetologia*, 52(7), 1409-1418. doi:10.1007/s00125-009-1364-1

- [97] Tamura, Y., Watanabe, K., Kantani, T., Hayashi, J., Ishida, N., & Kaneki, M. (2011). Upregulation of circulating IL-15 by treadmill running in healthy individuals: is IL-15 an endocrine mediator of the beneficial effects of endurance exercise? *Endocr J*, 58(3), 211-215.
- [98] Yang, H., Chang, J., Chen, W., Zhao, L., Qu, B., Tang, C., . . . Zhang, J. (2013). Treadmill exercise promotes interleukin 15 expression in skeletal muscle and interleukin 15 receptor alpha expression in adipose tissue of high-fat diet rats. *Endocrine*, 43(3), 579-585. doi:10.1007/s12020-012-9809-6
- [99] Alter, J., Rozentzweig, D., & Bengal, E. (2008). Inhibition of myoblast differentiation by tumor necrosis factor alpha is mediated by c-Jun N-terminal kinase 1 and leukemia inhibitory factor. *J Biol Chem*, 283(34), 23224-23234. doi:10.1074/jbc.M801379200
- [100] Broholm, C., & Pedersen, B. K. (2010). Leukaemia inhibitory factor--an exercise-induced myokine. *Exerc Immunol Rev*, 16, 77-85.
- [101] Diao, Y., Wang, X., & Wu, Z. (2009). SOCS1, SOCS3, and PIAS1 promote myogenic differentiation by inhibiting the leukemia inhibitory factor-induced JAK1/STAT1/STAT3 pathway. *Mol Cell Biol*, 29(18), 5084-5093. doi:10.1128/MCB.00267-09
- [102] Reza, M. M., Sim, C. M., Subramaniam, N., Ge, X., Sharma, M., Kambadur, R., & McFarlane, C. (2017). Irisin treatment improves healing of dystrophic skeletal muscle. *Oncotarget*, 8(58), 98553-98566. doi:10.18632/oncotarget.21636
- [103] Reza, M. M., Subramaniam, N., Sim, C. M., Ge, X., Sathiakumar, D., McFarlane, C., . . . Kambadur, R. (2017). Irisin is a pro-myogenic factor that induces skeletal muscle hypertrophy and rescues denervation-induced atrophy. *Nat Commun*, 8(1), 1104. doi:10.1038/s41467-017-01131-0
- [104] Spangenburg, E. E., & Booth, F. W. (2002). Multiple signaling pathways mediate LIF-induced skeletal muscle satellite cell proliferation. *Am J Physiol Cell Physiol*, 283(1), C204-211. doi:10.1152/ajpcell.00574.2001
- [105] Clow, C., & Jasmin, B. J. (2010). Brain-derived neurotrophic factor regulates satellite cell differentiation and skeletal muscle regeneration. *Mol Biol Cell*, 21(13), 2182-2190. doi:10.1091/mbc.E10-02-0154
- [106] Quinn, L. S., Anderson, B. G., Drivdahl, R. H., Alvarez, B., & Argiles, J. M. (2002). Overexpression of interleukin-15 induces skeletal muscle hypertrophy in vitro: implications for treatment of muscle wasting disorders. *Exp Cell Res*, 280(1), 55-63.
- [107] Quinn, L. S., Haugk, K. L., & Grabstein, K. H. (1995). Interleukin-15: a novel anabolic cytokine for skeletal muscle. *Endocrinology*, 136(8), 3669-3672. doi:10.1210/endo.136.8.7628408

- [108]Fukada, S., Uezumi, A., Ikemoto, M., Masuda, S., Segawa, M., Tanimura, N., . . . Takeda, S. (2007). Molecular signature of quiescent satellite cells in adult skeletal muscle. *Stem Cells*, 25(10), 2448-2459. doi:10.1634/stemcells.2007-0019
- [109]Mauro, A. (1961). Satellite cell of skeletal muscle fibers. *J Biophys Biochem Cytol*, 9, 493-495.
- [110]Kitamoto, T., & Hanaoka, K. (2010). Notch3 null mutation in mice causes muscle hyperplasia by repetitive muscle regeneration. *Stem Cells*, 28(12), 2205-2216. doi:10.1002/stem.547
- [111]Low, S., Barnes, J. L., Zammit, P. S., & Beauchamp, J. R. (2018). Delta-Like 4 Activates Notch 3 to Regulate Self-Renewal in Skeletal Muscle Stem Cells. *Stem Cells*, 36(3), 458-466. doi:10.1002/stem.2757
- [112]Fujimaki, S., Seko, D., Kitajima, Y., Yoshioka, K., Tsuchiya, Y., Masuda, S., & Ono, Y. (2018). Notch1 and Notch2 Coordinately Regulate Stem Cell Function in the Quiescent and Activated States of Muscle Satellite Cells. *Stem Cells*, 36(2), 278-285. doi:10.1002/stem.2743
- [113]Giordani, L., Parisi, A., & Le Grand, F. (2018). Satellite Cell Self-Renewal. *Curr Top Dev Biol*, 126, 177-203. doi:10.1016/bs.ctdb.2017.08.001
- [114]Seale, P., Sabourin, L. A., Girgis-Gabardo, A., Mansouri, A., Gruss, P., & Rudnicki, M. A. (2000). Pax7 is required for the specification of myogenic satellite cells. *Cell*, 102(6), 777-786.
- [115]Zammit, P. S., Golding, J. P., Nagata, Y., Hudon, V., Partridge, T. A., & Beauchamp, J. R. (2004). Muscle satellite cells adopt divergent fates: a mechanism for self-renewal? *J Cell Biol*, 166(3), 347-357. doi:10.1083/jcb.200312007
- [116]Zammit, P. S., Relaix, F., Nagata, Y., Ruiz, A. P., Collins, C. A., Partridge, T. A., & Beauchamp, J. R. (2006). Pax7 and myogenic progression in skeletal muscle satellite cells. *J Cell Sci*, 119(Pt 9), 1824-1832. doi:10.1242/jcs.02908
- [117]Pasut, A., Chang, N. C., Gurriaran-Rodriguez, U., Faulkes, S., Yin, H., Lacaria, M., . . . Rudnicki, M. A. (2016). Notch Signaling Rescues Loss of Satellite Cells Lacking Pax7 and Promotes Brown Adipogenic Differentiation. *Cell Rep*, 16(2), 333-343. doi:10.1016/j.celrep.2016.06.001
- [118]Mitchell, K. J., Pannerec, A., Cadot, B., Parlakian, A., Besson, V., Gomes, E. R., . . . Sassoon, D. A. (2010). Identification and characterization of a non-satellite cell muscle resident progenitor during postnatal development. *Nat Cell Biol*, 12(3), 257-266. doi:10.1038/ncb2025
- [119]Calegari, F., & Waskow, C. (2014). *Stem cells : from basic research to therapy*. Boca Raton, FL: CRC Press, Taylor & Francis Group.

- [120]Delfini, M. C., Hirsinger, E., Pourquie, O., & Duprez, D. (2000). Delta 1-activated notch inhibits muscle differentiation without affecting Myf5 and Pax3 expression in chick limb myogenesis. *Development*, *127*(23), 5213-5224.
- [121]Kopan, R., Nye, J. S., & Weintraub, H. (1994). The intracellular domain of mouse Notch: a constitutively activated repressor of myogenesis directed at the basic helix-loop-helix region of MyoD. *Development*, *120*(9), 2385-2396.
- [122]Kuroda, K., Tani, S., Tamura, K., Minoguchi, S., Kurooka, H., & Honjo, T. (1999). Delta-induced Notch signaling mediated by RBP-J inhibits MyoD expression and myogenesis. *J Biol Chem*, *274*(11), 7238-7244.
- [123]Zammit, P. S., Heslop, L., Hudon, V., Rosenblatt, J. D., Tajbakhsh, S., Buckingham, M. E., . . . Partridge, T. A. (2002). Kinetics of myoblast proliferation show that resident satellite cells are competent to fully regenerate skeletal muscle fibers. *Exp Cell Res*, *281*(1), 39-49.
- [124]Smith, H. K., Maxwell, L., Rodgers, C. D., McKee, N. H., & Pyley, M. J. (2001). Exercise-enhanced satellite cell proliferation and new myonuclear accretion in rat skeletal muscle. *J Appl Physiol* (1985), *90*(4), 1407-1414. doi:10.1152/jappl.2001.90.4.1407
- [125]Tsivitse, S. K., McLoughlin, T. J., Peterson, J. M., Mylona, E., McGregor, S. J., & Pizza, F. X. (2003). Downhill running in rats: influence on neutrophils, macrophages, and MyoD+ cells in skeletal muscle. *Eur J Appl Physiol*, *90*(5-6), 633-638. doi:10.1007/s00421-003-0909-0
- [126]Tamaki, T., Uchiyama, S., Uchiyama, Y., Akatsuka, A., Yoshimura, S., Roy, R. R., & Edgerton, V. R. (2000). Limited myogenic response to a single bout of weight-lifting exercise in old rats. *Am J Physiol Cell Physiol*, *278*(6), C1143-1152. doi:10.1152/ajpcell.2000.278.6.C1143
- [127]Der Vartanian, A., Audfray, A., Al Jaam, B., Janot, M., Legardinier, S., Maftah, A., & Germot, A. (2015). Protein O-fucosyltransferase 1 expression impacts myogenic C2C12 cell commitment via the Notch signaling pathway. *Mol Cell Biol*, *35*(2), 391-405. doi:10.1128/MCB.00890-14
- [128]Sun, D., Li, H., & Zolkiewska, A. (2008). The role of Delta-like 1 shedding in muscle cell self-renewal and differentiation. *J Cell Sci*, *121*(Pt 22), 3815-3823. doi:10.1242/jcs.035493
- [129]Smith, C. K., 2nd, Janney, M. J., & Allen, R. E. (1994). Temporal expression of myogenic regulatory genes during activation, proliferation, and differentiation of rat skeletal muscle satellite cells. *J Cell Physiol*, *159*(2), 379-385. doi:10.1002/jcp.1041590222

- [130]Kuang, S., Gillespie, M. A., & Rudnicki, M. A. (2008). Niche regulation of muscle satellite cell self-renewal and differentiation. *Cell Stem Cell*, 2(1), 22-31. doi:10.1016/j.stem.2007.12.012
- [131]Kuang, S., Kuroda, K., Le Grand, F., & Rudnicki, M. A. (2007). Asymmetric self-renewal and commitment of satellite stem cells in muscle. *Cell*, 129(5), 999-1010. doi:10.1016/j.cell.2007.03.044
- [132]Du, H., Shih, C. H., Wosczyzna, M. N., Mueller, A. A., Cho, J., Aggarwal, A., . . . Feldman, B. J. (2017). Macrophage-released ADAMTS1 promotes muscle stem cell activation. *Nat Commun*, 8(1), 669. doi:10.1038/s41467-017-00522-7
- [133]Zygmunt, D. A., Singhal, N., Kim, M. L., Cramer, M. L., Crowe, K. E., Xu, R., . . . Martin, P. T. (2017). Deletion of Pofut1 in Mouse Skeletal Myofibers Induces Muscle Aging-Related Phenotypes in cis and in trans. *Mol Cell Biol*, 37(10). doi:10.1128/MCB.00426-16
- [134]Schuster-Gossler, K., Cordes, R., & Gossler, A. (2007). Premature myogenic differentiation and depletion of progenitor cells cause severe muscle hypotrophy in Delta1 mutants. *Proc Natl Acad Sci U S A*, 104(2), 537-542. doi:10.1073/pnas.0608281104
- [135]Vasyutina, E., Lenhard, D. C., Wende, H., Erdmann, B., Epstein, J. A., & Birchmeier, C. (2007). RBP-J (Rbpsiuh) is essential to maintain muscle progenitor cells and to generate satellite cells. *Proc Natl Acad Sci U S A*, 104(11), 4443-4448. doi:10.1073/pnas.0610647104
- [136]Rosa de Andrade, I., Correa, S., Fontenele, M., de Oliveira Teixeira, J. D., Abdelhay, E., Costa, M. L., & Mermelstein, C. (2018). gamma-Secretase Inhibition Induces Muscle Hypertrophy in a Notch-Independent Mechanism. *Proteomics*, 18(3-4). doi:10.1002/pmic.201700423
- [137]Funahashi, Y., Shawber, C. J., Vorontchikhina, M., Sharma, A., Outtz, H. H., & Kitajewski, J. (2010). Notch regulates the angiogenic response via induction of VEGFR-1. *J Angiogenes Res*, 2(1), 3. doi:10.1186/2040-2384-2-3
- [138]Gamrekelashvili, J., Giagnorio, R., Jussofie, J., Soehnlein, O., Duchene, J., Briseno, C. G., . . . Limbourg, F. P. (2016). Regulation of monocyte cell fate by blood vessels mediated by Notch signalling. *Nat Commun*, 7, 12597. doi:10.1038/ncomms12597
- [139]Shang, Y., Smith, S., & Hu, X. (2016). Role of Notch signaling in regulating innate immunity and inflammation in health and disease. *Protein Cell*, 7(3), 159-174. doi:10.1007/s13238-016-0250-0
- [140]Kimball, A. S., Joshi, A. D., Boniakowski, A. E., Schaller, M., Chung, J., Allen, R., . . . Gallagher, K. A. (2017). Notch Regulates Macrophage-Mediated

- Inflammation in Diabetic Wound Healing. *Front Immunol*, 8, 635.
doi:10.3389/fimmu.2017.00635
- [141]Wei, X., Wang, J. P., Hao, C. Q., Yang, X. F., Wang, L. X., Huang, C. X., . . . Zhang, Y. (2016). Notch Signaling Contributes to Liver Inflammation by Regulation of Interleukin-22-Producing Cells in Hepatitis B Virus Infection. *Front Cell Infect Microbiol*, 6, 132. doi:10.3389/fcimb.2016.00132
- [142]Allen, D. L., Harrison, B. C., Sartorius, C., Byrnes, W. C., & Leinwand, L. A. (2001). Mutation of the IIB myosin heavy chain gene results in muscle fiber loss and compensatory hypertrophy. *Am J Physiol Cell Physiol*, 280(3), C637-645. doi:10.1152/ajpcell.2001.280.3.C637
- [143]Bentzinger, C. F., Lin, S., Romanino, K., Castets, P., Guridi, M., Summermatter, S., . . . Ruegg, M. A. (2013). Differential response of skeletal muscles to mTORC1 signaling during atrophy and hypertrophy. *Skelet Muscle*, 3(1), 6. doi:10.1186/2044-5040-3-6
- [144]Fuller, P. M., Baldwin, K. M., & Fuller, C. A. (2006). Parallel and divergent adaptations of rat soleus and plantaris to chronic exercise and hypergravity. *Am J Physiol Regul Integr Comp Physiol*, 290(2), R442-448. doi:10.1152/ajpregu.00578.2005
- [145]Marino, J. S., Tausch, B. J., Dearth, C. L., Manacci, M. V., McLoughlin, T. J., Rakyta, S. J., . . . Pizza, F. X. (2008). Beta2-integrins contribute to skeletal muscle hypertrophy in mice. *Am J Physiol Cell Physiol*, 295(4), C1026-1036. doi:10.1152/ajpcell.212.2008
- [146]Timson, B. F. (1990). Evaluation of animal models for the study of exercise-induced muscle enlargement. *J Appl Physiol (1985)*, 69(6), 1935-1945. doi:10.1152/jappl.1990.69.6.1935
- [147]Zushi, K., & Yamazaki, T. (2012). The Effect of Reloading on Disuse Muscle Atrophy: Time Course of Hypertrophy and Regeneration Focusing on the Myofiber Cross-sectional Area and Myonuclear Change. *J Jpn Phys Ther Assoc*, 15(1), 1-8. doi:10.1298/jjpta.Vol15_001
- [148]Terena, S. M., Fernandes, K. P., Bussadori, S. K., Deana, A. M., & Mesquita-Ferrari, R. A. (2017). Systematic review of the synergist muscle ablation model for compensatory hypertrophy. *Rev Assoc Med Bras (1992)*, 63(2), 164-172. doi:10.1590/1806-9282.63.02.164
- [149]Shan, T., Zhang, P., Xiong, Y., Wang, Y., & Kuang, S. (2016). Lkb1 deletion upregulates Pax7 expression through activating Notch signaling pathway in myoblasts. *Int J Biochem Cell Biol*, 76, 31-38. doi:10.1016/j.biocel.2016.04.017

- [150] Yue, F., Bi, P., Wang, C., Shan, T., Nie, Y., Ratliff, T. L., . . . Kuang, S. (2017). Pten is necessary for the quiescence and maintenance of adult muscle stem cells. *Nat Commun*, 8, 14328. doi:10.1038/ncomms14328
- [151] Bi, P., & Kuang, S. (2015). Notch signaling as a novel regulator of metabolism. *Trends Endocrinol Metab*, 26(5), 248-255. doi:10.1016/j.tem.2015.02.006
- [152] Pajvani, U. B., Shawber, C. J., Samuel, V. T., Birkenfeld, A. L., Shulman, G. I., Kitajewski, J., & Accili, D. (2011). Inhibition of Notch signaling ameliorates insulin resistance in a FoxO1-dependent manner. *Nat Med*, 17(8), 961-967. doi:10.1038/nm.2378
- [153] You, J. S., Anderson, G. B., Dooley, M. S., & Hornberger, T. A. (2015). The role of mTOR signaling in the regulation of protein synthesis and muscle mass during immobilization in mice. *Dis Model Mech*, 8(9), 1059-1069. doi:10.1242/dmm.019414
- [154] Palomero, T., Sulis, M. L., Cortina, M., Real, P. J., Barnes, K., Ciofani, M., . . . Ferrando, A. A. (2007). Mutational loss of PTEN induces resistance to NOTCH1 inhibition in T-cell leukemia. *Nat Med*, 13(10), 1203-1210. doi:10.1038/nm1636
- [155] Hinds, T. D., Peck, B., Shek, E., Stroup, S., Hinson, J., Arthur, S., & Marino, J. S. (2016). Overexpression of Glucocorticoid Receptor beta Enhances Myogenesis and Reduces Catabolic Gene Expression. *Int J Mol Sci*, 17(2), 232. doi:10.3390/ijms17020232
- [156] Agle, C. C., Velloso, C. P., Lazarus, N. R., & Harridge, S. D. (2012). An image analysis method for the precise selection and quantitation of fluorescently labeled cellular constituents: application to the measurement of human muscle cells in culture. *J Histochem Cytochem*, 60(6), 428-438. doi:10.1369/0022155412442897
- [157] Ciciliot, S., & Schiaffino, S. (2010). Regeneration of mammalian skeletal muscle. Basic mechanisms and clinical implications. *Curr Pharm Des*, 16(8), 906-914.
- [158] White, R. B., Bierinx, A. S., Gnocchi, V. F., & Zammit, P. S. (2010). Dynamics of muscle fibre growth during postnatal mouse development. *BMC Dev Biol*, 10, 21. doi:10.1186/1471-213X-10-21
- [159] Yin, H., Price, F., & Rudnicki, M. A. (2013). Satellite cells and the muscle stem cell niche. *Physiol Rev*, 93(1), 23-67. doi:10.1152/physrev.00043.2011
- [160] Ciofani, M., & Zuniga-Pflucker, J. C. (2005). Notch promotes survival of pre-T cells at the beta-selection checkpoint by regulating cellular metabolism. *Nat Immunol*, 6(9), 881-888. doi:10.1038/ni1234
- [161] Sade, H., Krishna, S., & Sarin, A. (2004). The anti-apoptotic effect of Notch-1 requires p56lck-dependent, Akt/PKB-mediated signaling in T cells. *J Biol Chem*, 279(4), 2937-2944. doi:10.1074/jbc.M309924200

- [162]Copp, J., Manning, G., & Hunter, T. (2009). TORC-specific phosphorylation of mammalian target of rapamycin (mTOR): phospho-Ser2481 is a marker for intact mTOR signaling complex 2. *Cancer Res*, *69*(5), 1821-1827. doi:10.1158/0008-5472.CAN-08-3014
- [163]Laplante, M., & Sabatini, D. M. (2012). mTOR signaling in growth control and disease. *Cell*, *149*(2), 274-293. doi:10.1016/j.cell.2012.03.017
- [164]Antikainen, H., Driscoll, M., Haspel, G., & Dobrowolski, R. (2017). TOR-mediated regulation of metabolism in aging. *Aging Cell*, *16*(6), 1219-1233. doi:10.1111/accel.12689
- [165]Harrison, D. E., Strong, R., Sharp, Z. D., Nelson, J. F., Astle, C. M., Flurkey, K., . . . Miller, R. A. (2009). Rapamycin fed late in life extends lifespan in genetically heterogeneous mice. *Nature*, *460*(7253), 392-395. doi:10.1038/nature08221
- [166]Lamming, D. W., Ye, L., Katajisto, P., Goncalves, M. D., Saitoh, M., Stevens, D. M., . . . Baur, J. A. (2012). Rapamycin-induced insulin resistance is mediated by mTORC2 loss and uncoupled from longevity. *Science*, *335*(6076), 1638-1643. doi:10.1126/science.1215135
- [167]Neff, F., Flores-Dominguez, D., Ryan, D. P., Horsch, M., Schroder, S., Adler, T., . . . Ehninger, D. (2013). Rapamycin extends murine lifespan but has limited effects on aging. *J Clin Invest*, *123*(8), 3272-3291. doi:10.1172/JCI67674
- [168]Wilkinson, J. E., Burmeister, L., Brooks, S. V., Chan, C. C., Friedline, S., Harrison, D. E., . . . Miller, R. A. (2012). Rapamycin slows aging in mice. *Aging Cell*, *11*(4), 675-682. doi:10.1111/j.1474-9726.2012.00832.x
- [169]Johnson, S. C., Rabinovitch, P. S., & Kaeberlein, M. (2013). mTOR is a key modulator of ageing and age-related disease. *Nature*, *493*(7432), 338-345. doi:10.1038/nature11861
- [170]Goodman, C. A., Frey, J. W., Mabrey, D. M., Jacobs, B. L., Lincoln, H. C., You, J. S., & Hornberger, T. A. (2011). The role of skeletal muscle mTOR in the regulation of mechanical load-induced growth. *J Physiol*, *589*(Pt 22), 5485-5501. doi:10.1113/jphysiol.2011.218255
- [171]Willett, M., Cowan, J. L., Vlasak, M., Coldwell, M. J., & Morley, S. J. (2009). Inhibition of mammalian target of rapamycin (mTOR) signalling in C2C12 myoblasts prevents myogenic differentiation without affecting the hyperphosphorylation of 4E-BP1. *Cell Signal*, *21*(10), 1504-1512. doi:10.1016/j.cellsig.2009.05.009
- [172]Cross, D. A., Alessi, D. R., Cohen, P., Andjelkovich, M., & Hemmings, B. A. (1995). Inhibition of glycogen synthase kinase-3 by insulin mediated by protein kinase B. *Nature*, *378*(6559), 785-789. doi:10.1038/378785a0

- [173]Glass, D. J. (2003). Signalling pathways that mediate skeletal muscle hypertrophy and atrophy. *Nat Cell Biol*, 5(2), 87-90. doi:10.1038/ncb0203-87
- [174]Rommel, C., Bodine, S. C., Clarke, B. A., Rossman, R., Nunez, L., Stitt, T. N., . . . Glass, D. J. (2001). Mediation of IGF-1-induced skeletal myotube hypertrophy by PI(3)K/Akt/mTOR and PI(3)K/Akt/GSK3 pathways. *Nat Cell Biol*, 3(11), 1009-1013. doi:10.1038/ncb1101-1009
- [175]Meloty-Kapella, L., Shergill, B., Kuon, J., Botvinick, E., & Weinmaster, G. (2012). Notch ligand endocytosis generates mechanical pulling force dependent on dynamin, epsins, and actin. *Dev Cell*, 22(6), 1299-1312. doi:10.1016/j.devcel.2012.04.005
- [176]Musse, A. A., Meloty-Kapella, L., & Weinmaster, G. (2012). Notch ligand endocytosis: mechanistic basis of signaling activity. *Semin Cell Dev Biol*, 23(4), 429-436. doi:10.1016/j.semcdb.2012.01.011
- [177]Arya, M. A., Tai, A. K., Wooten, E. C., Parkin, C. D., Kudryavtseva, E., & Huggins, G. S. (2013). Notch pathway activation contributes to inhibition of C2C12 myoblast differentiation by ethanol. *PLoS One*, 8(8), e71632. doi:10.1371/journal.pone.0071632
- [178]Jefferson, L. S., Fabian, J. R., & Kimball, S. R. (1999). Glycogen synthase kinase-3 is the predominant insulin-regulated eukaryotic initiation factor 2B kinase in skeletal muscle. *Int J Biochem Cell Biol*, 31(1), 191-200.
- [179]Brunet, A., Bonni, A., Zigmond, M. J., Lin, M. Z., Juo, P., Hu, L. S., . . . Greenberg, M. E. (1999). Akt promotes cell survival by phosphorylating and inhibiting a Forkhead transcription factor. *Cell*, 96(6), 857-868.
- [180]Waldemer-Streyer, R. J., & Chen, J. (2015). Myocyte-derived Tnfsf14 is a survival factor necessary for myoblast differentiation and skeletal muscle regeneration. *Cell Death Dis*, 6, e2026. doi:10.1038/cddis.2015.375
- [181]Ren, H., Koo, J., Guan, B., Yue, P., Deng, X., Chen, M., . . . Sun, S. Y. (2013). The E3 ubiquitin ligases beta-TrCP and FBXW7 cooperatively mediates GSK3-dependent Mcl-1 degradation induced by the Akt inhibitor API-1, resulting in apoptosis. *Mol Cancer*, 12, 146. doi:10.1186/1476-4598-12-146
- [182]Wilson, E. M., & Rotwein, P. (2007). Selective control of skeletal muscle differentiation by Akt1. *J Biol Chem*, 282(8), 5106-5110. doi:10.1074/jbc.C600315200
- [183]Gordon, B. S., Kelleher, A. R., & Kimball, S. R. (2013). Regulation of muscle protein synthesis and the effects of catabolic states. *Int J Biochem Cell Biol*, 45(10), 2147-2157. doi:10.1016/j.biocel.2013.05.039

- [184] Henning, R. J., Sanberg, P., & Jimenez, E. (2014). Human cord blood stem cell paracrine factors activate the survival protein kinase Akt and inhibit death protein kinases JNK and p38 in injured cardiomyocytes. *Cytotherapy*, *16*(8), 1158-1168. doi:10.1016/j.jcyt.2014.01.415
- [185] Jin, H., Sanberg, P. R., & Henning, R. J. (2013). Human umbilical cord blood mononuclear cell-conditioned media inhibits hypoxic-induced apoptosis in human coronary artery endothelial cells and cardiac myocytes by activation of the survival protein Akt. *Cell Transplant*, *22*(9), 1637-1650. doi:10.3727/096368912X661427
- [186] Karaboga Arslan, A. K., & Yerer, M. B. (2018). alpha-Chaconine and alpha-Solanine Inhibit RL95-2 Endometrium Cancer Cell Proliferation by Reducing Expression of Akt (Ser473) and ERalpha (Ser167). *Nutrients*, *10*(6). doi:10.3390/nu10060672
- [187] Saglam, A. S., Alp, E., Elmazoglu, Z., & Menevse, E. S. (2016). Effect of API-1 and FR180204 on cell proliferation and apoptosis in human DLD-1 and LoVo colorectal cancer cells. *Oncol Lett*, *12*(4), 2463-2474. doi:10.3892/ol.2016.4995
- [188] Mirzoev, T. M., Tyganov, S. A., & Shenkman, B. S. (2017). Akt-dependent and Akt-independent pathways are involved in protein synthesis activation during reloading of disused soleus muscle. *Muscle Nerve*, *55*(3), 393-399. doi:10.1002/mus.25235
- [189] Espinosa, L., Ingles-Esteve, J., Aguilera, C., & Bigas, A. (2003). Phosphorylation by glycogen synthase kinase-3 beta down-regulates Notch activity, a link for Notch and Wnt pathways. *J Biol Chem*, *278*(34), 32227-32235. doi:10.1074/jbc.M304001200
- [190] Foltz, D. R., Santiago, M. C., Berechid, B. E., & Nye, J. S. (2002). Glycogen synthase kinase-3beta modulates notch signaling and stability. *Curr Biol*, *12*(12), 1006-1011.
- [191] Guha, S., Cullen, J. P., Morrow, D., Colombo, A., Lally, C., Walls, D., . . . Cahill, P. A. (2011). Glycogen synthase kinase 3 beta positively regulates Notch signaling in vascular smooth muscle cells: role in cell proliferation and survival. *Basic Res Cardiol*, *106*(5), 773-785. doi:10.1007/s00395-011-0189-5
- [192] Mayhew, D. L., Hornberger, T. A., Lincoln, H. C., & Bamman, M. M. (2011). Eukaryotic initiation factor 2B epsilon induces cap-dependent translation and skeletal muscle hypertrophy. *J Physiol*, *589*(Pt 12), 3023-3037. doi:10.1113/jphysiol.2010.202432
- [193] Fryer, C. J., White, J. B., & Jones, K. A. (2004). Mastermind recruits CycC:CDK8 to phosphorylate the Notch ICD and coordinate activation with turnover. *Mol Cell*, *16*(4), 509-520. doi:10.1016/j.molcel.2004.10.014

- [194] Ilagan, M. X., Lim, S., Fulbright, M., Piwnicka-Worms, D., & Kopan, R. (2011). Real-time imaging of notch activation with a luciferase complementation-based reporter. *Sci Signal*, 4(181), rs7. doi:10.1126/scisignal.2001656
- [195] Jin, Y. H., Kim, H., Oh, M., Ki, H., & Kim, K. (2009). Regulation of Notch1/NICD and Hes1 expressions by GSK-3alpha/beta. *Mol Cells*, 27(1), 15-19. doi:10.1007/s10059-009-0001-7
- [196] Saint Just Ribeiro, M., Hansson, M. L., Lindberg, M. J., Popko-Scibor, A. E., & Wallberg, A. E. (2009). GSK3beta is a negative regulator of the transcriptional coactivator MAML1. *Nucleic Acids Res*, 37(20), 6691-6700. doi:10.1093/nar/gkp724
- [197] Ito, H., Ichiyanagi, O., Naito, S., Bilim, V. N., Tomita, Y., Kato, T., . . . Tsuchiya, N. (2016). GSK-3 directly regulates phospho-4EBP1 in renal cell carcinoma cell-line: an intrinsic subcellular mechanism for resistance to mTORC1 inhibition. *BMC Cancer*, 16, 393. doi:10.1186/s12885-016-2418-7
- [198] Shin, S., Wolgamott, L., Tcherkezian, J., Vallabhapurapu, S., Yu, Y., Roux, P. P., & Yoon, S. O. (2014). Glycogen synthase kinase-3beta positively regulates protein synthesis and cell proliferation through the regulation of translation initiation factor 4E-binding protein 1. *Oncogene*, 33(13), 1690-1699. doi:10.1038/onc.2013.113
- [199] Al-Khouri, A. M., Ma, Y., Togo, S. H., Williams, S., & Mustelin, T. (2005). Cooperative phosphorylation of the tumor suppressor phosphatase and tensin homologue (PTEN) by casein kinases and glycogen synthase kinase 3beta. *J Biol Chem*, 280(42), 35195-35202. doi:10.1074/jbc.M503045200
- [200] Maccario, H., Perera, N. M., Davidson, L., Downes, C. P., & Leslie, N. R. (2007). PTEN is destabilized by phosphorylation on Thr366. *Biochem J*, 405(3), 439-444. doi:10.1042/BJ20061837
- [201] Sieiro, D., Rios, A. C., Hirst, C. E., & Marcelle, C. (2016). Cytoplasmic NOTCH and membrane-derived beta-catenin link cell fate choice to epithelial-mesenchymal transition during myogenesis. *Elife*, 5. doi:10.7554/eLife.14847

APPENDIX 1: INSTITUTIONAL ANIMAL CARE AND USE COMMITTEE APPROVAL LETTER



Research and Economic Development

Office of Research Compliance

9201 University City Boulevard, Charlotte, NC 28223-0001
t/ 704.687.1876 | f/ 704.687.0980 | <http://research.uncc.edu/compliance-ethics>

Notice of Initial Protocol Approval

To: Dr. Susan Arthur
Department of Kinesiology

From: Dr. Yvette Huet
IACUC Chair

Subject: Approval of Protocol

Protocol #: 16-017

Title: The Myogenic Orchestration of Notch and mTOR

Approval Date: 01/13/2017

The Institutional Animal Care and Use Committee (IACUC) approved the protocol entitled "**The Myogenic Orchestration of Notch and mTOR.**" Approvals are valid for one year and may be renewed before the anniversary of the original approval date for a total of three years. After three years, a new protocol application must be submitted to continue the study. Please note the following information:

Initial Approval date: **01/13/2017**
Renewal 1 – due and approved before: 01/13/2018
Renewal 2 – due and approved before: 01/13/2019
Expiration date: **01/13/2020**

Please note that it is the investigator's responsibility to promptly inform the committee of any changes in the proposed research, as well as any unanticipated problems that may occur involving care and use of animals. All changes (e.g. personnel additions, change in animal strain, change in procedures, etc.) must be submitted to the IACUC via an Amendment. All forms (e.g. amendments, annual renewal, etc.) can be found at: <http://research.uncc.edu/departments/office-research-compliance-orc/animal-care-use/protocol-application-forms>

Before starting any protocol involving survival surgery, tumor and/or disease induction, and any other painful animal procedure, a meeting with the Attending Veterinarian, Vivarium Director, and Vivarium staff is required. If the research involves surgical procedures, it is also the investigator's responsibility to maintain detailed surgical records. These records must be approved by the Vivarium Director and the Attending Veterinarian and a copy must be kept with the animals at all times.

To better help you and your research team, please inform Vivarium personnel which phase/specific aim of your protocol is being conducted at any given time. It is helpful for the staff to know which endpoints are required for the phase/specific aim being investigated.

NOTES:

- This protocol requested reverse light cycle. Please consult with the Attending Veterinarian/Director of Laboratory Animal Resources to confirm start date of reverse light cycle.
- This protocol contains a pilot study. Per the reporting requirements policy, a progress report will be due to the IACUC approximately 90 days from the date of initiation of this study, or by **April 13, 2017**.

A renewal/status report is due annually for IACUC protocols. The annual renewal application can be accessed via the above-listed website. If you do not plan to continue your study at the time of your renewal anniversary date, please contact the Office of Research Compliance before the anniversary date to terminate your study.

If you need additional assistance, please contact Cindy Stone in the Office of Research Compliance at (704) 687-1872 or via email at C.Stone@uncc.edu.

APPENDIX 2: INSTITUTIONAL BIOSAFETY APPROVAL LETTER

**Institutional Biosafety Committee (IBC)***Certificate of Approval and Registration for BSL-2 work*

To: Dr. Susan Arthur
 Department of Kinesiology

From: Dr. Angelica N. Martins – Biosafety Officer

Protocol Title: “The Myogenic Orchestration of Notch and mTOR”

IBC Protocol #: 16-016

Agent/s and Material/s Declared: Lentivirus, mice.

BSL/Risk Group Classification: BSL-2/ RG-2

NIH Guidelines: Section III-D-1, III-D-3, III-D-4 and Section III-E-3

Approval Date: May 1st, 2017

The Institutional Biosafety Committee (IBC) has reviewed your proposed experiments using **Lentiviral particles** as described in your biosafety protocol. The IBC concurs with your classification and the stated BSL-2 precautions for using an RG-2 agent. Approvals are valid for one year and should be renewed before the anniversary of the original approval date for a total of three years. After three years, a new protocol application must be submitted to continue the study. Your protocol will reach 3-year expiration on **May 1st, 2020.**

The experiments are approved for execution only as proposed. It is the investigator’s responsibility to inform the IBC of any changes in the proposed research that potentially alters the BSL classification. Likewise, if there any changes to the proposed research involving this agent, (i.e. personnel changes, changes in the location of agents, change in manipulations of agents/materials, etc.); the investigator must inform the Committee of these changes via an amended protocol.

Please note that it is the investigator’s responsibility to promptly inform the committee of any unanticipated problems that may occur involving the use of this agent. If an accidental exposure or a spill using this agent occurs, please promptly forward a summary of the incident to the Office of Research Compliance for review by the IBC.

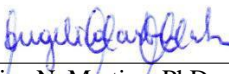
IBC Protocol # 16-016
Approval Certification Memorandum

A renewal/status report is due annually for IBC protocols. The Office of Research Compliance will send the annual renewal survey to you. If you do not plan to continue your study at the time of your renewal anniversary date, please contact the Office of Research Compliance before the anniversary date to terminate your study.

Also, the investigator is responsible for the following:

1. Posting "BIOHAZARD" warning signs with the universal biohazard-warning symbol on access doors to the laboratory area. NOTE: Signage should identify agent(s) in use, list the name of the laboratory supervisor or another responsible person(s), an after-hours contact telephone number and indicate any special conditions for entry into the room (e.g., immunizations, respirators).
2. Limiting access to your laboratory when experiments using these agents are in progress.
3. Ensuring that lab personnel read and become familiar with the contents of your protocol, any approved biosafety lab Standard Operating Procedures (SOPs), and the University [biosafety laboratory manual](#).

If you have any questions, please contact Dr. Angelica N. Martins in the Office of Research Compliance at 704-687-1825.



Angelica N. Martins, PhD
Biosafety Officer
Office of Research Compliance

May 5, 2017

Date

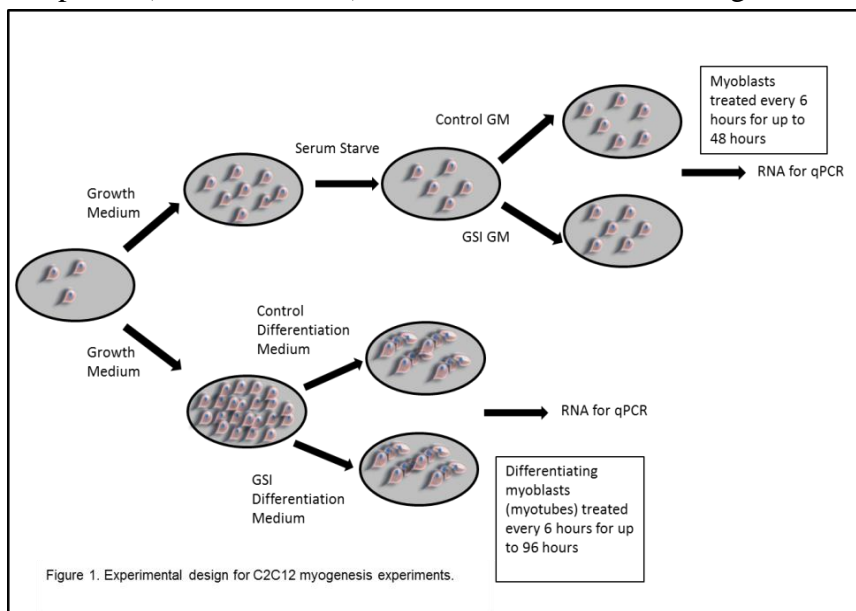
APPENDIX 3: SIGMA XI STUDENT RESEARCH GRANT

The Myogenic Switch of Notch and mTOR

Joshua R. Huot

Aging can be accompanied by aggressive loss of skeletal muscle mass (sarcopenia), and is thought to be a driving factor to a reduced ability of the elderly to accomplish basic activities of daily living (1). The prevalence of sarcopenia exceeds 30% in individuals 60 years and older and 50% in individuals 80 years and older, which results in excessive healthcare costs and impedes quality of life (2-4). Several mechanisms within aged skeletal muscle lead to development of sarcopenia, including a delayed myogenic response when exposed to injury. The process of myogenesis is comprised of activation of adult skeletal muscle stem cells (satellite cells), proliferation, differentiation, and fusion of these cells leading to formation of multinucleated myotubes. Aging is associated with deleterious modifications to the intrinsic properties of satellite cells and the signaling pathways that regulate myogenesis, including Notch and mammalian target of rapamycin (mTOR). Notch signaling regulates satellite cell activation and

proliferation, while mTOR appears to regulate differentiation and fusion (5-10). Although it is currently unknown if Notch and mTOR interact during the myogenic program, other disciplines (cancer research) have indicated that Notch regulates mTOR activity. Thus is



the basis for our testing whether Notch signaling affects mTOR signaling during myogenesis. Preliminary data from our lab indicates a possible myogenic switch of Notch and mTOR. Since these pathways are dysfunctional in aged skeletal

muscle, our overarching aim is to determine if Notch and mTOR contribute to the impaired repair of aged skeletal muscle and ultimately sarcopenia. To test this aim, we will first determine if inhibition of Notch signaling alters mTOR throughout the myogenic program using an *in vitro* model of skeletal muscle repair, a C2C12 cell line which is derived from mouse muscle tissue. C2C12 myoblasts will be seeded and

allowed to grow with or without treatment of a Notch inhibitor (Gamma Secretase Inhibitor). Separate experiments will be conducted allowing C2C12 cells to grow to full confluence followed by differentiation of the cells to form myotubes, with or without Notch Inhibition (Figure 1). Myoblast and myotube samples will be lysed and collected for quantitative PCR analysis, using the Radiant™ Green Hi-ROX qPCR Kit from Alkali Scientific Inc. We will confirm inhibition of Notch signaling (A.Notch and Hes1) and any changes in mTOR signaling (pmTOR, p70S6K, 4e-BP1) during early and late stages of myogenesis. The results of this study will be used as preliminary data for grants that will propose to determine Notch and mTOR dysfunction in aged skeletal muscle using *in vivo* techniques and strategies to rescue impaired Notch and mTOR orchestration during repair of aged skeletal muscle. We hypothesize that inhibiting Notch will reduce mTOR during the early stages of myogenesis, while increasing mTOR during the later stages of myogenesis. If expectations are met, we will shrink the current gap in knowledge regarding skeletal muscle repair and pave the way for rejuvenating repair capacity in aging skeletal muscle, leading to maintenance of skeletal muscle with increasing age and improved clinical practices for other muscle wasting diseases.

Project Budget

A. Radiant™ Green Hi-ROX qPCR Kit (2000 x 20µL reactions)- \$955.00

Total Amount Requested From Sigma Xi- \$955.00

Total Project Budget (\$2,500)

Budget Justification

The Radiant™ Green Hi-ROX qPCR Kit will be used to carry out quantitative PCR analysis for all myoblast and myotube samples of the proposed research. The supplies will help to delineate any differences in Notch and mTOR at the RNA level at several stages of the myogenic program. The Arthur Lab regularly quantifies protein levels of myogenesis; the use of qPCR in this proposal is a novel technique for our lab to analyze gene expression of key regulators of the myogenic program.

Literature Citations

- 1) Morley, J.E., et al., Sarcopenia. *J Lab Clin Med*, 2001. **137**(4): p. 231-43.
- 2) Buford, T.W., et al., Models of accelerated sarcopenia: critical pieces for solving the puzzle of age-related muscle atrophy. *Ageing Res Rev*, 2010. **9**(4): p. 369-83.
- 3) Janssen, I., et al., The healthcare costs of sarcopenia in the United States. *J Am Geriatr Soc*, 2004. **52**(1): p. 80-5.
- 4) Fielding, R., et al., Sarcopenia: An Undiagnosed Condition in Older Adults. Current Consensus Definition: Prevalence, Etiology, and Consequences. International Working Group on Sarcopenia. *Journal of the American Medical Directors Association*, 2011. **12**(4): p. 249–256.
- 5) Arthur, S.T. and I.D. Cooley, The effect of physiological stimuli on sarcopenia; impact of Notch and Wnt signaling on impaired aged skeletal muscle repair. *Int J Biol Sci*, 2012. **8**(5): p. 731-60.
- 6) Erbay, E. and J. Chen, The mammalian target of rapamycin regulates C2C12 myogenesis via a kinase-independent mechanism. *J Biol Chem*, 2001. **276**(39): p. 36079-82.
- 7) Park, I.H. and J. Chen, Mammalian target of rapamycin (mTOR) signaling is required for a late-stage fusion process during skeletal myotube maturation. *J Biol Chem*, 2005. **280**(36): p. 32009-17.
- 8) Ge, Y. and J. Chen, Mammalian target of rapamycin (mTOR) signaling network in skeletal myogenesis. *J Biol Chem*, 2012. **287**(52): p. 43928-35.
- 9) Ge, Y., et al., mTOR regulates skeletal muscle regeneration in vivo through kinase-dependent and kinase-independent mechanisms. *Am J Physiol Cell Physiol*, 2009. **297**(6): p. C1434-44.
- 10) Jansen, K.M. and G.K. Pavlath, Molecular control of mammalian myoblast fusion. *Methods Mol Biol*, 2008. **475**: p. 115-33.

APPENDIX 4: THOMAS L. REYNOLDS GRADUATE RESEARCH FELLOWSHIP

Application: The Thomas L. Reynolds Graduate Student Research Award

Title of Proposed Project:

INVESTIGATING NOTCH AS A MOLECULAR BRAKE ON SKELETAL MUSCLE
REPAIR AND GROWTH

PI Name: Joshua R. Huot (Doctoral Candidate, Biology/Kinesiology)

PI's Email: jhuot@uncc.edu

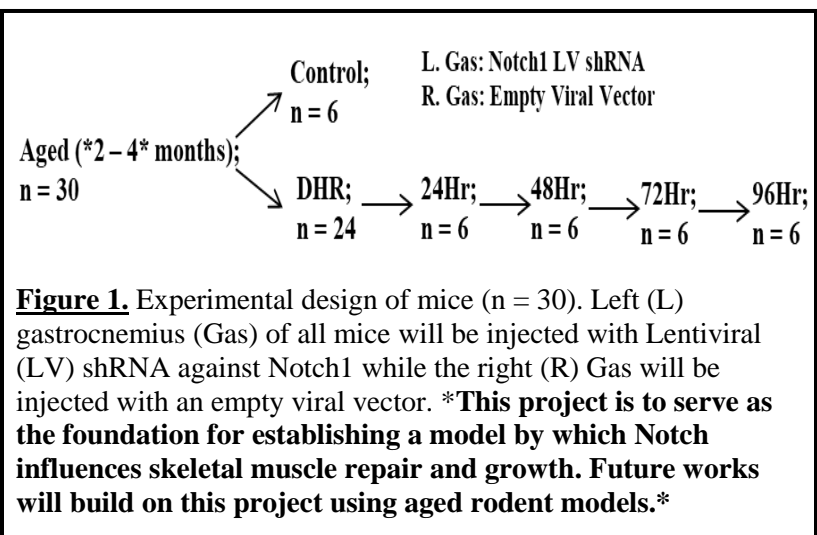
Dissertation Advisor: Dr. Susan T. Arthur (Associate Professor of Kinesiology)

1. Problem Statement: Aging is often accompanied by aggressive loss of skeletal muscle mass (sarcopenia) and is a primary component driving the reduced capacity of the elderly to accomplish basic activities of daily living (1, 2). Contributing to the development of sarcopenia is a faulty repair response and suppressed muscle protein synthesis (MPS) of aged muscle following injury (e.g. bout of exercise) (3, 4). The repair response includes activation and the resultant fusion of muscle stem cells. It is currently unknown to what extent key reparative factors and MPS pathways interact following muscle injury. Notch signaling is of great importance to skeletal muscle repair. Mechanistic target of rapamycin (mTOR) signaling is pivotal to MPS and has recently shown to regulate skeletal muscle repair (5, 6). It is unknown however, if these two signaling pathways interact within skeletal muscle. Delineation of the signaling pathways cross-talk that regulate skeletal muscle repair and MPS is crucial to our development of modalities aimed at treating and preventing the dysfunction that is seen with sarcopenia and other muscle wasting diseases. Our overarching hypothesis is that Notch acts as a molecular brake on skeletal muscle repair and MPS by regulating mTOR.

2. Objective and methodology of proposed project: OBJECTIVE: To determine the effects of Notch knockdown on skeletal muscle repair and MPS in mice following injurious downhill running.

Notch signaling is pivotal to the regulation of muscle stem cell activity. Specifically, following injury it is postulated that down regulation of Notch activates muscle stem cells leading to muscle repair (3, 7-9). A majority of studies investigating Notch's contribution

to skeletal muscle repair are artificial, however, and do not utilize physiological models of muscle injury. Furthermore, studies on Notch regulation of skeletal



muscle focus solely on its capacity to dictate muscle stem cell fate, ignoring other skeletal muscle processes such as MPS. Our lab is the first to utilize downhill running (DHR) as a model to study Notch signaling during skeletal muscle repair. This project is the first to study skeletal muscle repair and MPS using Notch knockdown and a physiological damaging stimuli. We hypothesize that knockdown of Notch will enhance skeletal muscle repair and MPS following DHR.

METHODS: The overall strategy of the proposed study is to investigate Notch's braking effect on repair and protein synthesis of skeletal muscle following DHR. To test our hypothesis, C57BL/6 mice (n = 6, [*2-4 months*]) will be randomly allocated into

exercise or control groups (Figure 1). The control group will simulate a sedentary lifestyle and the exercise groups will undergo an injurious bout of DHR (-15% grade; up to 20m/min until exhaustion). Prior to DHR, mice will receive five days of lentiviral injections into the right (control virus) and left (Notch1 shRNA knockdown virus) hindlimbs. Following completion of the DHR protocol, mice will be euthanized at either 24hr, 48hr, 72hr, or 96hr. Left and right hindlimb musculature will be harvested, and prepared for protein analysis via western blot and immunohistochemistry. Muscle samples will be first be analyzed to confirm Notch signaling was reduced (via measurement of Notch proteins: Cleaved Notch, Hairy and Enhancer of Split 1 [Hes1]). Samples will be measured for markers of muscle injury (centrally located nuclei, phagocytosis, pale cytoplasm), repair (Pax7, MyoD, Myogenin, Myosin Heavy Chain), and protein synthesis (mTOR and puromycin). Expected Outcomes: 1) Notch knockdown will increase injury following DHR. 2) Notch knockdown will lead to greater repair following DHR. 3) Notch knockdown will elevate mTOR and protein synthesis following DHR.

3. Timeline for project: This project has obtained both Institutional Biosafety Committee and Institutional Animal Care and Use Committee approval.

Table 1. *Proposed project timeline.*

| Present-May 14 th | May | June | July | August |
|-----------------------------------------------------------------|-----------------------------------------------------------------------------------------------------------------|-------------------------------------------------------------------------------------------------|-------------------------------------------------------------------------------|-----------------------------------------------------------------------------------------------------------------|
| Complete DHR experiment and process samples for tissue analysis | 14 th → 15 th Immunohistochemical (IHC) analysis on tissue samples from DHR experiment | 18 th → 29 th Automated data quantification on IHC markers of interest | 2 nd → 27 th Western blot analysis on tissue samples | 30 th → 17 th Data analysis and figure generation for all IHC and western blot samples |
| | 21 st → 30 th Manual data quantification on IHC markers of interest | | | |
| | | | | |

4. References Cited:

- 1) Morley JE, Baumgartner RN, Roubenoff R, Mayer J, Nair KS. Sarcopenia. *J Lab Clin Med.* 2001;137(4):231-43.
- 2) Lexell J. Human aging, muscle mass, and fiber type composition. *J Gerontol A Biol Sci Med Sci.* 1995;50 Spec No:11-6.
- 3) Arthur ST, Cooley ID. The effect of physiological stimuli on sarcopenia; impact of Notch and Wnt signaling on impaired aged skeletal muscle repair. *Int J Biol Sci.* 2012;8(5):731-60.
- 4) Carlson ME, Suetta C, Conboy MJ, Aagaard P, Mackey A, Kjaer M, et al. Molecular aging and rejuvenation of human muscle stem cells. *EMBO Mol Med.* 2009;1(8-9):381-91.
- 5) Ge Y, Chen J. Mammalian target of rapamycin (mTOR) signaling network in skeletal myogenesis. *J Biol Chem.* 2012;287(52):43928-35.
- 6) Ge Y, Wu AL, Warnes C, Liu J, Zhang C, Kawasome H, et al. mTOR regulates skeletal muscle regeneration in vivo through kinase-dependent and kinase-independent mechanisms. *Am J Physiol Cell Physiol.* 2009;297(6):C1434-44.

- 7) Mourikis P, Sambasivan R, Castel D, Rocheteau P, Bizzarro V, Tajbakhsh S. A critical requirement for notch signaling in maintenance of the quiescent skeletal muscle stem cell state. *Stem Cells*. 2012;30(2):243-52.
- 8) Mourikis P, Tajbakhsh S. Distinct contextual roles for Notch signaling in skeletal muscle stem cells. *BMC Dev Biol*. 2014;14:2.
- 9) Wen Y, Bi P, Liu W, Asakura A, Keller C, Kuang S. Constitutive Notch activation upregulates Pax7 and promotes the self-renewal of skeletal muscle satellite cells. *Mol Cell Biol*. 2012;32(12):2300-11.